Phytochem Rev (2022) 21:1761–1842
https://doi.org/10.1007/s11101-022-09808-1

# Anti-viral triterpenes: a review

**Priya Darshani · Shreya Sen Sarma · Amit K. Srivastava · Rinku Baishya · Deepak Kumar**

Received: 18 October 2021 / Accepted: 27 January 2022 / Published online: 5 March 2022
© The Author(s), under exclusive licence to Springer Nature B.V. 2022

**Abstract** Triterpenes are naturally occurring derivatives biosynthesized following the isoprene rule of Ruzicka. The triterpenes have been reported to possess a wide range of therapeutic applications including anti-viral properties. In this review, the recent studies (2010–2020) concerning the anti-viral activities of triterpenes have been summarized. The structure activity relationship studies have been described as well as brief biosynthesis of these triterpenes is discussed.

**Keywords** Triterpene · Anti-viral · Biosynthesis · Isoprenoid derivatives · Structure activity relationship

**Abbreviations**

| | |
|---|---|
| AIDS | Acquired immunodeficiency syndrome |
| ART | Antiretroviral therapy |
| AZT | Azidothymidine |
| BAS | *β*-Amyrin synthase |
| CAS | Cycloartane synthase |
| CAR | Coxsackievirus-adenovirus receptor |
| CAT | Cycloartane triterpene |
| $CC_{50}$ | Half maximal cytotoxic concentration |
| $CD4^{+}$ T | cluster of differentiation 4 |
| CLT | Cyclolanostane triterpene |
| CMV | Cytomegalovirus |
| CoV | Coronavirus |
| CPE | Cytopathic effect |
| CVB3 | Coxsackie B3 |
| DAF | Decay-accelerating factor |
| DDS | Dammarenediol synthase |
| DENV | Dengue virus |
| DMPP | Dimethylallyl pyrophosphate |
| DNA | Deoxyribonucleic acid |
| DT | Dammarane triterpene |
| EBV | Epstein-Barr virus |
| EBV-EA | Epstein-Barr virus early antigen |
| $EC_{50}$ | Half maximal effective concentration |
| EV | Enteroviruses |
| FDA | Food and drug administration |
| FPP | Farnesyl pyrophosphate |
| FRS | Friedelin synthase |
| GA | Glycyrrhizic acid |
| GGPP | Geranylgeranyl pyrophosphate |
| GPCMV | Guinea pig cytomegalovirus |
| GPEL | Guinea pig embryo lung fibroblasts |
| GPP | Geranyl pyrophosphate |

P. Darshani · S. Sen Sarma · D. Kumar (✉)
Organic and Medicinal Chemistry Division, CSIR-Indian Institute of Chemical Biology, 4, Raja SC Mullick Road, Jadavpur, Kolkata, India
e-mail: deepak@iicb.res.in; dkseervi@gmail.com

A. K. Srivastava
Cancer Biology and Inflammatory Disorder Division, CSIR-Indian Institute of Chemical Biology, 4, Raja SC Mullick Road, Jadavpur, Kolkata, India

R. Baishya
Natural Product Chemistry Group, CSIR-North East Institute of Science and Technology (NEIST), NH-37, Pulibor, Jorhat, Assam, India

| | |
|---|---|
| hACE2 | Human angiotensin-converting enzyme 2 |
| HbeAg | Hepatitis B e antigen |
| HbsAg | Hepatitis B surface antigen |
| HBV | Hepatitis B |
| HCV | Hepatitis C |
| HCoV | Human corona virus |
| HepG2 | Human hepatocellular carcinoma |
| HFMD | Hand–foot–mouth-disease |
| HIV | Human immunodeficiency viruses |
| HK/68 | Hong Kong/68 |
| HR1/HR2 | Hydrophobic internal fusion peptides |
| H1N1 | Hemagglutinin type 1 and neuraminidase type 1 |
| HSV | Herpes simplex virus |
| HV | Hepatitis virus |
| IV | Influenza virus |
| $IC_{50}$ | Half maximal inhibitory concentration |
| IPP | 3-Isopentenyl pyrophosphate |
| LAS | Lanosterol synthase |
| LUS | Lupeol synthase |
| LUT | Lupane triterpene |
| MDCK | Madin-Darby Canine kidney |
| MEP | Methylerythritol phosphate |
| MERS-CoV | Middle Eastrespiratory syndrome coronavirus |
| MNCC | Maximal noncytotoxic concentrations |
| MOSC | Multi-Functional Oxidosqualene Cyclase |
| MVA | Mevalonic acid |
| NA | Neuraminidase |
| NT | Nor-triterpene |
| OSC | Oxidosqualene cyclase |
| OT | Oleanane triterpene |
| P450 | Cytochrome P450 monooxygenase |
| PEDV | Porcine epidemic diarrhoea virus |
| RD | Rhabdomyosarcoma |
| RSV | Respiratory syncytial virus |
| RT | Reverse transcriptase |
| SAR | Structure–activity relationship |
| SFV | Semliki forest virus |
| SHT | Shionone triterpene |
| SARS-CoV | Severe acute respiratory syndrome coronavirus |
| SHS | Shionone synthase |
| SI | Selective index |
| $TCID_{50}$ | Median tissue culture infectious dose; therapeutic index |
| TPA | 12-*O*-Tetradecanoylphorbol 13-acetate |
| TT | Taraxerane triterpenes |
| UT | Ursane triterpene |
| ZIKV | Zika virus |

## Introduction

Triterpenes with diverse anti-viral activity reported during 2010–2020 are summarized here with a focus on their brief biogenesis, structure–activity relationship, and reported mode of anti-viral actions. The information presented in this article is retrieved from the database search e.g. SciFinder, PubMed, and Google Scholar for the "triterpene" with "virus" or "anti-viral" as keywords and full text were obtained from the respective publisher's/journal's website. The retrieved information is further summarized according to the virus followed by the triterpene sub-class they belong to. In summary, a total of 342 triterpenoids belonging to 10 sub-classes were found to exert anti-viral effects against 14 different viruses (Fig. 1). These triterpenes were identified from 42 plant species belonging to 25 families. Several triterpenes were explored against more than one virus, therefore, the total number of entries has been increased to 406 and a network-based correlation between viruses, plant species, and their families are displayed in Fig. 2. This review further highlights their structure–activity relationship (SAR) and the biosynthesis of representative examples.

Its in-fact evident from the current pandemic that despite tremendous advancement in drug discovery and development, the human race is still vulnerable to ever-evolving viral viruses. Therefore, emphasis on lead identification and drug development on a larger scale is required where triterpenes could play a major role.

## Biosynthetic aspects of triterpenes

Plant secondary metabolites are synthesized through complex biosynthetic pathways which are tuned by the presence of relevant enzymes catalyzing the synthesis of a diverse array of derivatives. It is evident that these metabolites are not essential for the survival of plants, however, they may help in combating the stress, and

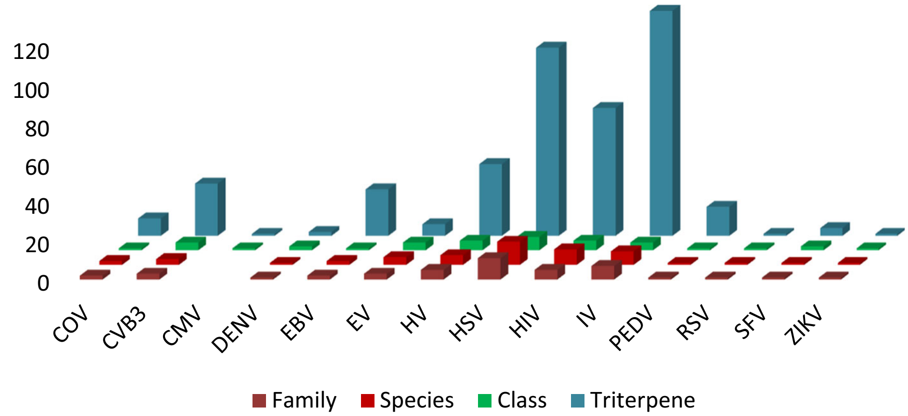


**Fig. 1** Chart displays the number of families, species, sub-classes and triterpenes against studied viruses

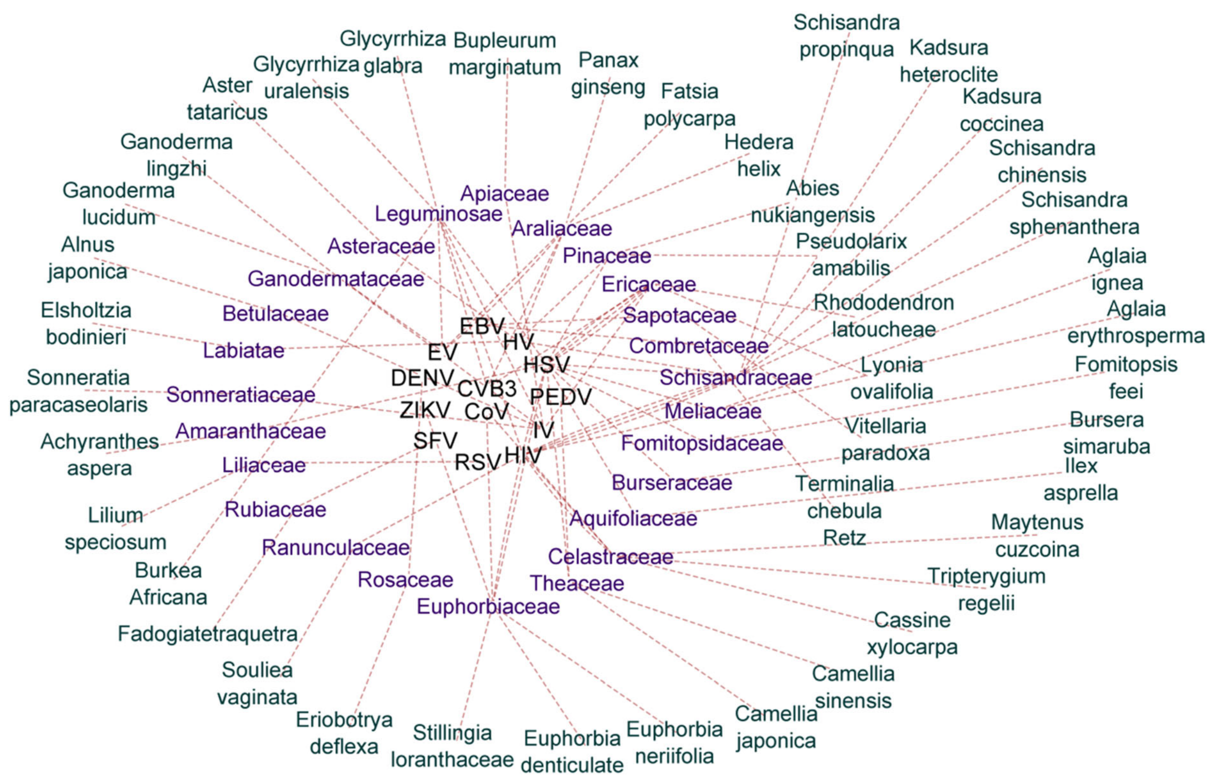


**Fig. 2** Cytoscape network between the plant species, families they belong to, and virus against which they were evaluated. The network shows a total of 42 plant species of 25 different families acting on 13 different viruses. The most prominent point of interest illustrated in the network shows that, out of 25 plant families, 12 have activity against HSV, followed by 6 plant families acting on IV and 5 having efficacy against HV. Network analysis also indicates Leguminosae, Araliaceae, Ericaceae, and Euphorbiaceae being the most interacting plant families acting on more than three viruses. The majority of the plant species that displayed effectiveness against HIV are falling under the Schisandraceae family

pathogenic attack, or may act as a self-defense tool against the herbivorous (Wink 1988; Isah 2019). Also, many secondary metabolites play a significant role in the dissemination of pollens by attracting bees and insects (Glover 2011; Rivest and Forrest 2020). The biosynthesis of a particular class of secondary metabolites is restricted to the plant species belonging to related genus or families, suggesting the presence of genes responsible for the production of relevant enzymes and catalytic systems for the biosynthesis (Xu et al. 2004; Zhou and Pichersky 2020). Among these secondary metabolites, terpene constitutes a major class that is further sub-classified into monoterpene, sesquiterpene, diterpene, sesterterpene, triterpene, and tetraterpenoids.

The triterpenoids are the most widely disseminated class of natural products typically derived from the C30 backbone biosynthesized with rearrangement of six isoprene units following the isoprene rule of Ruzicka (Ruzicka 1953). Triterpenoids with over 100 different carbon skeletons arising out of rearrangements have been reported, among which tetracyclic (C6–C6–C6–C5) and pentacyclic (C6–C6–C6–C6–C6 or C6–C6–C6–C6–C5) are the most abundant (Xu et al. 2004). They continuously find importance due to the enormous pharmacological activities displayed owing to the structural diversity and complexity offered through the protonation, deprotonation, hydroxylation, cyclization, and ring arrangement cascade on the 2,3-oxidosqualene, an indispensable intermediate (Fig. 3). In addition, they may also possess the sugar moieties, either linear or branched to generate mono- bis- or tri-desmosides (Eschenmoser et al. 1955; Morita et al. 2000).

A general scheme for the biosynthesis of terpenes is depicted in Fig. 3 which essentially starts via the mevalonic acid or 2-C-methyl-D-erythritol-4-phosphate (non-mevalonate) pathway to synthesize inositol pyrophosphate (IPP), the primary C-5 unit, which is further converted to GPP (C-10), FPP (C-15), GGPP (C-20) and 2,3-oxidosqualene, a C-30 carbon skeleton (Xu et al. 2004; Hunter 2007; Vranová et al. 2013; Wang et al. 2021). It is now well documented that oxidosqualene cyclases (OSCs) act on 2,3-oxidosqualene to catalyze protosteryl and dammarenyl cation mediated pathways (Xue et al. 2012; Hou et al. 2021). The first pathway mediated through protosteryl cation intermediate leads to the genesis of tetracyclic cycloartenol, lanosterol, and cucrbitadienol, while the second intermediate dammarenyl cation generates both tetracyclic (dammarane) and pentacyclic (lupane, oleanane, and ursane) class of triterpenes. These transformations are mediated via chair/boat/chair and chair/chair/chair conformation, respectively (Xu et al. 2004, 2012; Thimmappa et al. 2014; Hu et al. 2020a; Hou et al. 2021).

Cycloartane triterpenes are widespread among the plants with several new compounds in the series being reported in the past few years and getting attention due to their potential hypo-lipidemic, anti-inflammatory, cytotoxic and anti-viral properties (Xiao et al. 2008; Fang et al. 2019; Shi et al. 2020). It is now evident that a relevant enzyme i.e. cycloartane synthase (CAS), a 2,3-oxidosqualene cyclase (OSC), is required for the biosynthesis of cycloartane skeleton (Haralampidis et al. 2002). Further, it is relevant to highlight that several ring-opened cycloartane derivatives such as 3,4-*seco*-cycloartane, or expended B ring 9,10-*seco*-cycloartane have marked their presence in nature. 3,4-*seco*-triterpenes are common in nature while 9,10-*seco*-triterpenes are rare and biosynthesized through bond modifications. Almeida et al. 2020 reported the genesis of 9,10-*seco*-cycloartane by the activation of cyclopropane methylene (C-25) leading to the cleavage of the C9–C10 bond and thus generating an expanded B-ring with unsaturation (Almeida et al. 2020; Shenvi et al. 2008) and possibly the same pathway is followed by **10–23** (Lv et al. 2016) (Fig. 4).

At the same time, 3,4-*seco*-cycloartanes are proposed to be generated through a photolytic cleavage of 3-oxo bearing cycloartenoids (Norrish I pathway or Baeyer–Villiger oxidation) (Almeida et al. 2020). This is evident from the co-occurrence of 3-oxo bearing cycloartenoids (**105**, **107**, **110**) and 3,4-*seco*-cycloartenoids (**104**, **106**, **108**, **109**) in the seeds of *Pseudolarix amabilis* (Zhao et al. 2020) and **194–196** in the *Kadsura heteroclite* (Xu et al. 2010). Interesting diversifications are also observed through the side chain; such as the formation of spiro lactone, an $\alpha,\beta$-unsaturated-$\gamma$-lactone (**104–106**, **108**, **109**) via intramolecular rearrangements involving C-23 keto and C-25 acid groups (**107**, **110**) (Fig. 4) (Zhao et al. 2020). Transformations of A-ring into lactones is another remarkable modification reported leading to the generation of an unprecedented skeleton 7/6/6/5/6 (**198**) and 7/7/6/5/6 (**199**) wherein, precisely, A-ring is transformed into 7 membered $\alpha,\beta$-unsaturated lactone along with the generation of six-membered $\alpha,\beta$-

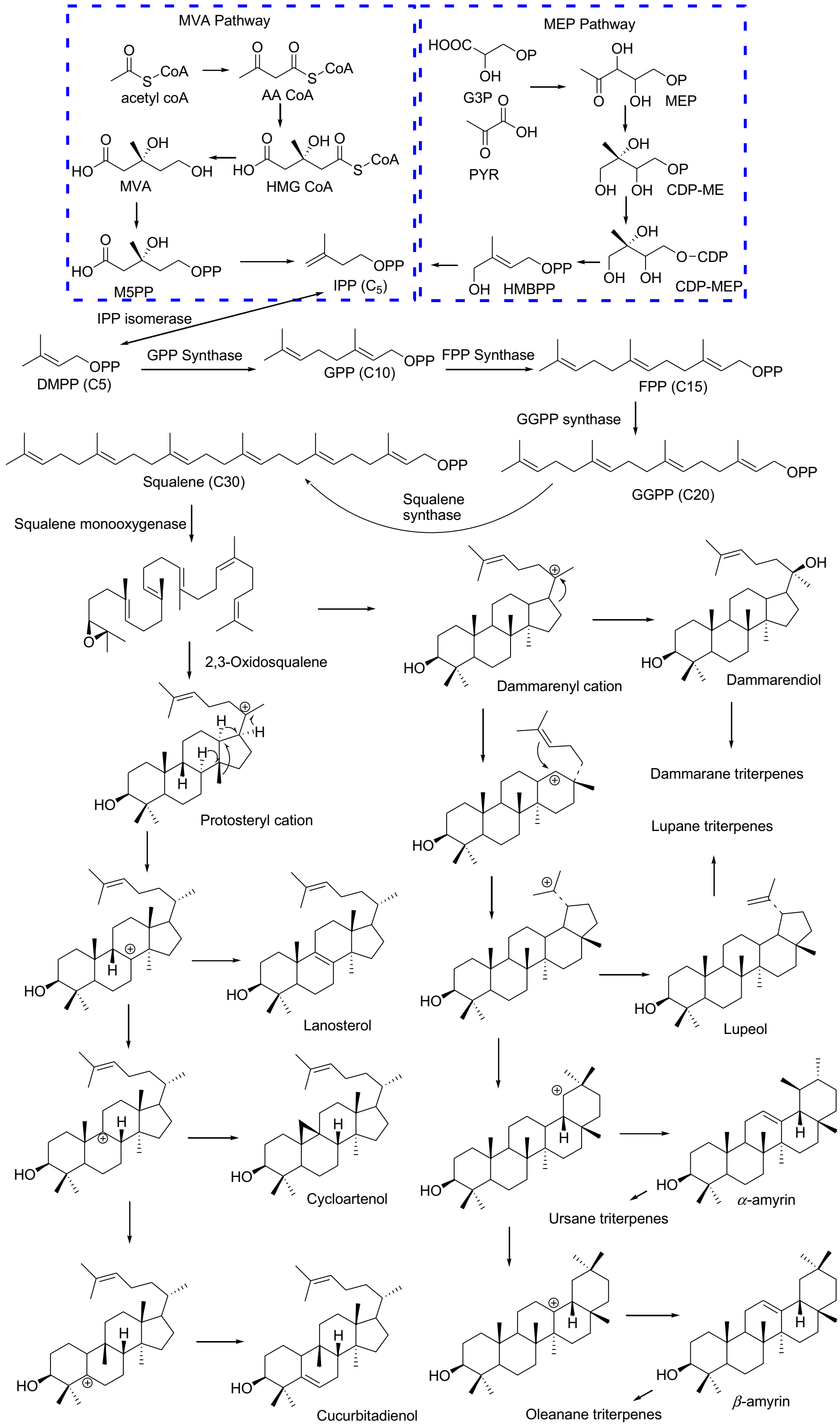


**Fig. 3** General scheme for the biosynthesis of different classes of triterpenes

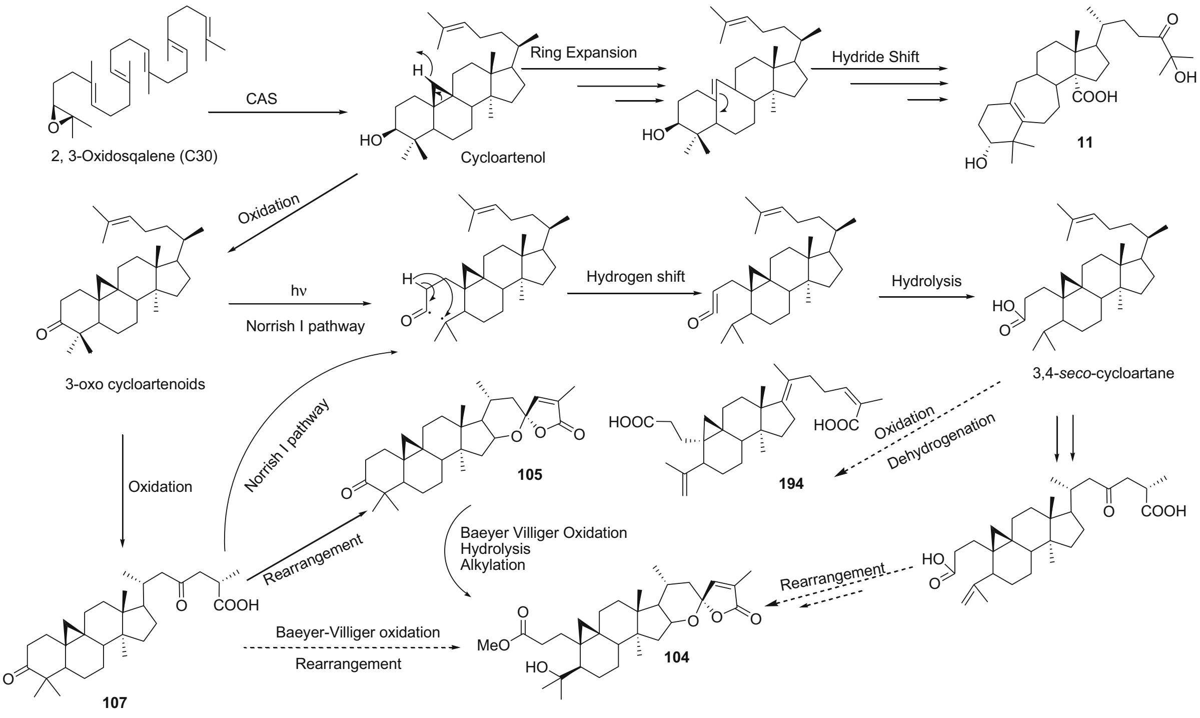


**Fig. 4** Plausible scheme for the biosynthesis of cycloartane derivatives

unsaturated lactone via cyclization of the side chain along with B-ring modifications (Liang et al. 2014).

Another interesting triterpene sub-class, lanostanes, along with cycloartanes are the precursors for the biosynthesis of steroids which are devoid of C-28 and C-29 methyl groups on the parent triterpenes (Sandjo and Kuete 2013). Earlier it was believed that the steroids are synthesized in animals through the cyclization of 2,3-oxidosqualene to lanosterol and via cycloartenol in the plants. Now it is evident that the plants also can synthesize lanosterol via cyclization of 2,3-oxidosqualene catalyzed by functional lanosterol synthase (LAS) (Suzuki et al. 2006; Ohyama et al. 2009). Cycloartanols differ from lanosterols by possessing a characteristic tetra-substituted cyclopropane ring and their co-occurrence has been documented in many plants. The lanosterols are also reported to possess a diverse array of biological activities including anti-cancer, anti-inflammatory, anti-diabetic, and anti-viral (Lyu et al. 2016; Lv et al. 2016; Shehla et al. 2020; Su et al. 2020).

Similar to the cycloartanes, the side chain of the lanostanes also provides scope for structural diversification owing to glycosylation (**28, 30–35**), unsaturation (**64–65**), ring modifications (**118–119, 201–203**), and hydroxylation (**241–270**). Ring-opening rearrangements mediated through relevant enzymes may result in a completely new skeleton, one such modified tricyclic lanosterol (**201**) is reported to possess an 18(13 → 12)-*abeo*-13,17-*seco*-6/6/6-fused tricyclic system generated by cleavage of the bond between C-13 and C-17 i.e. D-ring opening (Liang et al. 2013). Attention-grabbing modifications constructed a tetra substituted cyclopropane bearing 17,18-cyclolanosterol (6/6/6/5/3), along with a butyrolactone moiety generated through the enzymatic cascades on the side chain (**67**, Fig. 5) (Li et al. 2019a).

Cycloartane and lanostane offer similar ring-opening cascades leading to the genesis of *seco*-derivatives, and side-chain modifications. The side chain cyclization leading to the generation of $\alpha,\beta$-unsaturated lactone are reported for both the cycloartane and lanostane class of compounds (**67**, **104–106**, **108**, and **109**) reported from *Abies nukiangensis* and *Pseudolarix amabilis*. This could be attributed to the presence of similar catalytic enzymes owing to the similarity in the genetic makeup, as both these plants

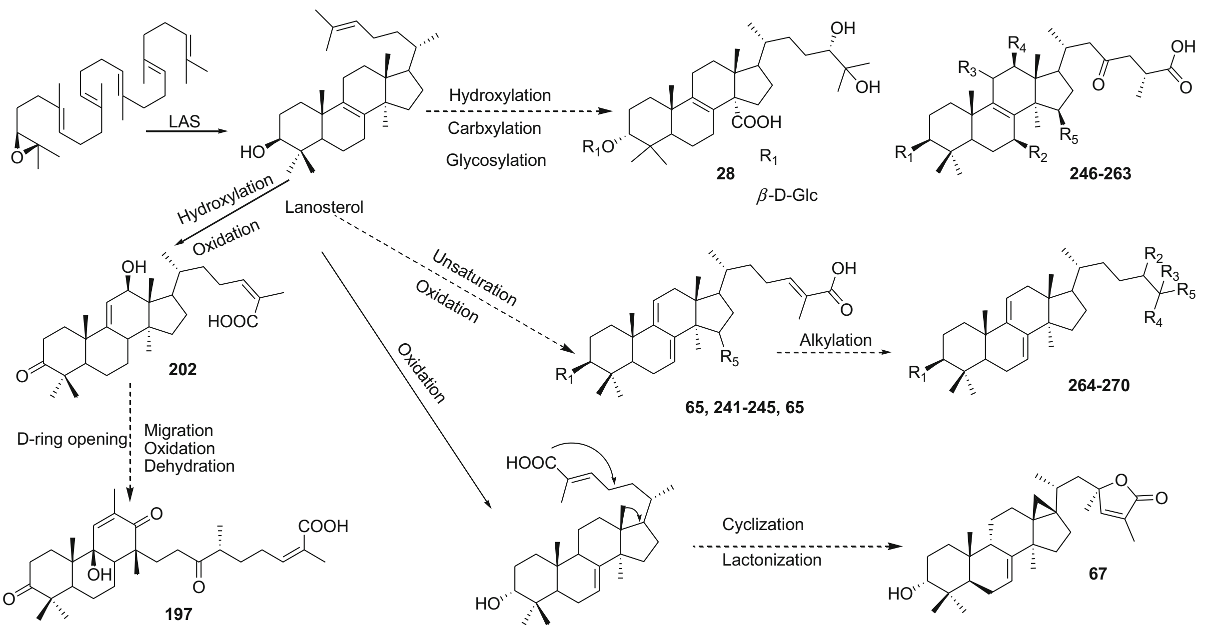


**Fig. 5** Plausible scheme for the biosynthesis of lanostane derivatives

belong to the Pinaceae family (Table 1) (Suzuki and Muranaka 2007; Ohyama et al. 2009; Li et al. 2019a; Zhao et al. 2020).

Dammaranes has marked their presence in many medicinally and traditionally important plants, i.e. *Panax ginseng, Bacopa monnierie*, displaying diverse biological potential, but their contribution as anti-viral agents are surprisingly less. The basic skeleton of dammarane triterpenes consists of a tetracyclic ring system possessing a side chain at C-17 position, which is constructed in plants by cyclization of 2,3-oxidosqualene with the assistance of OSC dammarenediol synthase (DDS) enzymes. Ginsenosides, the most promising anti-viral dammaranes covered in the present article, are synthesized by dammarenediol-II synthase in *Panax ginseng* (Chu et al. 2020; Sawai and Saito 2011) involving three major steps - cyclization, hydroxylation followed by glycosylation (Tansakul et al. 2006; Sawai and Saito 2011) of aglycone protopanax-diol and protopanax-triol (**24–27**). The distinctive diversifications of the ginsenosides are offered through the hydroxylation and glycosylation at C-3, C-6, C-12 positions (**24–27**).

Like cycloartanes and lanostanes, modifications on the side chain of dammaranes generate chemically diverse natural products having butyrolactone (**115**), tetrahydrofuran (**116**), and oxane (**339**) moieties. A-ring opened 3,4-*seco*-dammaranoids (**200**) also marked their presence in concurrence with the side chain modifications (**116**). The A-ring opening could be mediated via Norrish I pathway affording *seco*-dammarane type triterpenoids (**200**), and further intramolecular arrangements and hydroxylation may generate tetrahydrofuran (**116**) or butyrolactone (**115**) moieties (Fig. 6).

Lupanes are another important group of pentacyclic triterpenoids containing 6/6/6/6/5 ring system. Cyclization and rearrangement of 2,3-oxidosqualene through lupeol synthase (LUS) enzyme constructs the basic lupane skeleton. Subsequent deprotonation from one of the methyl groups permits the synthesis of very well-known pentacyclic triterpene lupeol. Oxidation of lupeol at C-28 by cytochrome P450, specifically CYP716A12 enzyme produces another well-known lupane triterpene betulinic acid (**38**) (Fukushima et al. 2011; Hu et al. 2020b). Hydroxylations at C-1, C-3, C-6, C-7, and C-28, carboxylation at C-28, and oxidation of hydroxyl to carbonyl at C-3 are the usual modifications involved in the formation of lupane derivative (**121–132; 206–230**). 2,3-*seco*-lupane triterpene (**127**) is another remarkable modification found in nature; synthesis of which is proposed by Almeida et al. (2020) via oxidation of a 3-hydroxylated lupane skeleton, resulting in 2,3-diketone

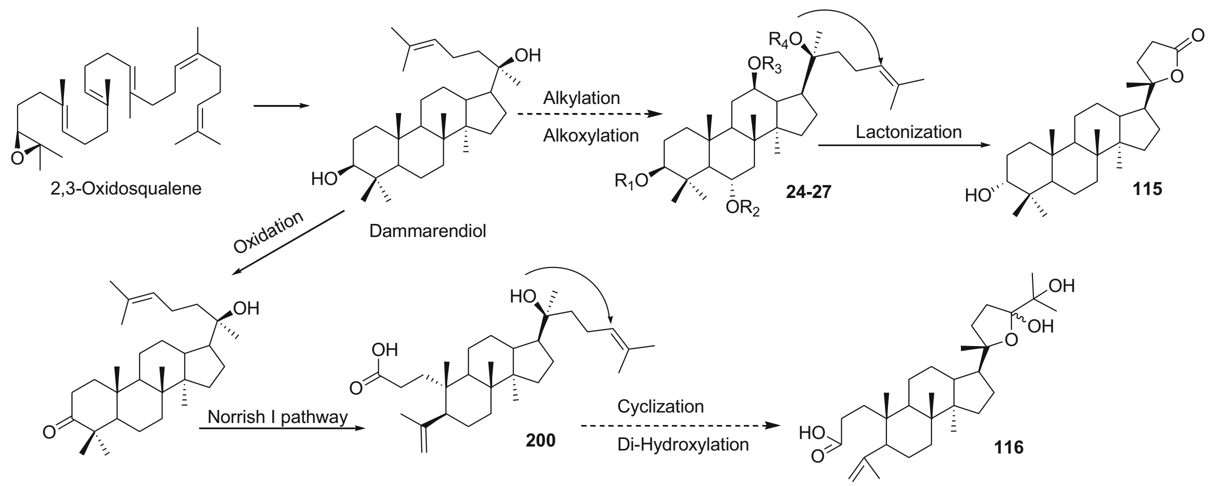


**Fig. 6** Plausible scheme for the biosynthesis of dammarane derivatives

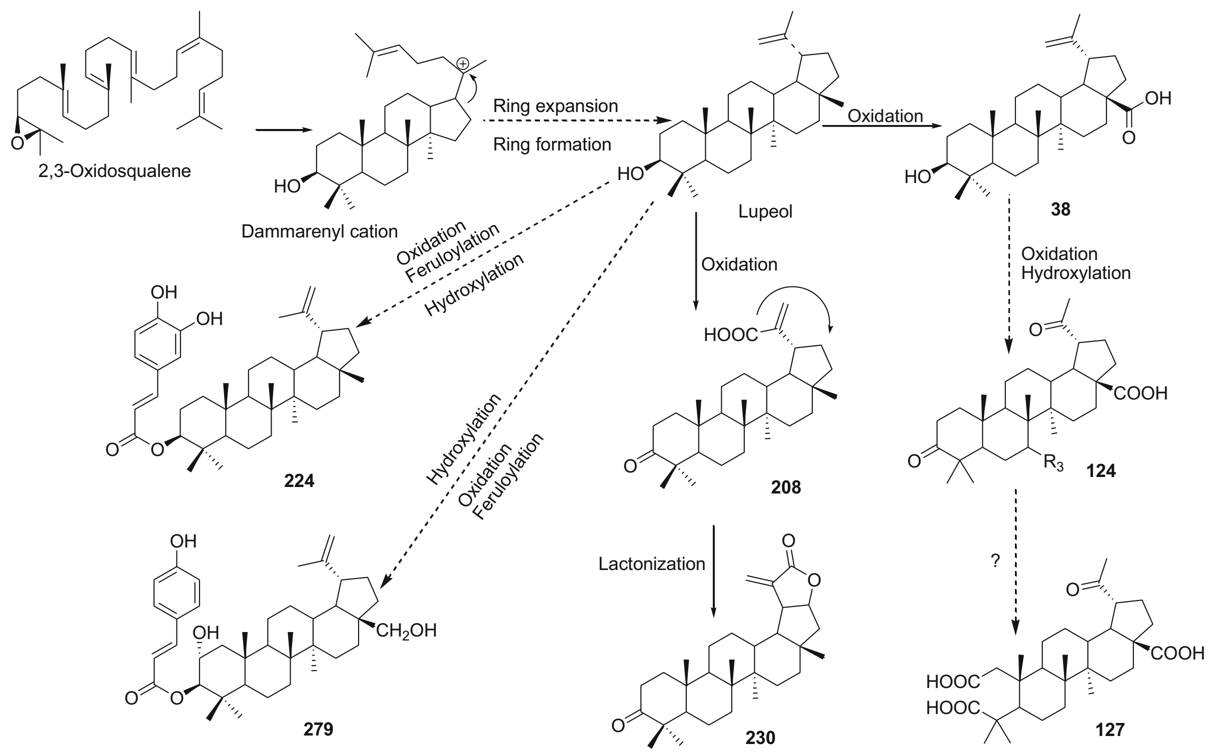


**Fig. 7** Plausible scheme for the biosynthesis of lupane derivatives

followed by Bayer-Villiger oxidation to form an anhydride, which is further hydrolyzed into 2,3-*seco* derivative (Almeida et al. 2020). The introduction of groups like feruloyl at C-3 as observed in **129**, **130**, **132**, **224**, and **279** might be due to the involvement of specific enzyme like feruloyl transferase (Fig. 7).

Dammarenyl cation generated by the action of OSC leads to the formation of lupenyl cation, which in presence of amyrin synthase transform into pentacyclic ring system (6/6/6/6/6), α or β-amyrin. α-Amyrin with the assistance of multi-functional oxidosqualene cyclase (MOSC) form ursane class of

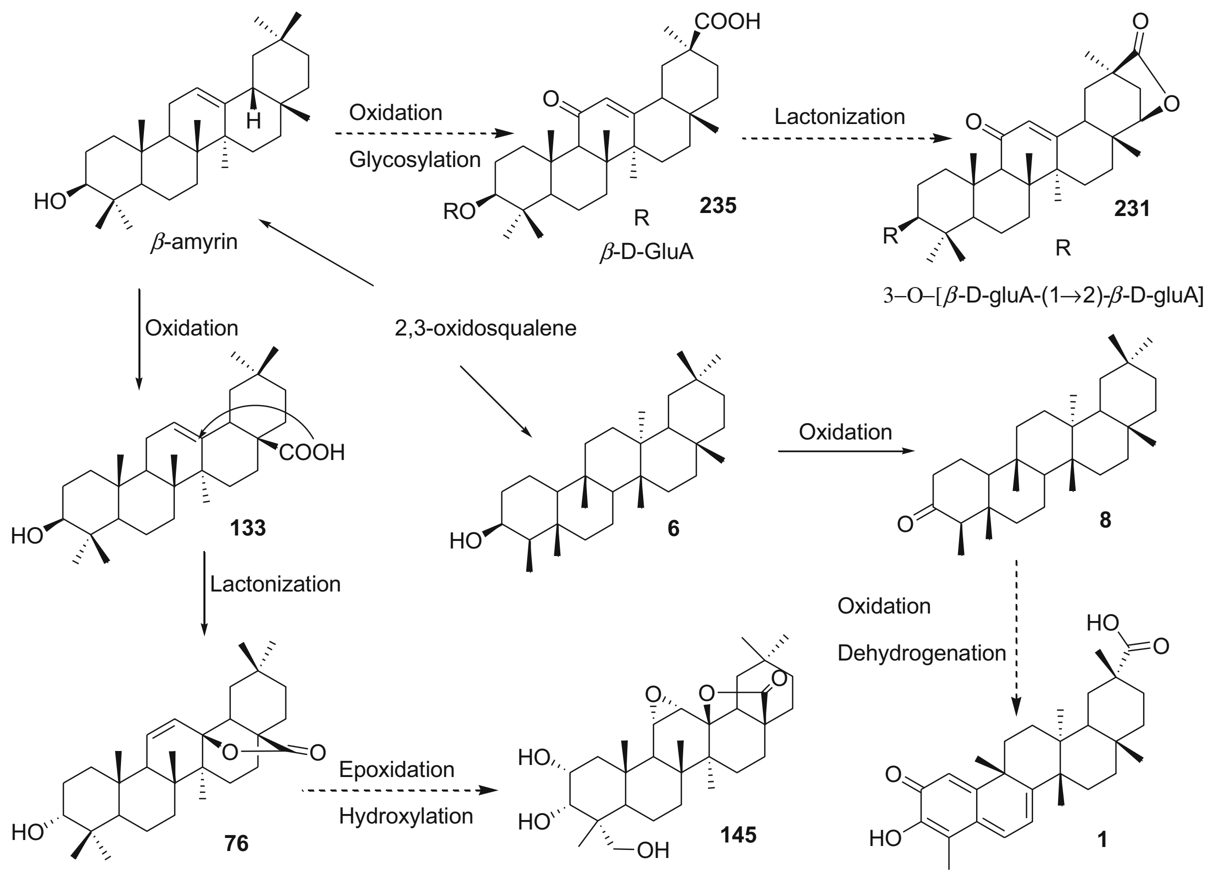


**Fig. 8** Plausible scheme for the biosynthesis of oleanane derivatives

triterpenes and β-amyrin with the action of β-amyrin synthase (BAS) generate widely distributed and most extensively studied class of triterpenes i.e. oleanane (Lu et al. 2018; Stephenson et al. 2019). Further, oxidative reactions on β-amyrin at C-30, and/or C-11 and/or glycosyl transfer reactions form the most popular derivatives like **36**, **133**, and **235**. Hydroxylation reactions are also known to occur at many positions leading to the generation of poly-oxygenated derivatives (**40–43**, **134–138**) but glycosylation reactions occur mostly at C-3 and C-28 positions (**44–57**, **324–328**). Beside these, several other modifications such as C-3=O (**237–240**), C-11=O (**36**, **282–290**, **292–299**), double bond migration (**72**, **236–240**), multiple unsaturation (**61–63**, **68–71**, **75**, **291**) or intramolecular lactonization (**74**, **76**, **145**, **231**) are widespread among oleananes. Other interesting modification of oleanane includes feruloylation (**142**) and epoxidation (C-11–O–C-12) (**145**). Oleanane saponins are found to undergo oxidation to attain ketone at C-3, C-11, and C-16, as evident from **231–240, 335–338** (Fig. 8). These events may be mediated by the involvement of specific enzymes.

Another biologically interesting modification on the A-ring led to the genesis of quinone methide derivatives (**1–4**). The quinone methides in detail have been reported earlier (Rokita 2009; Zhou 2009); biogenesis of quinone methides has been linked with the precursors 3β-friedelanol (**6**) and friedelin (**8**) generated from the oxidosqualene in the *Maytenusa quifolium* and *Salacia campestris* (Corsino et al. 2000). This finding is further supported by a recent study on the *Tripterygium wilfordii* wherein Zhou and co-workers described the biosynthesis of celastrol (**1**) involving TwOSC1 and TwOSC3, the multiproduct friedelin synthases (FRS; Fig. 8) (Zhou et al. 2019).

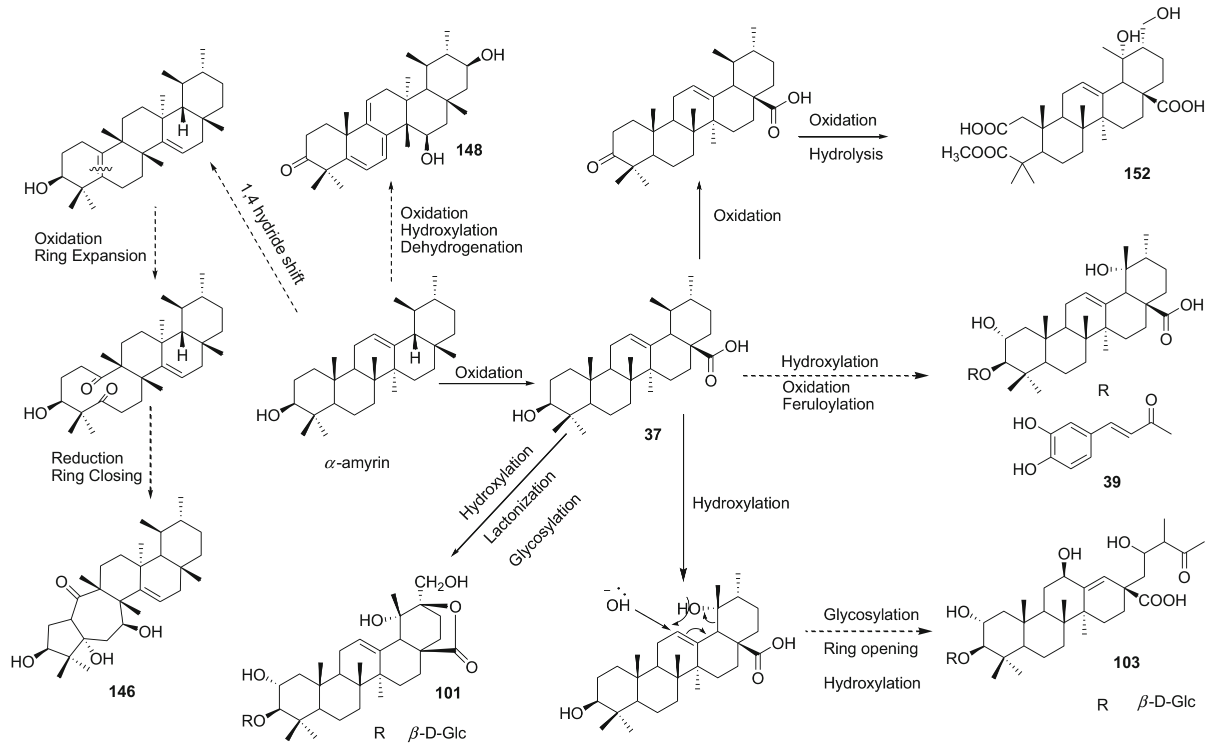


**Fig. 9** Plausible scheme for the biosynthesis of ursane derivatives

This indicates that the friedelin skeleton acts as the key intermediate in the biosynthesis of anti-covid natural products (Corsino et al. 2000; Ryu et al. 2010; Chang et al. 2012).

Oleanane and ursane triterpenoids are mostly found together, as they share similar biosynthetic precursors. The only significant difference in both skeletons occurs at C-19 and C-20 methyl groups of ring E. The most common example of a ursane backbone is ursolic acid (**37**) generated from the α-amyrin. Ursane undergoes similar reactions as oleanane to build its derivatives imparting exclusive bioactivities. The usual reaction like esterification to attain feruloyl moiety at C-3 (**39**, **166–168**), lactonization (**101**), glycosylation at C-3, C-24, or C-18 (**98–103**), and hydroxylation/oxidation on A-E rings are reported in ursane skeleton as well. An 18,19-*seco*-ursane generated by enzymatic or photolytic cleavage of E-ring functionalized with hydroxyl and carbonyl along with migrated double bond (C13/C18) is also observed in nature (**103**). Formation of 2,3-*seco* derivatives like **152** might follow the same pathway as for lupane 2,3-*seco* derivatives (**127**). A series of reactions such as dehydrogenation, oxidative ring-opening, and cyclization are reported to construct an unprecedented 5/7/6/6/6 fused pentacyclic ring system (**146–147**) (Fig. 9) which is unique in this class and a plausible biogenetic pathway is reported in detail earlier (Liu et al. 2017). Apart from these, sulfur-containing triterpenoid saponin (**169**) reported from *Ilex asprella* suggests interesting phylogenetic modification by the involvement of imperative enzymes, which needs exploration to understand the possible diversification of triterpenoids.

Shionones are the rare tetracyclic skeleton (6/6/6/6) bearing triterpenoids with a side chain and a C-3 carbonyl in most of the derivatives. Sawai and coworkers identified a shionone synthase (SHS), evolved from the BAS, responsible for the cyclization of 2,3-oxidosqualene into shionones via dammarenyl, baccharenyl, and an intermediate C-4 cation (Sawai et al. 2011). The shionones are known to exert in the roots and rhizomes of *Aster* species and examples covered in the current study are mostly side-chain derivatives (**83–97**) (Fig. 10).

The last classes of triterpenes covered under the present study are structurally unique skeleton bearing anti-viral nor-triterpenoids reported from the *Schisandra propinqua* var. *propinqua* and *Schisandra chinensis* (Schisandraceae). A couple of review in past has detailed the triterpenoids (cycloartane, lanostane, and norterpenoids) of the Schisandraceae family. These norterpenoids are derived from the cycloartane and can be further sub classified into schisanartane, schiartane, 18-norschiartane, 18(13/14)-*abeo*-schiartane, pre-schisanartane, and wuweiziartane (Xiao et al. 2008; Xia et al. 2015). A hypothetical biosynthetic pathway for the genesis of **77** is displayed in Fig. 11 wherein its biosynthesis is proposed via the generation of 3,4-*seco*- and 9,10-*seco*-cycloartane skeletons followed by rearrangements on the A-ring leading to the generation of fused tetrahydro furan and butyrolactone moieties and then the side chain rearrangements leading to the genesis of **77** with the help of relevant enzymes. A similar pathway may be followed for the biosynthesis of **171** and other related compounds.

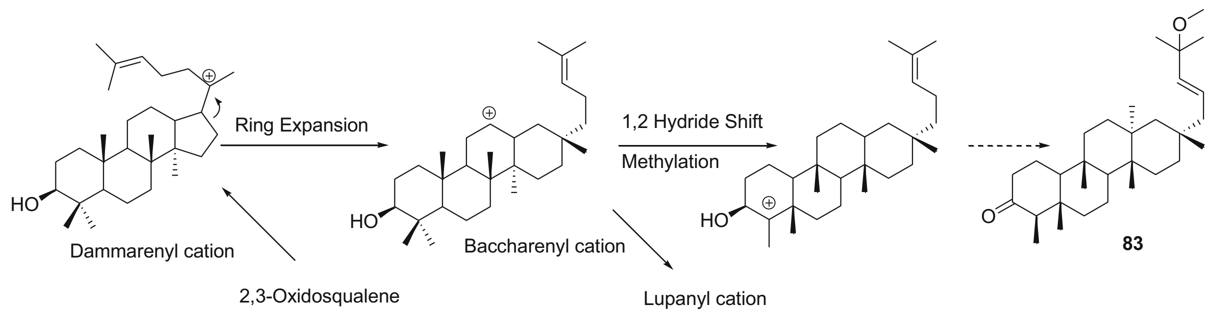


**Fig. 10** Plausible scheme for the biosynthesis of shionone derivatives

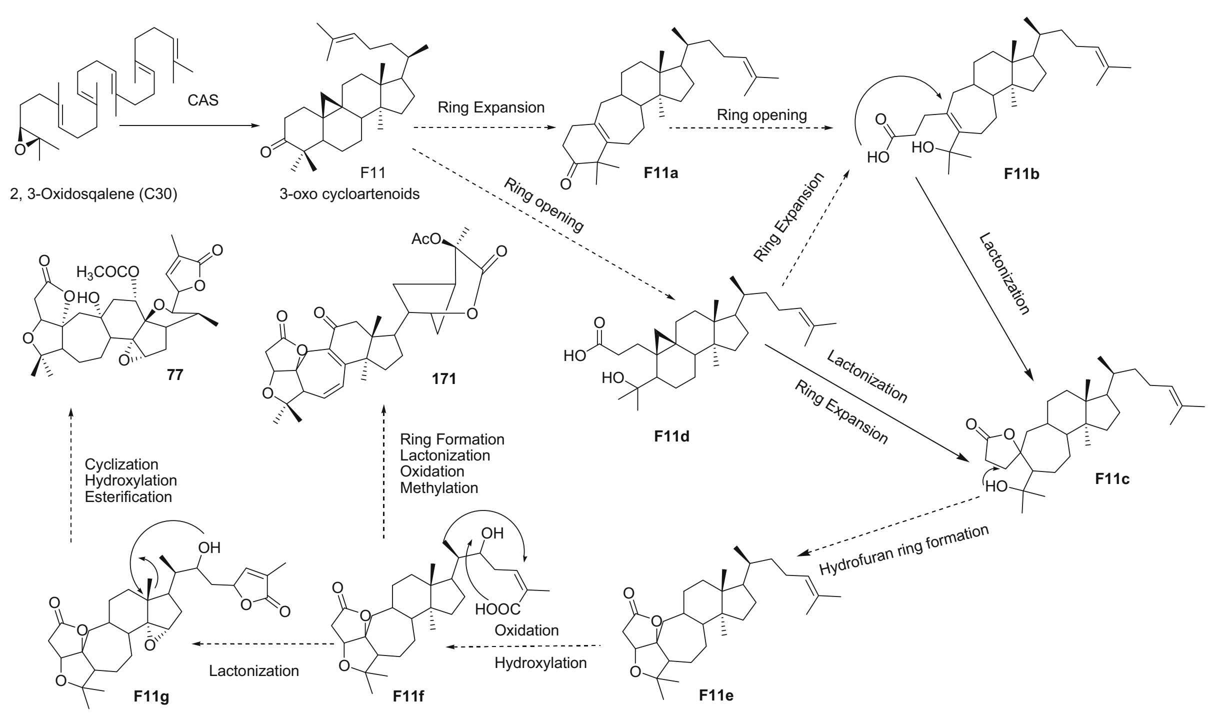


**Fig. 11** Plausible scheme for the biosynthesis of nor-terpene derivatives

**Table 1** Anti-viral triterpenes

| S. no. | Virus | Class | Plant species and family | Compound | $IC_{50}$ or $EC_{50}$ | Cell lines | References |
|---|---|---|---|---|---|---|---|
| 1 | CoV | OT | *Tripterygium regelii* | Celastrol (**1**) | 10.3 ± 0.2 µM | – | Ryu et al. ( 2010) |
| 2 | | | (Celastraceae) | Pristimerin (**2**) | 5.5 ± 0.7 µM | | |
| 3 | | | | Tingenone (**3**) | 9.9 ± 0.1 µM | | |
| 4 | | | | Iguesterin (**4**) | 2.6 ± 0.3 µM | | |
| 5 | | | | Dihydrocelastrol (**5**) | 21.7 ± 1.9 µM | | |
| 6 | | | *Euphorbia neriifolia* | 3*β*-friedelanol (**6**) | – | MRC-5 | Chang et al. (2012) |
| 7 | | | (Euphorbiaceae) | 3*β*-acetoxy friedelane (**7**) | – | | |
| 8 | | | | Friedelin (**8**) | – | | |
| 9 | | | | Epitaraxerol (**9**) | – | | |
| 10 | CVB3 | CAT | *Lyonia ovalifolia* | Lyonifoloside A (**10**) | 11.1 ± 1.98 µM/L | Vero | Lv et al. (2016) |
| 11 | | | (Ericaceae) | Lyonifolic acid A (**11**) | 2.1 ± 0.30 µM/L | | |
| 12 | | | | Lyonifoloside B (**12**) | ≥ 33.3 µM/L | | |
| 13 | | | | Lyofoligenic acid (**13**) | 4.8 ± 1.20 µM/L | | |
| 14 | | | | Lyonifoloside C (**14**) | ≥ 33.3 µM/L | | |
| 15 | | | | Lyonifoloside D (**15**) | ≥ 33.3 µM/L | | |
| 16 | | | | Lyonifoloside E (**16**) | ≥ 33.3 µM/L | | |
| 17 | | | | Lyonifoloside F (**17**) | ≥ 33.3 µM/L | | |
| 18 | | | | Lyonifoloside G (**18**) | ≥ 33.3 µM/L | | |
| 19 | | | | Lyonifolic Acid B (**19**) | ≥ 33.3 µM/L | | |
| 20 | | | | Lyonifoloside H (**20**) | ≥ 33.3 µM/L | | |
| 21 | | | | Lyonifoloside I (**21**) | ≥ 33.3 µM/L | | |
| 22 | | | | Lyonifoloside J (**22**) | ≥ 33.3 µM/L | | |
| 23 | | | | Lyonifoloside K (**23**) | ≥ 33.3 µM/L | | |
| 24 | | DT | *Panax pseudoginseng* | 20(S)-protopanaxtriol (**24**) | 2.74 µg/mL | HeLa | Song et al. (2014a), Wang et al. (2012) |
| 25 | | | (Araliaceae) | Ginsenoside Re (**25**) | – | Vero | |
| 26 | | | | Ginsenoside Rf (**26**) | – | | |
| 27 | | | | Ginsenoside Rg2 (**27**) | – | | |
| 28 | | LAT | *Lyonia ovalifolia* | Lyonifoloside L (**28**) | ≥ 33.3 µM/L | Vero | Lv et al. (2016) |
| 29 | | | (Ericaceae) | Lyonifolic acid C (**29**) | 4.8 ± 1.16 µM/L | | |
| 30 | | | | Lyonifoloside M (**30**) | 11.1 ± 1.17 | | |
| 31 | | | | Lyonifoloside N (**31**) | ≥ 33.3 µM/L | | |
| 32 | | | | Lyonifoloside O (**32**) | ≥ 33.3 µM/L | | |
| 33 | | | | Lyonifoloside P (**33**) | ≥ 33.3 µM/L | | |
| 34 | | | | Lyonifoloside Q (**34**) | ≥ 33.3 µM/L | | |
| 35 | | | | Lyonifoloside R (**35**) | ≥ 33.3 µM/L | | |

**Table 1** continued

| S. no. | Virus | Class | Plant species and family | Compound | $IC_{50}$ or $EC_{50}$ | Cell lines | References |
|---|---|---|---|---|---|---|---|
| 36 | | OT | *Glycyrrhiza uralensis* (Leguminosae) | Glycyrrhizic acid (**36**) | – | Vero | Wang et al. (2013) |
| 37 | CMV | UT | – | Ursolic acid (**37**) | 6.8 µg/mL | GPEL | Zhao et al. (2012) |
| 38 | DENV | LUT | - | Betulinic acid (**38**) | 0.9463 µM | Huh7 | Loe et al. (2020) |
| 39 | | UT | *Eriobotrya deflexa* f. *buisanensis* (Rosaceae) | 3-*O*-trans-caffeoyltormentic acid (**39**) | 12.4 ± 1.1 µM | C6/36 | Chen et al. (2019a) |
| 40 | EBV | OT | *Terminalia chebula* Retz (Combretaceae) | Arjungenin (**40**) | 271 | Raji | Manosroi et al. (2013) |
| 41 | | | | Arjunolic acid (**41**) | 283 | | |
| 42 | | | | Arjunic acid (**42**) | 279 | | |
| 43 | | | | Terminolic acid (**43**) | 269 | | |
| 44 | | | | Arjunglucoside I (**44**) | 346 | | |
| 45 | | | | Arjunglucoside II (**45**) | 363 | | |
| 46 | | | | Arjunetin (**46**) | 359 | | |
| 47 | | | | Chebuloside II (**47**) | 350 | | |
| 48 | | | *Vitellaria paradoxa* (Sapotaceae) | Paradoxoside A (**48**) | 455 | Raji | Zhang et al. (2014a) |
| 49 | | | | Paradoxoside B (**49**) | 456 | | |
| 50 | | | | Tieghemelin A (**50**) | 470 | | |
| 51 | | | | Butyroside D (**51**) | 460 | | |
| 52 | | | | Arginine C (**52**) | 479 | | |
| 53 | | | | 3-*O*-β-D-glucuronopyranosyl 16-α-hydroxyprotobassic acid (**53**) | 348 | | |
| 54 | | | | 3-*O*-β-D-glucopyranosyl 16α-hydroxyprotobassic acid (**54**) | 335 | | |
| 55 | | | | Paradoxoside C (**55**) | 368 | | |
| 56 | | | | Paradoxoside D (**56**) | 410 | | |
| 57 | | | | 3-*O*-β-D-glucuronopyranosyl protobassic acid (**57**) | 360 | | |
| 58 | | | | mi-glycoside I (**58**) | 353 | | |
| 59 | | | | Protobassic acid (**59**) | 330 | | |
| 60 | | | | 16α-hydroxy protobassic acid (**60**) | – | | |
| 61 | | | | Paradoxoside E (**61**) | 380 | | |
| 62 | | | | 3-*O*-β-D-glucopyranosyl bassic acid (**62**) | 371 | | |
| 63 | | | | Bassic acid (**63**) | 339 | | |

**Table 1** continued

| S. no. | Virus | Class | Plant species and family | Compound | $IC_{50}$ or $EC_{50}$ | Cell lines | References |
|---|---|---|---|---|---|---|---|
| 64 | EV | DT | *Panax pseudoginseng* (Araliaceae) | Ginsenoside Rg2 (**27**) | – | Vero | Song et al. (2014a) |
| 65 | | LAT | *Ganoderma lucidum* | Lanosta-7,9(11),24-trien-3-one,15;26-dihydroxy (**64**) | < 100 µg/mL | RD | Zhang et al. (2014b) |
| 66 | | | (Ganodermataceae) | Ganoderic acid Y (**65**) | < 100 µg/mL | | |
| 67 | | OT | *Glycyrrhiza uralensis* (Leguminosae) | Glycyrrhizic acid (**36**) | – | Vero | Wang et al. (2013) |
| 68 | | | *Hedera helix* (Araliaceae) | Hederasaponin B (**66**) | 24.77 ± 12.56 µg/mL<br>41.77 ± 0.76 µg/mL | Vero | Song et al. (2014b) |
| 69 | | UT | – | Ursolic acid (**37**) | – | RD | Zhao et al. (2014) |
| 70 | HV | CLT | *Abies nukiangensis* (Pinaceae) | Abinukitrine A (**67**) | 6.52 µM | GT1b | Li et al. (2019a) |
| 71 | | OT | *Fatsia polycarpa* | Fatsicarpain A (**68**) | 18.9 µM | HepG2 2.2.15 | Cheng et al. (2011) |
| 72 | | | (Araliaceae) | Fatsicarpain B (**69**) | > 50 µM | | |
| 73 | | | | Fatsicarpain C (**70**) | 16.7 µM | | |
| 74 | | | | Fatsicarpain D (**71**) | 28.8 µM | | |
| 75 | | | | Fatsicarpain E (**72**) | > 50 µM | | |
| 76 | | | | Fatsicarpain F (**73**) | 23.9 µM | | |
| 77 | | | | Fatsicarpain G (**74**) | 29.2 µM | | |
| 78 | | | | 3α-hydroxyolean- 11,13(18)-dien-28-oic acid (**75**) | > 50 µM | | |
| 79 | | | | 3α-hydroxyolean- 11-en-28,13β-olide (**76**) | > 50 µM | | |
| 80 | | NT | *Schisandra propinqua* var. *propinqua* | Propindilactone P (**77**) | – | Hep G 2.2.15 | Lei et al. (2010) |
| 81 | | | (Schisandraceae) | Propindilactone Q (**78**) | – | | |
| 82 | | | | Propindilactone R (**79**) | – | | |
| 83 | | | | Propindilactone S (**80**) | – | | |
| 84 | | | | Wuweizidilactone B (**81**) | 0.806 mg/mL | | |
| 85 | | | | Wuweizidilactone H (**82**) | – | | |
| 86 | | SHT | *Aster tataricus* | Shion-22-methoxy-20(21)-en-3-one (**83**) | 0.89 µg/mL | HepG 2.2.15 | Zhou et al. (2010) |
| 87 | | | (Asteraceae) | Shion-22(30)-en- 3,21-dione (**84**) | 4.49 µg/mL | | |
| 88 | | | | Shion-22-methoxy-20(21)-en-3β-ol (**85**) | – | | |
| 89 | | | | Astataricusone A (**86**) | – | | Zhou et al. (2013) |
| 90 | | | | Astataricusone B (**87**) | 2.7 µM | | |
| 91 | | | | Astataricusone C (**88**) | – | | |
| 92 | | | | Astataricusone D (**89**) | – | | |
| 93 | | | | Astataricusol A (**90**) | – | | |
| 94 | | | | Epishionol (**91**) | 30.7 µM | | |

**Table 1** continued

| S. no. | Virus | Class | Plant species and family | Compound | $IC_{50}$ or $EC_{50}$ | Cell lines | References |
|---|---|---|---|---|---|---|---|
| 95 | | | | Astershionone A (**92**) | – | | Zhou et al. (2014) |
| 96 | | | | Astershionone B (**93**) | – | | |
| 97 | | | | Astershionone C (**94**) | 22.4 μM | | |
| 98 | | | | Astershionone D (**95**) | – | | |
| 99 | | | | Astershionone E (**96**) | – | | |
| 100 | | | | Astershionone F (**97**) | – | | |
| 101 | | UT | *Elsholtzia bodinieri* | Bodinioside O (**98**) | 0.41 nM | Huh7.5.1 | Xiang et al. (2019) |
| 102 | | | (Labiatae) | Bodinioside P (**99**) | 1.58 nM | | |
| 103 | | | | Bodinioside M (**100**) | 11.50 nM | | Zhong et al. (2016) |
| 104 | | | | Bodinioside N (**101**) | 13.25 nM | | |
| 105 | | | | Oblonganoside I (**102**) | 160.36 nM | | |
| 106 | | | | Bodinioside A (**103**) | 32.86 nM | | |
| 107 | HSV | CAT | *Pseudolarix amabilis* | Pseudolarnoid A (**104**) | – | Vero | Zhao et al. (2020) |
| 108 | | | (Pinaceae) | Pseudolarnoid C (**105**) | – | | |
| 109 | | | | Pseudolarnoid D (**106**) | – | | |
| 110 | | | | Pseudolarnoid F (**107**) | 15.3 ± 1.9 μM | | |
| 111 | | | | Pseudolarolide C (**108**) | 4.3 ± 0.4 μM | | |
| 112 | | | | Pseudolarolide C acid (**109**) | – | | |
| 113 | | | | 3,23-dioxo-cycloart-24-en-26-oic acid (**110**) | – | | |
| 114 | | | | Pseudolarolide F (**111**) | – | | |
| 115 | | | | Pseudolarolide E (**112**) | – | | |
| 116 | | | | Pseudolarnoid G (**113**) | 1.1 ± 0.2 μM | | |
| 117 | | | *Lyonia ovalifolia* | Lyonifoloside A (**10**) | 11.1 ± 2.31 μM/L | | Lv et al. (2016) |
| 118 | | | (Ericaceae) | Lyonifolic acid A (**11**) | 3.7 ± 1.35 μM/L | | |
| 119 | | | | Lyonifoloside B (**12**) | > 33.3 μM/L | | |
| 120 | | | | Lyofoligenic acid (**13**) | 11.1 ± 1.65 μM/L | | |
| 121 | | | | Lyonifoloside C (**14**) | > 33.3 μM/L | | |
| 122 | | | | Lyonifoloside D (**15**) | > 33.3 μM/L | | |
| 123 | | | | Lyonifoloside E (**16**) | > 33.3 μM/L | | |
| 124 | | | | Lyonifoloside F (**17**) | > 33.3 μM/L | | |
| 125 | | | | Lyonifoloside G (**18**) | > 33.3 μM/L | | |
| 126 | | | | Lyonifolic Acid B (**19**) | > 33.3 μM/L | | |
| 127 | | | | Lyonifoloside H (**20**) | 19.3 ± 3.31 μM/L | | |
| 128 | | | | Lyonifoloside I (**21**) | > 33.3 μM/L | | |
| 129 | | | | Lyonifoloside J (**22**) | > 33.3 μM/L | | |
| 130 | | | | Lyonifoloside K (**23**) | > 33.3 μM/L | | |

**Table 1** continued

| S. no. | Virus | Class | Plant species and family | Compound | $IC_{50}$ or $EC_{50}$ | Cell lines | References |
|---|---|---|---|---|---|---|---|
| 131 | | | *Euphorbia denticulate* (Euphorbiaceae) | Cycloart-23*E*-ene-3$\beta$,25-diol (**114**) | 86.63 ± 0.03 µg/mL | | Shamsabadipour et al. (2013) |
| 132 | | DT | *Aglaia erythrosperma* | Cabraleahydroxylactone (**115**) | 3.20 mg/mL | | Phongmaykin et al. (2011) |
| 133 | | | (Meliaceae) | Aglinin A (**116**) | – | | |
| 134 | | LAT | *Fomitopsis feei* | Fomitopsin D (**117**) | 17 µg/mL | | Isaka et al. (2017) |
| 135 | | | (Fomitopsidaceae) | Fomitopsin E (**118**) | > 50 µg/mL | | |
| 136 | | | | Fomitopsin F (**119**) | > 50 µg/mL | | |
| 137 | | | | Compound (**120**) | > 50 µg/mL | | |
| 138 | | | *Lyonia ovalifolia* | Lyonifoloside L (**28**) | > 33.3 µM/L | | Lv et al. (2016) |
| 139 | | | (Ericaceae) | Lyonifolic acid C (**29**) | 2.1 ± 1.13 µM/L | | |
| 140 | | | | Lyonifoloside M (**30**) | 6.4 ± 3.32 µM/L | | |
| 141 | | | | Lyonifoloside N (**31**) | 23.1 ± 7.23 µM/L | | |
| 142 | | | | Lyonifoloside O (**32**) | > 33.3 µM/L | | |
| 143 | | | | Lyonifoloside P (**33**) | 14.3 ± 2.10 µM/L | | |
| 144 | | | | Lyonifoloside Q (**34**) | > 33.3 µM/L | | |
| 145 | | | | Lyonifoloside R (**35**) | > 33.3 µM/L | | |
| 146 | | LUT | *Bursera simaruba* (Burseraceae) | (3$\beta$,18$\beta$)-lupa-5,20(29)-dien-3-ol (**121**) | 26.0 ± 10.2 µg/mL<br>14.9 ± 1.4 µg/mL | | Álvarez et al. (2015) |
| 147 | | | | (3$\beta$,18$\beta$)-lupa-12,20(29)-dien-3-ol (**122**) | 17.7 ± 1.5 µg/mL<br>9.6 ± 3.6 µg/mL | | |
| 148 | | | | Lup-20(29)-ene-3$\beta$,28-diol (betulin; **123**) | 75.3 ± 6.1 µg/mL<br>110.6 ± 5.9 µg/mL | | |
| 149 | | | *Euphorbia denticulate* (Euphorbiaceae) | Lup-20(29)-ene-3$\beta$,28-diol (betulin; **123**) | 84.37 ± 0.02 µg/mL | | Shamsabadipour et al. (2013) |

**Table 1** continued

| S. no. | Virus | Class | Plant species and family | Compound | $IC_{50}$ or $EC_{50}$ | Cell lines | References |
|---|---|---|---|---|---|---|---|
| 150 | | | *Rhododendron latoucheae* | 7$\beta$-hydroxy-3,20-dioxo-30 norlupane-28-oic acid (**124**) | 25.87 ± 2.2 μM | Vero | Liu et al. (2019) |
| 151 | | | (Ericaceae) | 6$\alpha$-hydroxy-3,20-dioxo-30 norlupane-28-oic acid (**125**) | 20.61 ± 1.8 μM | | |
| 152 | | | | 3-dihydroxy-30-nor-28-lupanoic acid (**126**) | > 33.3 μM | | |
| 153 | | | | 2,3-seco-lup-29-nor-20-oxo-2,3,28-trioic acid (**127**) | > 33.3 μM | | |
| 154 | | | | Alphitolic acid (**128**) | > 33.3 μM | | |
| 155 | | | | 13$\beta$-*O*-cis-ferulyl-2$\alpha$-hydroxy-lup-20(29)-ene-28-oic acid (**129**) | > 33 μM | | |
| 156 | | | | Eucalyptic acid (**130**) | 3.70 ± 0.2 μM | | |
| 157 | | | | 3$\beta$,20-dihydroxy-28-lupanoic acid (**131**) | > 33.3 μM | | |
| 158 | | | | 3$\beta$-*O*-trans-ferulyl-20-hydroxy-lup-28-oic acid (**132**) | 0.71 ± 0.06 μM | | |
| 159 | | OT | *Achyranthes aspera* (Amaranthaceae) | Oleanolic acid (**133**) | 6.8 μg/mL<br>7.8 μg/mL | Vero | Mukherjee et al. (2013) |
| 160 | | | *Glycyrrhiza glabra* (Leguminosae) | Glycyrrhizic acid (**36**) | | Hela | Laconi et al. (2014) |
| 161 | | | *Camellia sinensis* | Chakasapogenin I (**134**) | – | Vero | Yoneda et al. (2018) |
| 162 | | | (Theaceae) | Chakasapogenin II (**135**) | – | | |
| 163 | | | | 21-*O*-tigloyl-28-*O*-acetyl-barringtogenol C (**136**) | – | | |
| 164 | | | | Jegosapogenin (**137**) | – | | |
| 165 | | | | R1-barrigenol (**138**) | – | | |
| 166 | | | *Rhododendron latoucheae* | 6-hydroxy-23-norpristimerin (**139**) | 3.70 ± 0.3 μM | Vero | Liu et al. (2019) |
| 167 | | | (Ericaceae) | 6-hydroxy-pristimerin (**140**) | 8.62 ± 0.5 μM | | |
| 168 | | | | 2$\alpha$,3$\beta$-dihydroxyolean-12-en-28-oic acid (**141**) | > 33.3 μM | | |
| 169 | | | | 3$\beta$-*O*-cis-ferulyl-2$\alpha$-hydroxy-olean-12-ene-28-oic acid (**142**) | > 33.3 μM | | |
| 170 | | | | Eucalyptolic acid (**143**) | 3.70 ± 0.3 μM | | |
| 171 | | | | Ovalifoliogenin (**144**) | > 33.3 μM | | |
| 172 | | | | 2$\alpha$,3$\alpha$,23-trihydroxy-11$\alpha$,12$\alpha$-epoxy-olean-28,13$\beta$-olide (**145**) | > 33.3 μM | | |
| 173 | | UT | *Rhododendron latoucheae* | Rhodoterpenoid A (**146**) | 8.62 μM | | Liu et al. (2017) |
| 174 | | | (Ericaceae) | Rhodoterpenoid B (**147**) | > 33.33 μM | | |
| 175 | | | | Rhodoterpenoid D (**148**) | 6.87 μM | | |

Table 1 continued

| S. no. | Virus | Class | Plant species and family | Compound | $IC_{50}$ or $EC_{50}$ | Cell lines | References |
|---|---|---|---|---|---|---|---|
| 176 | | | *Rhododendron latoucheae* | (3S)-3,23-dihydroxy-12-oxo-ursa-9(11)-ene (**149**) | > 33.3 μM | | Liu et al. (2019) |
| 177 | | | (Ericaceae) | 3β,24-dihydroxy-12-oxo-ursa-9(11)-ene (**150**) | > 33.3 μM | | |
| 178 | | | | 3β-hydroxy-12-oxoursa-9(11)-ene-24-acid (**151**) | > 33.3 μM | | |
| 179 | | | | 19α,30-dihydroxy-2,3-seco-urs-12-ene-2,3,28-trioic acid 3-methyl ester (**152**) | 14.62 ± 1.3 μM | | |
| 180 | | | | 2α,3α,23-trihydroxy-urs12,19-diene-28-oic acid 30-ethyl ether (**153**) | > 33.3 μM | | |
| 181 | | | | 3α,24-dihydroxy-urs-12,19-diene-28-oic acid 30-ethyl ether (**154**) | > 33.3 μM | | |
| 182 | | | | 24,30-dihydroxy-urs-3-oxo-12,19-diene-28-oic acid (**155**) | 33.33 ± 3.1 μM | | |
| 183 | | | | 2α,3α,24-trihydroxy-urs-12,18-diene-28-oic acid (**156**) | 33.33 ± 2.5 μM | | |
| 184 | | | | 2α,3α,23-trihydroxyurs-12,18-dien28-oic acid (**157**) | > 33.3 μM | | |
| 185 | | | | 19α,22α,24-trihydroxy-urs3-oxo-12-ene-28-oic acid (**158**) | > 33.3 μM | | |
| 186 | | | | 7β,30-dihydroxy-urs-3-oxo-12-ene-28-oic acid (**159**) | 33.33 ± 2.8 μM | | |
| 187 | | | | 3β,24-dihydroxy-19-oxo18,19-seco-urs-11,13(18)-diene-28-oic acid (**160**) | > 33.3 μM | | |
| 188 | | | | 18,19-seco,2a,3β -dihydroxy-19-oxo-urs-11,13(18)-diene-28-oic acid (**161**) | > 33.3 μM | | |
| 189 | | | | 2α,3β -dihydroxyurs-12-en-28-oic acid (**162**) | > 33.3 μM | | |
| 190 | | | | 19,23-dihydroxy-3-oxo-urs-12-en-28-oic acid (**163**) | > 33.3 μM | | |
| 191 | | | | Pomolic acid (**164**) | > 33.3 μM | | |
| 192 | | | | 2α,3α,19α,23-tetrahydroxyurs-12-en-28-oic acid (**165**) | > 33.3 μM | | |
| 193 | | | | 3β-*O*-trans-ferulyl-19α-hydroxy-urs-12-ene-28-oic acid (**166**) | 1.23 ± 0.1 μM | | |
| 194 | | | | 3β-*O*-trans-ferulyl-2α-hydroxy-urs-l2-ene-28-oic acid (**167**) | 2.87 ± 0.2 μM | | |
| 195 | | | | 3β-*O*-cis-ferulyl-19α-hydroxy-urs-12-ene-28-oic acid (**168**) | > 33.3 μM | | |
| 196 | | | *Ilex asprella* | Asprellanoside A (**169**) | 0.14 mM | Vero | Zhou et al. (2012) |
| 197 | | | (Aquifoliaceae) | Oblonganoside H (**170**) | 0.18 mM | | |
| 198 | | NT | *Schisandra chinensis* | Schinchinenin A (**171**) | 0.94 μg/mL | Vero | Song et al. (2013) |
| 199 | | | (Schisandraceae) | Schinchinenin B (**172**) | 0.94 μg/mL | | |
| 200 | | | | Schinchinenin G (**173**) | 0.47 μg/mL | | |
| 201 | | | | Henrischinin A (**174**) | 0.24 μg/mL | | |
| 202 | | | | Henrischinin B (**175**) | 0.24 μg/mL | | |
| 203 | | | | Henrischinin C (**176**) | 0.24 μg/mL | | |

**Table 1** continued

| S. no. | Virus | Class | Plant species and family | Compound | $IC_{50}$ or $EC_{50}$ | Cell lines | References |
|---|---|---|---|---|---|---|---|
| 204 | HIV | CAT | *Souliea vaginata* | Beesioside I (**177**) | 2.32 ± 0.46 μM | MT-4 | Wu et al. (2019) |
| 205 | | | (Ranunculaceae) | Beesioside K (**178**) | 4.65 ± 1.15 μM | | |
| 206 | | | | Soulieoside M (**179**) | – | | |
| 207 | | | | Beesioside M (**180**) | 4.85 ± 1.40 μM | | |
| 208 | | | | Soulieoside N (**181**) | – | | |
| 209 | | | | Soulieoside R (**182**) | > 10 μM | | |
| 210 | | | | Soulieoside Q (**183**) | > 10 μM | | |
| 211 | | | | Beesioside O (**184**) | > 10 μM | | |
| 212 | | | | (20S,24S)-15α-acetoxy-16β,24; 20,24-diepoxy-3β-(β-D-xylopyranosyloxy)-9,19-cyclolanostane-18,25-diol (**185**) | – | | |
| 213 | | | | Soulieoside S (**186**) | 3.76 ± 1.4 μM | | |
| 214 | | | | Soulieoside O (**187**) | > 10 μM | | |
| 215 | | | | Soulieoside P (**188**) | > 30 μM | | |
| 216 | | | *Kadsura heteroclite* | Kadheterilactone A (**189**) | > 10 μg/mL | – | Xu et al. (2010) |
| 217 | | | (Schisandraceae) | Kadheterilactone B (**190**) | > 10 μg/mL | | |
| 218 | | | *Schisandra sphenanthera* | Longipedlactone H (**191**) | > 10 μg/mL | | |
| 219 | | | (Schisandraceae) | Longipedlactone A (**192**) | > 10 μg/mL | | |
| 220 | | | | Longipedlactone F (**193**) | > 10 μg/mL | | |
| 221 | | | | Kadsuranic acid A (**194**) | < 10 μg/mL | | |
| 222 | | | | Nigranoic acid (**195**) | < 10 μg/mL | | |
| 223 | | | | Schisandronic acid (**196**) | < 10 μg/mL | | |
| 224 | | | *Schisandra sphenanthera* | Nigranoic acid (**195**) | 28.97 μg/mL | C8166 | Liang et al. (2014) |
| 225 | | | (Schisandraceae) | Lancifoic acid A (**197**) | 0.52 μg/mL | | |
| 226 | | | | Schisphendilactone A (**198**) | 8.79 μg/mL | C8166 | Liang et al. (2014) |
| 227 | | | | Schisphendilactone B (**199**) | 1.09 μg/mL | | |
| 228 | | DT | *Aglaia ignea* (Meliaceae) | Dammarenolic acid (**200**) | 0.48 μg/mL | HeLa | Esimone et al. (2010) |
| 229 | | LAT | *Kadsura coccinea* | Kadcotrione A (**201**) | 30.29 μM | C8166 | Liang et al. (2013) |
| 230 | | | (Schisandraceae) | Kadcotrione B (**202**) | – | | |
| 231 | | | | Kadcotrione C (**203**) | – | | |
| 232 | | | | 12-β-hydroxycoccinic acid (**204**) | 54.81 μM | | |
| 233 | | | *Schisandra sphenanthera* (Schisandraceae) | Kadsuric acid (**205**) | 8.23 μg/mL | C8166 | Liang et al. (2014) |

**Table 1** continued

| S. no. | Virus | Class | Plant species and family | Compound | $IC_{50}$ or $EC_{50}$ | Cell lines | References |
|---|---|---|---|---|---|---|---|
| 234 | | LUT | *Cassine xylocarpa* | 6β,30-dihydroxylup-20(29)-en-3-one (**206**) | 9.5 ± 2.6 μM | MT-2 | Callies et al. (2015) |
| 235 | | | *Maytenus cuzcoina* | 6β-hydroxy-3-oxolup-20(29)-en-30-al (**207**) | 7.9 ± 2.6 μM | | |
| 236 | | | (Celastraceae) | 3-oxolup-20(29)-en-30-oic acid (**208**) | – | | |
| 237 | | | | 3β,6β,20-trihydroxylupane (**209**) | – | | |
| 238 | | | | 1β,3α,28-trihydroxylup-20(29)-ene (**210**) | – | | |
| 239 | | | | 11α,28- dihydroxylup-20(29)-en-3-one (**211**) | – | | |
| 240 | | | | 3-oxolup-20(29)-en-30-al (**212**) | 1.4 ± 0.2 μM | | |
| 241 | | | | 3-oxo-30-hydroxylupane (**213**) | – | | |
| 242 | | | | Lupenone (**214**) | – | | |
| 243 | | | | 6β,20-dihydroxylupan-3-one (**215**) | 7.0 ± 3.3 μM | | |
| 244 | | | | Glochidiol (**216**) | 13.9 ± 3.2 μM | | |
| 245 | | | | Betulone (**217**) | 4.1 ± 1.8 μM | | |
| 246 | | | | Rigidenol (**218**) | – | | |
| 247 | | | | Glochidone (**219**) | – | | |
| 248 | | | | 11α-hydroxyglochidone (**220**) | 8.7 ± 1.9 μM | | |
| 249 | | | | Lupeol (**221**) | – | | |
| 250 | | | | 25-hydroxylupeol (**222**) | 6.9 ± 1.9 μM | | |
| 251 | | | | 3β,30-dihydroxylupane (**223**) | – | | |
| 252 | | | | Lupan-3β-caffeate (**224**) | – | | |
| 253 | | | | Betulin-3β-caffeate (**225**) | – | | |
| 254 | | | | 3-*epi*-nepeticin (**226**) | – | | |
| 255 | | | | Nepeticin (**227**) | 0.4 ± 5.0 μM | | |
| 256 | | | | 3-*epi*-betulin (**228**) | 8.8 ± 0.5 μM | | |
| 257 | | | | Betulin (**123**) | – | | |
| 258 | | | | 3-epiglochidiol (**229**) | – | | |
| 259 | | | | Ochraceolide A (**230**) | 39.0 ± 2.8 μM | | |
| 260 | | OT | *Glycyrrhiza uralensis* | Licorice saponin E2 (**231**) | 87.1 μM | 293 T | Song et al. (2014c) |
| 261 | | | (Leguminosae) | Licorice saponin B2 (**232**) | 83.2 μM | | |
| 262 | | | | Araboglycyrrhizin (**233**) | 85.1 μM | | |
| 263 | | | | 22β-acetoxyglycyrrhizin (**234**) | 29.5 μM | | |
| 264 | | | | 3-*O*-β-D-glucuronopyranosyl glycyrrhetinic acid (**235**) | 41.7 μM | | |
| 265 | | | *Cassine xylocarpa* | 3β,29-dihydroxy-olean-18-ene (**236**) | 10.38 μM | MT2 | Osorio et al. (2012) |
| 266 | | | (Celastraceae) | 6β,29-dihydroxy-3-oxo-olean-18-ene (**237**) | 65.58 μM | | |
| 267 | | | | 6β-hydroxy-3-oxo-olean-18-ene (**238**) | 23.8 μM | | |
| 268 | | | | 21α-hydroxy-3-oxo-olean-18-ene (**239**) | – | | |
| 269 | | | | 3,21-dioxo-olean-18-ene (**240**) | 4.038 μM | | |

**Table 1** continued

| S. no. | Virus | Class | Plant species and family | Compound | $IC_{50}$ or $EC_{50}$ | Cell lines | References |
|---|---|---|---|---|---|---|---|
| 270 | IV | CAT | *Lyonia ovalifolia* | Lyonifoloside A (**10**) | > 11.1 µM/L | MDCK | Lv et al. (2016) |
| 271 | | | (Ericaceae) | Lyonifolic acid A (**11**) | 2.1 ± 0.56 µM/L | | |
| 272 | | | | Lyonifoloside B (**12**) | 33.3 ± 2.97 µM/L | | |
| 273 | | | | Lyofoligenic acid (**13**) | 4.8 ± 3.16 µM/L | | |
| 274 | | | | Lyonifoloside C (**14**) | > 11.1 µM/L | | |
| 275 | | | | Lyonifoloside D (**15**) | > 33.3 µM/L | | |
| 276 | | | | Lyonifoloside E (**16**) | > 33.3 µM/L | | |
| 277 | | | | Lyonifoloside F (**17**) | > 33.3 µM/L | | |
| 278 | | | | Lyonifoloside G (**18**) | > 33.3 µM/L | | |
| 279 | | | | Lyonifolic acid B (**19**) | 25.9 ± 4.77 µM/L | | |
| 280 | | | | Lyonifoloside H (**20**) | > 33.3 µM/L | | |
| 281 | | | | Lyonifoloside I (**21**) | > 33.3 µM/L | | |
| 282 | | | | Lyonifoloside J (**22**) | 33.3 ± 6.69 µM/L | | |
| 283 | | | | Lyonifoloside K (**23**) | > 33.3 µM/L | | |
| 284 | | LAT | | Lyonifoloside L (**28**) | > 33.3 µM/L | | |
| 285 | | | | Lyonifolic acid C (**29**) | 3.7 ± 1.08 µM/L | | |
| 286 | | | | Lyonifoloside M (**30**) | 11.1 ± 3.29 µM/L | | |
| 287 | | | | Lyonifoloside N (**31**) | > 33.3 µM/L | | |
| 288 | | | | Lyonifoloside O (**32**) | > 33.3 µM/L | | |
| 289 | | | | Lyonifoloside P (**33**) | 33.3 ± 6.31 µM/L | | |
| 290 | | | | Lyonifoloside Q (**34**) | > 33.3 µM/L | | |
| 291 | | | | Lyonifoloside R (**35**) | > 33.3 µM/L | | |

**Table 1** continued

| S. no. | Virus | Class | Plant species and family | Compound | $IC_{50}$ or $EC_{50}$ | Cell lines | References |
|---|---|---|---|---|---|---|---|
| 292 | | | *Ganoderma lingzhi* | Ganoderic acid T-Q (**241**) | 1.2 ± 1.0 µM | – | Zhu et al. (2015) |
| 293 | | | (Ganodermataceae) | Ganoderic acid TR (**242**) | 10.9 ± 6.4 µM | | |
| 294 | | | | Ganoderic acid T-N (**243**) | 2.7 ± 0.4 µM | | |
| 295 | | | | Ganoderic acid Sz (**244**) | > 200 µM | | |
| 296 | | | | Ganoderic acid S (**245**) | > 200 µM | | |
| 297 | | | | Ganoderic acid Y (**65**) | > 200 µM | | |
| 298 | | | | Ganoderic acid A (**246**) | > 200 µM | | |
| 299 | | | | Ganoderenic acid A (**247**) | > 200 µM | | |
| 300 | | | | Ganoderic acid C2 (**248**) | > 200 µM | | |
| 301 | | | | Ganoderic acid AM1 (**249**) | 135.3 ± 24.6 µM | | |
| 302 | | | | Ganoderic acid K (**250**) | 173.0 ± 5.2 µM | | |
| 303 | | | | Ganoderenic acid H (**251**) | 28.0 ± 10.9 µM | | |
| 304 | | | | Ganoderic acid H (**252**) | 143.9 ± 46.3 µM | | |
| 305 | | | | Ganoderic acid B (**253**) | > 200 µM | | |
| 306 | | | | Ganoderenic acid F (**254**) | 142.6 ± 43.1 µM | | |
| 307 | | | | Ganoderenic acid C (**255**) | > 200 µM | | |
| 308 | | | | Ganoderenic acid D (**256**) | 123.4 ± 22.5 µM | | |
| 309 | | | | Ganoderic acid C6 (**257**) | > 200 µM | | |
| 310 | | | | Ganoderic acid C1 (**258**) | > 200 µM | | |
| 311 | | | | Ganoderic acid DM (**259**) | > 200 µM | | |
| 312 | | | | Ganolucidic acid A (**260**) | > 200 µM | | |
| 313 | | | | Ganoderic acid Zeta (**261**) | > 200 µM | | |
| 314 | | | | Ganoderic acid LM2 (**262**) | 130.0 ± 25.5 µM | | |
| 315 | | | | Ganoderic acid F (**263**) | > 200 µM | | |
| 316 | | | | Ganoderol A (**264**) | 60.3 ± 13.7 µM | | |
| 317 | | | | Ganoderol B (**265**) | 35.5 ± 11 µM | | |
| 318 | | | | Ganoderiol F (**266**) | > 200 µM | | |
| 319 | | | | Ganodermanondiol (**267**) | 2.7 ± 0.6 µM | | |
| 320 | | | | Ganodermanontriol (**268**) | > 200 µM | | |
| 321 | | | | Lucialdehyde A (**269**) | 164.3 ± 18.0 µM | | |
| 322 | | | | Lucialdehyde B (**270**) | 1.8 ± 1.6 µM | | |

**Table 1** continued

| S. no. | Virus | Class | Plant species and family | Compound | $IC_{50}$ or $EC_{50}$ | Cell lines | References |
|---|---|---|---|---|---|---|---|
| 323 | | LUT | *Alnus japonica* (Betulaceae) | Betulinic aldehyde (**271**) | 12.5 µg/ML | – | Tung et al. (2010) |
| 324 | | | *Burkea Africana* | 3-*O*-*β*-D-xylopyranosyl-(1 → 2)-*β*-D-glucopyranosylalphitolic acid (**272**) | 38.6 ± 15.7 µM | MDCK | Mair et al. (2018) |
| 325 | | | (Leguminosae) | 3-*O*-*β*-D-xylopyranosyl-(1 → 2)-[α-L-rhamnopyranosyl-(1 → 4)]-*β*-D-glucopyranosylalphitolic acid (**273**) | 1.9 ± 0.08 µM | | |
| 326 | | | | 3-*O*-*β*-D-xylopyranosyl-(1 → 2)-*β*-D-glucopyranosyl-27-hydroxyalphitolic acid (**274**) | – | | |
| 327 | | | | 3-*O*-*β*-D-glucopyranosyl-(1 → 2)-*β*-D-glucopyranosyl-27-hydroxyalphitolicacid (**275**) | 43.0 ± 11.8 µM | | |
| 328 | | | *Sonneratia paracaseolaris* | Paracaseolin A (**276**) | 28.4 µg/mL | MDCK | Gong et al. (2017) |
| 329 | | | (Sonneratiaceae) | Paracaseolin B (**277**) | – | | |
| 330 | | | | Paracaseolin C (**278**) | – | | |
| 331 | | | | Paracaseolin D (**279**) | – | | |
| 332 | | | | Lupeol (**221**) | – | | |
| 333 | | | | Betulin (**123**) | – | | |
| 334 | | | | Betulinic acid (**38**) | – | | |
| 335 | | | | Alphitolic acid (**128**) | – | | |
| 336 | | | | 3*β*-*O*-cis-*p*-coumaroylalphitolic acid (**280**) | – | | |
| 337 | | | | 3*β*-*O*-trans-*p*-coumaroyl betulinic acid (**281**) | – | | |

**Table 1** continued

| S. no. | Virus | Class | Plant species and family | Compound | $IC_{50}$ or $EC_{50}$ | Cell lines | References |
|---|---|---|---|---|---|---|---|
| 338 | | OT | *Glycyrrhiza uralensis* | Glycyrrhizic acid (**36**) | 158.0 µM | MDCK | Song et al. (2014c) |
| 339 | | | (Leguminosae) | Licorice saponin E2 (**231**) | – | | |
| 340 | | | | Licorice saponin B2 (**232**) | – | | |
| 341 | | | | Araboglycyrrhizin (**233**) | – | | |
| 342 | | | | 22*β*-acetoxyglycyrrhizin (**234**) | 49.1 µM | | |
| 343 | | | | 3-*O*-*β*-D-glucuronopyranosyl glycyrrhetinic acid (**235**) | – | | |
| 344 | | | | Uralsaponin M (**282**) | 48.0 µM | | |
| 345 | | | | Uralsaponin N (**283**) | – | | |
| 346 | | | | Uralsaponin O (**284**) | – | | |
| 347 | | | | Uralsaponin P (**285**) | – | | |
| 348 | | | | Uralsaponin Q (**286**) | – | | |
| 349 | | | | Uralsaponin R (**287**) | – | | |
| 350 | | | | Uralsaponin S (**288**) | 42.7 µM | | |
| 351 | | | | Uralsaponin T (**289**) | 39.6 µM | | |
| 352 | | | | Uralsaponin U (**290**) | – | | |
| 353 | | | | Uralsaponin V (**291**) | – | | |
| 354 | | | | Ualsaponin W (**292**) | – | | |
| 355 | | | | Uralsaponin X (**293**) | – | | |
| 356 | | | | Uralsaponin Y (**294**) | – | | |
| 357 | | | | Uralsaponin C (**295**) | – | | |
| 358 | | | | Uralsaponin F (**296**) | – | | |
| 359 | | | | Licorice saponin A3 (**297**) | – | | |
| 360 | | | | Licorice saponin G2 (**298**) | – | | |
| 361 | | | | Licorice saponin H2 (**299**) | – | | |
| 362 | | | | Licorice saponin B (**300**) | – | | |
| 363 | | | | Licorice saponin J2 (**301**) | – | | |
| 364 | | | | 22*β*-acetoxyglycyrrhetaldehyde (**302**) | – | | |
| 365 | | | | 3*β*-*O*-[*β*-D-glucuronopyranosyl-(1 → 2)-*β*-D-glucuronopyranosyl]olean-9,12-dien-30-oic-acid (**303**) | – | | |
| 366 | | | *Burkea africana* (Leguminosae) | 3-*O*-*β*-D-xylopyranosyl-(1 → 2)-[α-L-rhamnopyranosyl-(1 → 4)]-*β*-D-glucopyranosylmaslinic acid (**304**) | 1.7 ± 0.07 µM | MDCK | Mair et al. (2018) |
| 367 | | | | 3-*O*-*β*-D-xylopyranosyl-(1 → 2)-[α-L-rhamnopyranosyl-(1 → 4)]-*β*-D-glucopyranosyl-21-cinnamoyloxymaslinic acid (**305**) | 1.8 ± 0.23 µM | | |
| 368 | | | | 3-*O*-α-L-rhamnopyranosyl-(1 → 2)-*β*-D-xylopyranosyl-(1 → 2)-*β*-D-xylopyranosyl-21-cinnamoyloxyolean-olic acid (**306**) | 0.05 ± 0.02 µM | | |
| 369 | | | | 3-*O*-α-L-rhamnopyranosyl-(1 → 2)-*β*-D-xylopyranosyl-(1 → 2)-[α-L-rhamnopyranosyl-(1 → 4)]-*β*-D-xylopyranosyl-21-cinnamoyloxy oleanolic acid (**307**) | 0.17 ± 0.18 µM | | |
| 370 | | | | 21-cinnamoyloxy-maslinic acid (**308**) | 11.3 ± 7.35 µM | | |
| 371 | | | | 21-cinnamoyloxy-oleanolic acid (**309**) | 8.9 ± 3.95 µM | | |

**Table 1** continued

| S. no. | Virus | Class | Plant species and family | Compound | $IC_{50}$ or $EC_{50}$ | Cell lines | References |
|---|---|---|---|---|---|---|---|
| 372 | | | *Bupleurum marginatum* var. stenophyllum | 6″-*O*-crotonyl-saikosaponin a (**310**) | 8.92 ± 0.87 µM | 293 T-Gluc | Fang et al. (2017) |
| 373 | | | (Apiaceae) | Tibesaikosaponin I (**311**) | > 20 µM | | |
| 374 | | | | Tibesaikosaponin II (**312**) | > 20 µM | | |
| 375 | | | | Tibesaikosaponin III (**313**) | 21.77 ± 0.75 µM | | |
| 376 | | | | Tibesaikosaponin IV (**314**) | > 20 µM | | |
| 377 | | | | Saikosaponin e (**315**) | 2.14 ± 0.72 µM | | |
| 378 | | | | 23-hydroxy-13*β*, 28*β*-epoxy-olean-11-ene-16-one-3-*O*-*β*-D-glucopyranosyl-(1 → 3)-*β*-D-fucopyranoside (**316**) | 2.66 ± 0.78 µM | | |
| 379 | | | | Prosaikosaponin d (**317**) | 8.48 ± 0.84 µM | | |
| 380 | | | | 3*β*,23,28-trihydroxy-11, 13(18)-diene-16-one-3-*O*-*β*-D-glucopyranosyl-(1 → 3)-*β*-D-fucopyranoside (**318**) | – | | |
| 381 | | | | Saikosaponin g (**319**) | 15.82 ± 0.91 µM | | |
| 382 | | | | 11-*α*-methoxy-saikosaponin f (**320**) | > 20 µM | | |
| 383 | | | | Nepasaikosaponin k (**321**) | 17.91 ± 9.9 µM | | |
| 384 | | | | Saikosaponin n (**322**) | 7.67 ± 2.48 µM | | |
| 385 | | | | Saikosaponin h (**323**) | 10.09 ± 0.34 µM | | |
| 386 | PEDV | | *Camellia japonica* | Camellenodiol 3-*O*-*β*-D-glucuronopyranoside (**324**) | – | Vero | Yang et al. (2015) |
| 387 | | | (Theaceae) | Camellenodiol 3-*O*-6′-methoxy-*β*-D-glucuronopyranoside (**325**) | 1.94 ± 0.39 µM | | |
| 388 | | | | Camellenodiol 3-*O*-6′-ethoxy-*β*-D-glucuronopyranoside (**326**) | 1.09 ± 0.22 µM | | |
| 389 | | | | Camellenodiol 3-*O*-[*β*-D-glucopyranosyl(1 → 2)-*β*-D-galactopyranosyl(1 → 3)]-*β*-D-glucuronopyranoside (**327**) | – | | |
| 390 | | | | Camellioside A (**328**) | – | | |
| 391 | | | | Schimperinon (**329**) | 0.28 ± 0.09 µM | | |
| 392 | | | | Compound (**330**) | 0.91 ± 0.07 µM | | |
| 393 | | | | Primulagenin A (**331**) | 0.06 ± 0.02 µM | | |
| 394 | | | | 3*β*,16*α*-Dihydroxyolean-12-en-28-al 3-*O*-*β*-D-glucuronopyranoside (**332**) | 0.34 ± 0.01 µM | | |
| 395 | | | | Echinocystic acid 3-*O*-[*β*-D-galactopyranosyl(1 → 2)]-[*β*-D-glucopyranosyl(1 → 2)-*β*-D-galactopyranosyl(1 → 3)]-*β*-D-glucuronopyranoside (**333**) | – | | |
| 396 | | | | Echinocystic acid 3-*O*-*β*-D-glucuronopyranoside (**334**) | 3.70 ± 0.68 µM | | |
| 397 | | | | 3*β*-hydroxy-28-norolean-12,17-dien-16-on (**335**) | 0.28 ± 0.11 µM | | |
| 398 | | | | 3*β*-hydroxy-28-norolean-12,17-dien-16-one 3-*O*-6′-methoxy-*β*-D-glucuronopyranoside (**336**) | 2.90 ± 0.25 µM | | |
| 399 | | | | 3*β*-hydroxy-28-norolean-12,17-dien-16-one 3-*O*-6′-methoxy-*α*-D-glucuronopyranoside (**337**) | 0.93 ± 0.22 µM | | |
| 400 | | | | 1*β*-hydroxy-28-norolean-12,17-dien-3,11,16-trione (**338**) | – | | |

**Table 1** continued

| S. no. | Virus | Class | Plant species and family | Compound | $IC_{50}$ or $EC_{50}$ | Cell lines | References |
|---|---|---|---|---|---|---|---|
| 401 | RSV | DT | *Lilium speciosum var* (Liliaceae) | (20R)-20,25-epoxy-3-methyldammaran-2-en-6α,12β-diol,(20R)-20,25-epoxy dammaran-2-en-6α,12β-diol (**339**) | 2.9 µg/mL | – | Chen et al. (2019b) |
| 402 | SFV | OT | *Fadogia tetraquetra* var. tetraquetra (Rubiaceae) | Oleanolic acid (**133**) | – | BHK21 | Mulholland et al. (2011) |
| 403 | | | | 3β-hydroxy-11α,12α-epoxyoleanan-28,13β-olide (**340**) | > 50 µM | | |
| 404 | | UT | | 3β-hydroxyurs-11-en-28,13β-olide (**341**) | > 50 µM | | |
| 405 | | | | Ursolic acid (**37**) | 14.7 µM | | |
| 406 | ZIKV | TT | *Stillingia loranthaceae* (Euphorbiaceae) | Loranthones B (**342**) | – | Vero | Abreu et al. (2019) |

The http://www.theplantlist.org/ was referred for extracting the families wherever not mentioned

## Anti-viral triterpenes

### Coronavirus (CoV)

Coronavirus is a single-stranded enveloped RNA virus that belongs to the Coronaviridae family and subfamily Coronavirinae. These viruses are further classified into four subgroups, *Alphacoronavirus*, *Betacoronavirus*, *Gammacoronavirus*, and *Deltacoronavirus*, based on the genome structure. Out of these four subtypes, alpha and beta coronaviruses are known to infect mammals while gamma and delta coronavirus infect birds (Weiss and Leibowitz 2011; Woo et al. 2012; Li 2016; Payne 2017; Schwartz and Graham 2020; Pal et al. 2020). Of the one infecting mammals, seven viruses, HCoV 229E, HCoV OC43, HCoVNL63, HCoVHKU1, SARS-Cov, MERS-CoV, and SARS-CoV-2, are known to cause mild to serious infections in humans (Liu et al. 2021). The most recent outbreak caused by SARS-Cov-2, a new member of the coronavirus family and betacoronavirus genus, turned out to be the most fatal pandemics of the century (Pal et al. 2020). The SARS-CoV-2 RNA is a 30 kb single positive-strand RNA which encodes 27 proteins including the S protein which can bind with the angiotensin-converting enzyme 2 receptors on the cells (Bar-On et al. 2020; Pal et al. 2020).

It is pertinent to mention that both SARS-CoV and SARS-CoV-2 share 89.8% identical sequences in the S2 subunit of spike proteins which is essential for the process of membrane fusion. The S1 subunits of both of these viruses bind to the human angiotensin-converting enzyme 2 (hACE2) for entry into the cells via the receptor-binding domain. The S2 unit consists of two hydrophobic internal fusion peptides (HR1 and HR2) that form a six-helix bundle (6-HB) fusion core upon binding of RBD to the ACE-2 on the target cells. This interaction brings the viral and cellular membranes into close proximity leading to the fusion of the virus with the host cells (Harrison 2008; Si et al. 2018; Xia et al. 2020). Given the fact that the triterpenoids are well known to inhibit the fusion process by blocking the HR1–HR2 interactions; it's high time for their evaluation against SARS-CoV-2 and other corona viruses (Si et al. 2018; Li et al. 2020a). Besides this, an investigation by Ryu et al. (2010) suggests that the triterpenoid may also act as viral replication inhibitors, and thus they may act at multiple targets simultaneously. However, substantial efforts are required towards triterpenoid-based anti-covid drug discovery and development.

*Oleanane triterpenoids*

In their phytochemical investigation on *Tripterygium regelii*, Ryu and co-workers reported quinone-methide triterpenes having potent dose-dependent SARS-CoV 3CLpro inhibitory activities. These quinone-methides, namely celastrol (**1**), pristimerin (**2**), tingenone (**3**), and iguesterin (**4**) displayed $IC_{50}$ of 10.3 ± 0.2, 5.5 ± 0.7, 9.9 ± 0.1, and 2.6 ± 0.3 μM, respectively (Table 1), compared to curcumin (23.5 ± 3.7 μM) as a positive control (Ryu et al. 2010). These triterpenoids feature partial oxidation of the C-29 methyl group (**1**, **2**) or loss of C-29 due to decarboxylation (**3**, **4**) besides the presence of quinone-methide moiety. They are relatively rare molecules featuring D:A-friedo-*nor*-oleanane skeleton mostly present in the Celastraceae family (Gunatilaka 1996; Taddeo et al. 2019). The reported kinetic analysis revealed a competitive mode of action of these compounds. It was further detailed that iguesterin (**4**) possessing double bond bearing E ring displayed potent activity while substitution at C-20 or C-21 position along with the removal of double bond decreased the activity. The presence of quinone-methide moiety is also essential for the activity as the reduced analog (**5**) of **1** displayed an $IC_{50}$ 21.7 ± 1.9 μM (Ryu et al. 2010).

In general, the quinone methides are reported to exert their action via the formation of covalent interactions with the bio-molecules like DNA, proteins, and 3CLpro in the present case; and the *O*-hydroxyl group enhances the activity via the formation of hydrogen bonds (Zhou 2009; Ryu et al. 2010). This is supported by the molecular docking analysis of **4** wherein C-3-OH is reported to form a hydrogen bond with Cys44 carbonyl and Thr25 OH in domain I (Ryu et al. 2010).

Another study reported the isolation of triterpenoids from the leaves of *Euphorbia neriifolia* L. and found that 3*β*-friedelanol (**6**) exhibited the most potent anti-viral activity against human coronavirus (HCoV-229E) cultured in MRC-5 cells, followed by 3*β*-acetoxy friedelane (**7**) and friedelin (**8**) (Table 1), in comparison with actinomycin D as a positive control (Chang et al. 2012). This suggests that the friedelane skeleton has a potential role to play against HCoV, whereas epitaraxerol (**9**) was most active among taraxeranes, the other class of triterpenes reported. The anti-viral potential was reported in terms of MRC-5 (human fibroblasts) cell survival on infection with HCoV229E strain. It was further detailed that the C-3 position in friedelanes is decisive to exert activity whereas acetylation or substitutions significantly affect the activity; acetylation led to the loss of activity in taraxeranes (Chang et al. 2012). Further comparison of the structural features of these two skeletons suggests that the orientation of methyl groups and the absence of E-ring olefinic bond could provide selectivity to friedelanes skeleton over taraxeranes towards HCoV, however, this needs further experimental validation.

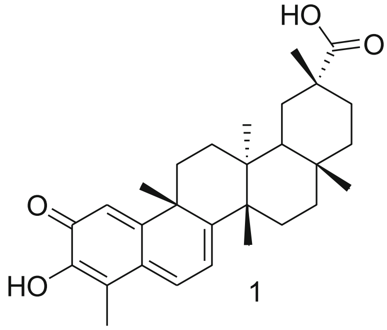


1

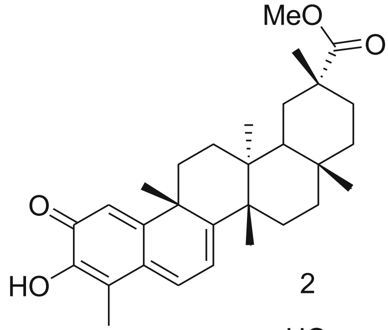


2

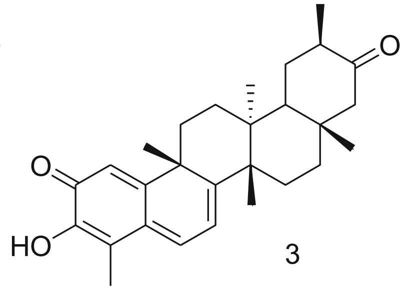


3

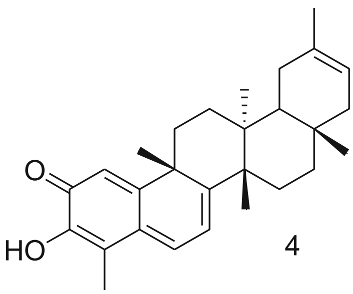


4

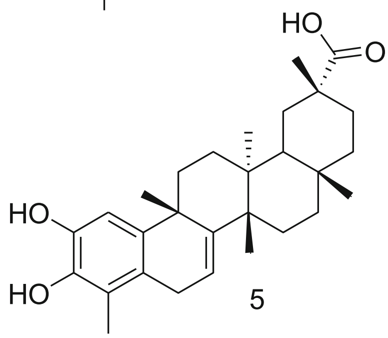


5

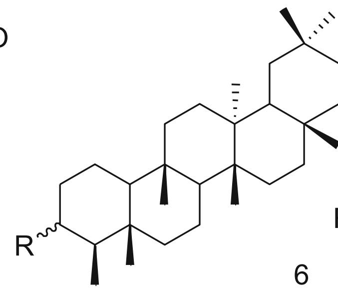


R
6 β-OH
7 β-OAc
8 =O

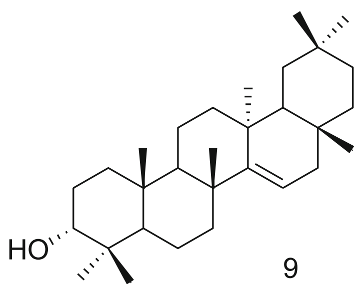


9

Coxsackie B3 (CVB3)

Coxsackie B3 (CVB3) is a serotype of the coxsackie virus belonging to the Picornaviridae family of the genus *Enterovirus*. CVB3 is a non-enveloped, positive sensed, single-stranded RNA virus, which transmits through the gastrointestinal route (Feuer et al. 2002; Lasrado et al. 2021). Interaction of virus with receptor proteins coxsackievirus–adenovirus receptor (CAR) and the decay-accelerating factor (DAF) play a significant role in the pathogenesis of Coxsackie B virus infection to the myocardial cells, which ultimately leads to myocarditis (Feuer et al. 2002; Shieh and Bergelson 2002; Lasrado et al. 2021; Milstone et al. 2005). It is pertinent to mention that there is no specific treatment for the CVB infection to date, however, few reports suggested a potential inhibitory role of different skeletons bearing triterpenes. Moreover, the available reports suggest that therapeutic interventions for the treatment of myocarditis and viral infection-induced active inflammatory destruction of the myocardium are limited to immunosuppressive and immunomodulatory therapies (Pollack et al. 2015). No wonder that the triterpenoids are well reported to exert these properties and demonstrated their beneficial effects in myocarditis as well (Martín et al. 2014; Xu et al. 2020).

Several studies have chalked out the role of triterpenoids, as described below, belonging to the four different skeletons. A total of 27 triterpenoids have been reported in these studies, among which only glycyrrhizic acid (GA; **36**) was evaluated extensively in *in-vitro* and *in-vivo* models while other compounds were evaluated for indicative anti-viral properties without exploring the detailed mode of action. Therefore, extensive anti-viral activities need to be undertaken for exploration of the complete potential of these triterpenes; further experimental and clinical correlation concerning viral myocarditis is warranted.

*Cycloartane triterpenoids*

Lv et al. (2016) isolated a series of cycloartane, lanostane, and ursane classes of triterpenes from twigs and leaves of *Lyonia ovalifolia* and evaluated them against Coxsackie B3, HSV-1, and influenza A/95–359. Among the cycloartanes, lyonifolosides A-K and their aglycones (**10–23**) obtained by acid hydrolysis, compound 3α-[(*β*-D-glucopyranosyl)-oxy]-25-hydroxy-9,10-*seco*-cycloartan-24-oxo-5(10)-en-30-oic acid (lyonifoloside A; **10**) its aglycone lyonifolic acid A (**11**), lyofoligenic acid (**13**) the aglycone of 3α-[(*β*-D-glucopyranosyl)-oxy]-24S,25-dihydroxy-9,10-*seco*-cycloartan-5(10)-en-30-oic acid (lyonifoloside B; **12**) has displayed potent activity against CVB3 with $IC_{50}$ value of 11.1 ± 1.98, 2.1 ± 0.30, 4.8 ± 1.20 μM/L (Table 1), respectively against the positive control pleconarild ($IC_{50}$ 0.001 ± 0.0001 μM/L) and ribavirin ($IC_{50}$ 292 ± 9.04 μM/L) (Lv et al. 2016).

The $IC_{50}$ of these cycloartane shows that 9,10-*seco*-cycloartane skeleton bearing olefinic bond at 1(10) position are less active in comparison with the one bearing olefinic bond at 5(10) position. Furthermore, the aglycones are more potent compared to their respective glycosides, suggesting the potential role of the C-3 bearing hydroxyl group. The presence of the keto group at C-21 instead of the hydroxyl group favored the CVB3 inhibition and further glycosylation at C-21 hydroxy resulted in a loss of the activity (Lv et al. 2016).

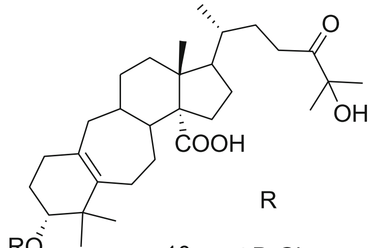

| | R |
|---|---|
| 10 | β-D-Glc |
| 11 | H |

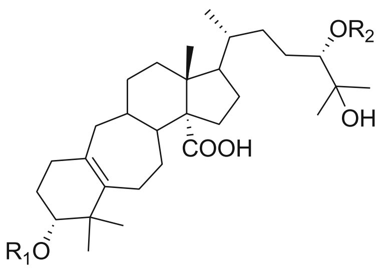

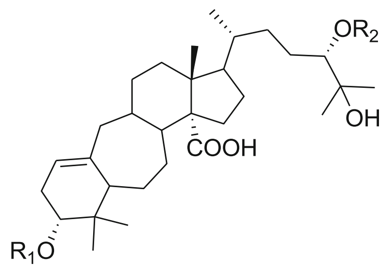

| | $R_1$ | $R_2$ |
|---|---|---|
| 12 | β-D-Glc | H |
| 13 | H | H |
| 14 | β-D-Glc _ Ac | H |
| 15 | β-D-Glc | α-L-Ara |
| 16 | β-D-Glc _ Ac | α-L-Ara |
| 17 | α-L-Ara | α-L-Ara |

| | $R_1$ | $R_2$ |
|---|---|---|
| 18 | β-D-Glc _ Ac | H |
| 19 | H | H |
| 20 | β-D-Glc _ Ac | α-L-Ara |
| 21 | β-D-Glc | α-L-Ara |
| 22 | β-D-Glc | β-D-Glc |
| 23 | α-L-Ara | α-L-Ara |

*Dammarane triterpenes*

20(S)-Protopanaxtriol (**24**), of *Panax pseudoginseng*, was reported to be potent anti-viral both in *in-vitro* ($IC_{50}$ 2.74 μg/mL, HeLa cells) and *in-vivo*. It also lowered the virus titers and pathological alterations in the hearts along with the plasma lactate dehydrogenase and creatine kinase, the biochemical markers of myocardial injury (Wang et al. 2012). In another study protopanaxatriol type ginsenoside Re, Rf, and Rg2 (**25–27**) demonstrated significant anti-viral activity against CVB3 at 100 μg/mL concentration (Table 1). At the same time the protopanaxadiol type ginsenosides (Rb1, Rb2, Rc, and Rd), were ineffective (Song et al. 2014a); suggesting the possible involvement of the C-6 α-OH.

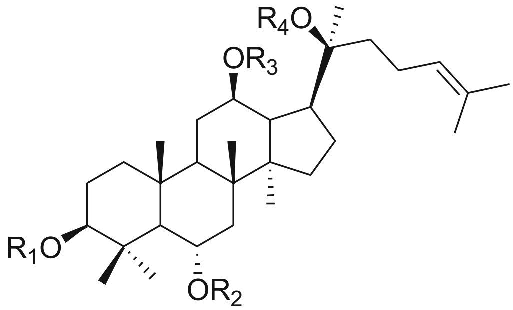


| | R1 | R2 | R3 | R4 |
|---|---|---|---|---|
| 24 | H | H | H | H |
| 25 | H | Glc$^{2}$-Rha | H | Glc |
| 26 | H | Glc$^{2}$-Glc | H | H |
| 27 | OH | Glc$^{2}$-Rha | H | H |

*Lanostane triterpenoids*

Among the lanostane triterpenoids (**28–35**) reported by Lv et al. 2016 from leaves and twigs of *Lyonia ovalifolia*, the aglycone, lyonifolic acid C (**29**) of 3α-[(*β*-D-glucopyranosyl)-oxy]-24(S),25-dihydroxy-lanost-8-en-30-oic acid (lyonifoloside L; **28**) and 3α-[(6-*O*-acetyl-*β*-D-glucopyranosyl)-oxy]-24(S),25-dihydroxylanost-8-en-30-oic acid (lyonifoloside M; **30**) have displayed potent activity against CVB3 with $IC_{50}$ value of 4.8 ± 1.16 and 11.1 ± 1.17 µM/L, respectively (Table 1). This suggests that the C-21 position is important for the activity as the glycosylation resulted in the loss of activity. Further, the aglycone is more potent compared to their respective glycoside, but acetylation of the attached sugar at C-3 facilitated the activity (Lv et al. 2016).

*Oleanane triterpenes*

GA (**36**) (*Glycyrrhiza uralensis*) is reported to block viral replication, of CVA16, in a dose-dependent manner and the anti-viral effects were found to be via inactivation of viral particles. GA (**36**) markedly inhibited the CVA16 associated cytopathic effect and was reported to reduce CVA16 production by 3.5 and 6.0 logs at 3 and 5 mM, respectively. Time-of-drug analysis conducted by the author suggested that GA interferes with an early event of the CVA16 replication cycle (Wang et al. 2013).

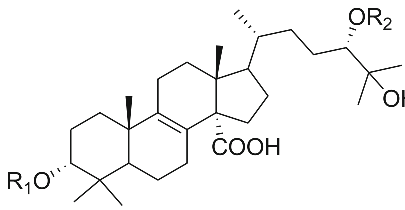

| | $R_1$ | $R_2$ | | $R_1$ | $R_2$ |
|---|---|---|---|---|---|
| 28 | β-D-Glc | H | 32 | β-D-Glc | α-L-Ara |
| 29 | H | H | 33 | β-D-Glc _ Ac | α-L-Ara |
| 30 | β-D-Glc _ Ac | H | 34 | β-D-Glc | β-D-Glc |
| 31 | H | β-D-Glc | 35 | α-L-Ara | α-L-Ara |

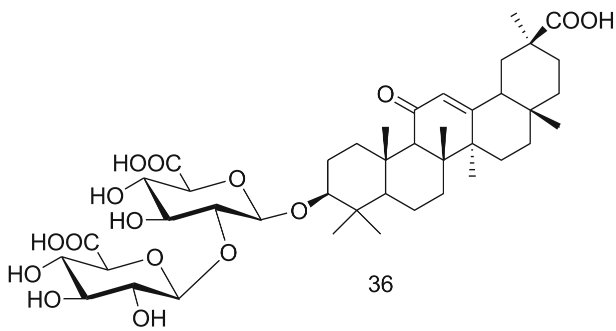

36

Cytomegalo virus (CMV)

Cytomegalovirus (CMV) is the largest member of the Herpesviridae family and belongs to the subfamily Betaherpesvirinae. Currently, the available drug includes viral DNA polymerase inhibitors like ganciclovir, foscarnet, cidofovir, and acyclovir. But there is no single drug that is adequately potent and safe; also the resistance mutations to gancyclovir have been reported. This resistance mutation is suspected to develop cross-resistance to other available anti-viral drugs (Griffiths and Whitley 2002; Lurain and Chou 2010; Krishna et al. 2019).

The available therapies or more precisely the targets for the development of anti-virals against CMV are viral DNA polymerase UL54, viral terminase complex inhibitor, and viral kinase UL97 inhibitor against which the drugs are available (Schulz et al. 2016; Krishna et al. 2019). The suggested course of action also includes therapies against the CMV latency, since pro-inflammatory signals and myeloid differentiation may reactivate these latently infected cells (Sinclair and Sissons 2006; Krishna et al. 2019). Moreover, during this latency period, the viral replicase inhibitors are ineffective in absence of any viral replication and the US28 is expressed by CMV during latent infection which could serve as a potential therapeutic target (Lee et al. 2017). Flavonoid-based molecules have already been explored against US28 (Kralj et al. 2013). Surprisingly, we could trace only one report in the last decade, therefore, effort towards the identification of potential therapeutic triterpenoid leads is warranted to target both the latency and replication stages.

*Ursane triterpene*

The only available study on triterpenoids reported that ursolic acid (**37**) targeted guinea pig cytomegalo virus (GPCMV-22122) replication in guinea pig embryo lung fibroblasts (GPEL), but it could not prevent viral entry into the cells. It displayed $CC_{50}$ of 86.7 μg/mL and $EC_{50}$ 6.8 μg/mL (Table 1) with a therapeutic index of 13 (Zhao et al. 2012).

Dengue virus (DENV)

Dengue virus (DENV), a viral virus counting millions of infections, is a member of the family Flaviviridae and genus *Flavivirus*. It is the most common vector-borne (*Aedes* mosquitos) viral disease counting millions of cases in tropical and subtropical regions every year (https://www.who.int/news-room/fact-sheets/detail/dengue-and-severe-dengue). DENV is a single-stranded, positive-sense RNA virus that consists of approximately 11 kb genome. Antigenically four serotypes of DENV are found worldwide i.e. DENV-1, DENV-2, DENV-3, and DENV-4. The treatment of which mostly lies around the management of the symptoms, as over 90 years of efforts towards the development of vaccines could achieve limited success; and at the same time there is no specific anti-viral drug is available to treat dengue virus infection (Seema 2005; Halstead 2015; Behnam et al. 2016; Murugesan and Manoharan 2019). Hence, the development of a safe and effective anti-DENV agent is required to reduce the mortality and morbidity burden of the infection (Guzman et al. 2010; Tuiskunen and Lundkvist 2013).

It is to mention that targets identified for the development of drugs against the dengue virus includes (i) stem domain, hydrophobic pocket (*β*-OG pocket), and receptor-binding domain III of the DENV envelope (E) glycoprotein, responsible for receptor recognition, have been pursued as DENV entry inhibitor drug targets; (ii) DENV capsid protein C hydrophobic core and N-terminal region are encouraging targets for anti-dengue drug development; (iii) inhibitors of the NS3 helicase, NS2B-NS3 helicase, NS2B-NS3 protease, NS4B, NS5 methyltransferase, and NS5 polymerase; and (iv) blocking NS5 nuclear localization (Behnam et al. 2016). Despite the availability of several targets, only a few reports could be traced in the last decade on natural products and rarely triterpenoids as anti-DENV agents.

*Lupane triterpenes*

Recently, Loe et al. 2020 detailed the anti-viral mechanism of betulinic acid (**38**) with $CC_{50}$ and $IC_{50}$ values of 28.24 and 0.9463 μM in the DENV2-infected Huh7 cells (Table 1), and a similar observation was recorded in other cells (BHK21, HepG2, HEK293T and Vero) as well. The study concluded that betulinic acid decreased the DENV2 envelope protein and NS4B proteins expression, a decrease in nanoluciferase signal was also recorded supporting the reduction in viral protein synthesis after infection. It was found not to affect the viral binding or entry into the cells. This is supported by several previous studies where it is reported to inhibit viral NS5 RNA-dependent RNA polymerase (RdRp) activities (Bourjot et al. 2012; Peyrat et al. 2017; Loe et al. 2020).

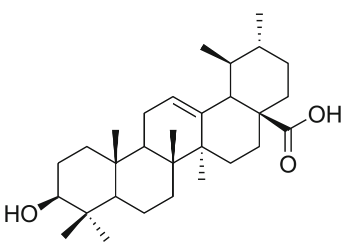

37

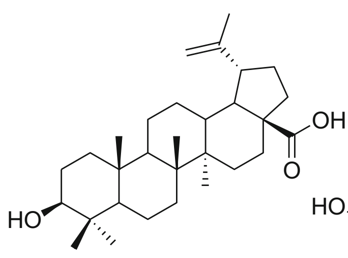

38

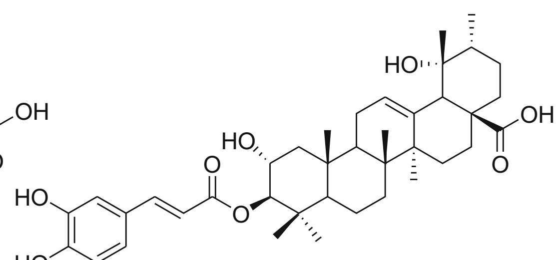

39

*Ursane triterpenes*

3-*O*-Trans-caffeoyltormentic acid (**39**) reported from the leaves of *Eriobotrya deflexa* f. *buisanensis* exhibited the most potent activity against dengue virus ($IC_{50}$ 12.4 ± 1.1 μM; serotype 2 strain PL046; Table 1) (Chen et al. 2019a).

Epstein-Barr virus (EBV)

Epstein-Barr virus (EBV) is a type of $\gamma$-herpes, contains a double-stranded DNA genome of approximately 184 kb pair in length which encodes nearly 100 proteins. Two different types of EBV infection, EBV-1, and EBV-2 (or A, and B), are documented and both have more than 70–80% sequence homology. EBV is known to infect more than 90% of the adult population worldwide and persists for lifelong in a person with latent infection of the B-lymphocytes and saliva (Arai 2021; Jenson 2011; Sausen et al. 2021).

Many of the nucleoside and nucleotide anti-viral approved by US-FDA against other viral disorders were not effective against EBV infections probably due to the difficulty in timely diagnosis, the required high concentrations of anti-viral in the oropharynx. The signs and symptoms associated with the disease are not related to the viral replication but are the immunological implications (Ernberg and Andersson 1986; Gershburg and Pagano 2005; Poole and James 2018; Keith et al. 2018; Andrei et al. 2019). Therefore, there is no effective treatment available against this virus. Several classes of synthetic (nucleoside, nucleotide, and pyrophosphate analogs) and natural products (including herbal extracts) are being explored and developed against different targets like EBV protein kinase BGLF4, EBV DNA polymerase, EBV nuclear antigen 1 (EBNA1), and other cellular targets essential for viral replication such as topoisomerases I and II (Kapadia et al. 2002; Cui et al. 2014; Andrei et al. 2019).

In the literature, only two studies concerning 24 oleanane triterpenoids were traced to exert their action by inhibiting the EBV early antigen (EBV-EA) activation. Both these studies, as described below, reported poly-oxygenated oleanane skeleton bearing aglycones and glycosides wherein the respective aglycones displayed better activity owing to the C-28 –COOH group.

*Oleanane triterpenes*

*Terminalia chebula* Retz is one of the most widely acknowledged medicinal plants as a folklore medicine. An investigation of the galls of *T. chebula* collected from Chiang Mai province in Thailand led to the isolation of eight oleanane triterpenoids and their glycosides along with hydrolyzable tannins. These triterpenoids (**40–47**), exerted potent diminishing effects on the 12-*O*-tetradecanoylphorbol 13-acetate (TPA) induced EBV early antigen (EBV-EA) activation in Raji cells ($IC_{50}$ 269–363 mol ratio/32 pmol TPA). The number of hydroxyl groups may influence the activity (**43**) as the presence of glycosidic linkage at C-28 have diminishing effects (Table 1) (Manosroi et al. 2013).

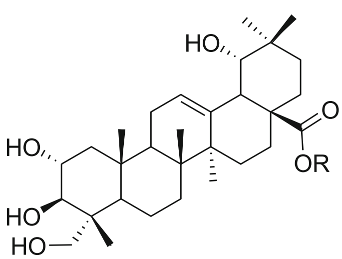


| | R |
|---|---|
| 40 | H |
| 44 | β-D-Glc |

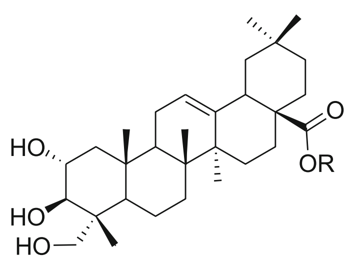


| | R |
|---|---|
| 41 | H |
| 45 | β-D-Glc |

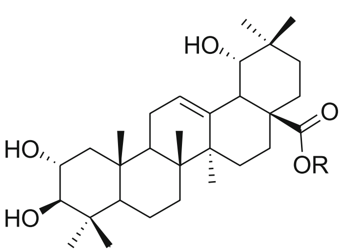


| | R |
|---|---|
| 42 | H |
| 46 | β-D-Glc |

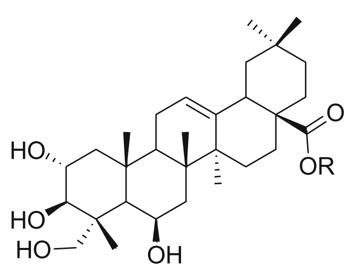


| | R |
|---|---|
| 43 | H |
| 47 | β-D-Glc |

Similarly, triterpenoids and other compounds isolated from the kernels of *Vitellaria paradoxa* displayed activity against EBV early antigen (EBV-EA) activation induced by TPA in Raji cells. The isolated oleanane triterpenoids, **48–59**, displayed $IC_{50}$ of 455, 456, 470, 460, 479, 348, 335, 368, 410, 360, 353, and 330, and compound **61–63** displayed $IC_{50}$ of 380, 371, and 339 M ratio 32 pmol 1 TPA respectively (Table 1) (Zhang et al. 2014a). It was further concluded by the authors that derivatives without any sugar attachment at C-28 were more active suggesting the possible involvement of the C-28 –COOH group in the activity, whereas an increase in the number of sugars at the C-3 position reduced the activity (Zhang et al. 2014a).

Enterovirus (EV)

Enteroviruses (EV) of the family Picornaviridae are the non-enveloped, positive sensed, single-stranded RNA virus and contain a genome of approximately 7500 bases. The disease is named after its route of transmission that is through the intestine and causes hand, foot, and mouth disease (HFMD). It also causes neurological disorders like brainstem encephalitis, acute meningitis, and/or cardiopulmonary complications, hemorrhagic conjunctivitis, myocarditis, and acute flaccid paralysis, etc. Although a couple of vaccines have been approved for the prevention of HFMD in China, the clinically approved anti-virals are still far away from reality (Oberste et al. 1999; Lin et al. 2013; Zhai et al. 2016; Tang et al. 2020).

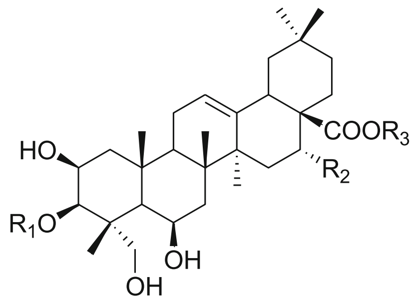


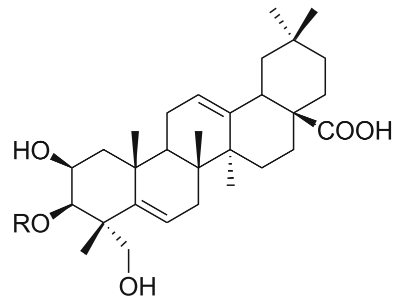


| | R |
|---|---|
| 61 | *β*-D-MeGlcA |
| 62 | *β*-D-Glc |
| 63 | H |

| | $R_1$ | $R_2$ | $R_3$ |
|---|---|---|---|
| 48 | *β*-D-GlcA | OH | *α*-L-Rha-(1→2)-*α*-L-Ara- |
| 49 | *β*-D-GlcA | OH | *β*-D-Xyl-(1→4)-*α*-L-Rha-(1→2)-*α*-L-Ara- |
| 50 | *β*-D-GlcA | OH | *α*-L-Rha-(1→3)-*β*-D-Xyl-(1→2)-*α*-L-Rha-(1→2)-*α*-L-Ara- |
| 51 | *β*-D-GlcA | OH | *β*-D-Api-(1→3)-*β*-D-Xyl-(1→2)-*α*-L-Rha-(1→2)-*α*-L-Ara- |
| 52 | *β*-D-Glc | OH | *α*-L-Rha-(1→3)-*β*-D-Xyl-(1→2)-*α*-L-Rha-(1→2)-*α*-L-Ara- |
| 53 | *β*-D-GlcA | OH | H |
| 54 | *β*-D-Glc | OH | H |
| 55 | *β*-D-MeGlcA | H | H |
| 56 | *β*-D-Glc-(1→3)-*β*-D-Glc | H | H |
| 57 | *β*-D-GlcA | H | H |
| 58 | *β*-D-Glc | H | H |
| 59 | H | H | H |
| 60 | H | OH | H |

Some of the potential targets against which several synthetic molecules are being developed include viral 3C protein (3Cpro), a cysteine protease with chymotrypsin-like specificity, VP1 one of the four coat proteins of the capsid, 2C helicases, entry, and replication inhibitors (Shia et al. 2002; Zhai et al. 2016; Ma et al. 2018; Tang et al. 2020). It is evident from the literature that several natural products have been reported to possess anti-EV activity with little contribution from the triterpenes (Wang et al. 2015).

Only six triterpenes have been found in the literature to exert their action either by inhibiting cell adhesion and uncoating, or blocking VP1 and VP2 protein expression; therefore, it is recommended that more triterpenoids should be explored and a detailed mechanism of action should be delineated which is lacking at this moment. Further, it is dubious to conclude the SARs due to the limited reports.

*Dammarane triterpenes*

Protopanaxatriol type ginsenoside Rg2 (**27**) of *Panax ginseng* displayed anti-EV71 activity in Vero cells among the seven tested ginsenosides (Table 1) (Song et al. 2014a).

*Lanostane triterpenes*

*Oleanane triterpenes*

GA (**36**) (*Glycyrrhiza uralensis*) is reported to block viral replication of EV71 in a dose-dependent manner (Table 1) and the anti-viral effects were found to be via the blockage of VP1 protein expression and post virus cell entry events (Wang et al. 2013).

Hederasaponin B (**66**) from *Hedera helix* was reported to possess significant EV71 C3 ($EC_{50}$ 24.77 ± 12.56 µg/mL) and C4a ($EC_{50}$ 41.77 ± 0.76 µg/mL; Table 1) in Vero cells by inhibiting viral capsid protein synthesis via blocking the viral VP2 protein expression. Under the specified condition the positive control ribavirin was ineffective (Song et al. 2014b).

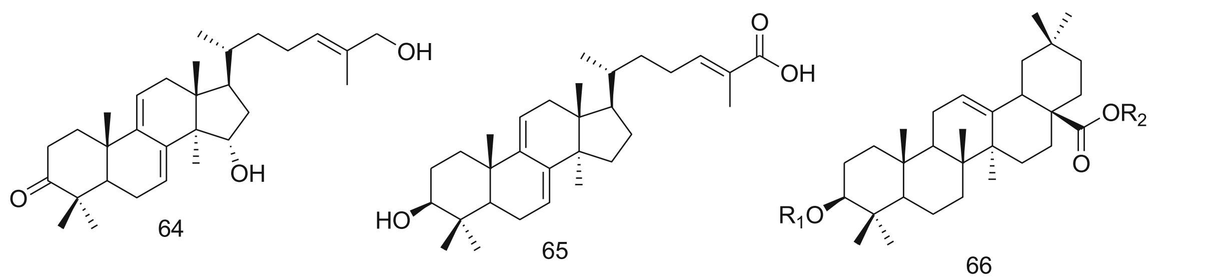


R1 α–L-Rha-(1→2)-α–L-Ara-

R2 α-L-Rha-(1→4)-β-D-Glu-(1→6)-β-D-Glu-

*Ganoderma lucidum*, a mushroom used in traditional Chinese medicines, derivatives lanosta-7,9(11),24-trien-3-one,15;26-dihydroxy (**64**) and ganoderic acid Y (**65**) displayed significant anti-EV71 activities (strain-XiangYang-Hubei-09); at the same time, they were reported to be non-cytotoxic in human rhabdomyosarcoma (RD) cells (Table 1). The author further reported that **64** and **65**, featuring a conjugates diene (C7=C8–C9 =C10), blocked the virus particle adsorption to the cells and thus prevented uncoating of the virus supported with computational interactions. Accordingly, these compounds were reported to inhibit the replication of the viral RNA by blocking the cell adhesion and uncoating (Zhang et al. 2014b).

*Ursane triterpenes*

Another investigation evaluated ursolic acid, oleanolic acid, and asiatic acid against EV71 among which ursolic acid (**37**) displayed the greatest inhibition of EV71 in the human rhabdomyosarcoma (RD) cells (Table 1) by decreasing the levels of VP1 viral protein (Zhao et al. 2014).

Hepatitis virus (HV)

Hepatitis virus (HV), a member of Hepadnaviridae, containing double-stranded circular DNA causes inflammation of the liver and may lead to liver cirrhosis or fibrosis. Hepatitis viruses are the most common cause of hepatitis, a major health concern all over the globe affecting millions of people each year. Five main HV includes hepatitis A, B, C, D, and E, among which hepatitis B (HBV) and C (HCV) are causing chronic diseases like liver cirrhosis and cancer (Zuckerman 1996; Yuen et al. 2018; Naggie and Lok 2021; https://www.who.int/publications/i/item/global-hepatitis-report-2017).

On the therapeutic front, the interferon-based therapies and viral polymerase transcriptase inhibitors, nucleotides/nucleosides, are the targets which gained most of the attention for the drug development. However, other targets for the development of anti-HBV agents gaining attention includes viral entry inhibitors, capsid assembly modulator, transcription modulators, and HBV surface antigen (HBsAg) secretion inhibitors, etc. Similarly, several targets like viral entry inhibitor, RNA dependent RNA polymerase inhibitor, capsid modulator, etc. are being explored for the design and synthesis of tailor-made molecules against HCV (Naggie and Lok 2021; O'leary and Davis 2010; Haudecoeur et al. 2011; Colpitts et al. 2016; Pei et al. 2017).

However, despite being a viral virus counting millions of infections every year, very limited efforts are documented towards the therapeutic interventions employing natural products. Overall 37 anti-HBV and anti-HCV triterpenoids bearing five different skeletons are documented here. Among these, ursane appears to be most potent however the testimonial needs further experimental validation under identical test conditions and could join hands with other natural products evaluated against the HV both in preclinical and clinical studies (Wohlfarth and Efferth 2009; Parvez et al. 2016; El-Tantawy and Temraz 2020). Further target-specific evaluation is recommended to delineate the mechanism of action and development of potential leads against the available targets.

*Cyclolanostane triterpenes*

Li et al. 2019a reported the isolation of 17,18-cyclolanostane triterpene, containing a unique 6/6/6/5/3 ring system, abinukitrine A (**67**) from the leaves and twigs of *Abies nukiangensis*. It was reported to display *in-vitro* anti-hepatitis C virus (HCV) activity using GT1b cells ($EC_{50}$ 6.52 μM) and was considered a moderate inhibitor as compared to sofosbuvir ($EC_{50}$ 0.04 μM; Table 1) (Li et al. 2019a).

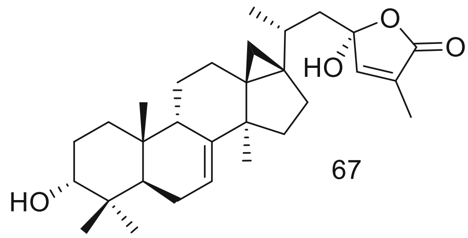


67

*Oleanane triterpenes*

Cheng et al. 2011 reported the bio-assay-guided isolation of nine oleanane triterpenoids against HBV using the HepG2 2.2.15 (human hepatocellular carcinoma) cells. The oleananes fatsicarpains A-G (**68–74**), 3α-hydroxyolean-11,13(18)-dien-28-oic acid (**75**), 3α-hydroxyolean-11-en-28,13*β*-olide (**76**) were isolated from the twigs and leaves of *Fatsia polycarpa*. Among these **68**, **70**, **71**, **73**, and **74** were reported with $IC_{50}$ values of 18.9, 16.7, 28.8, 23.9, and 29.2 μM, respectively, while compound **69**, **72**, **75**, and **76** displayed $IC_{50} > 50$ μM (Table 1). The author further reported that the tested compound could not inhibit the hepatitis B surface antigen (HbsAg) and hepatitis B e antigen (HbeAg) in HepG2 2.2.15 cells (Cheng et al. 2011). The better activity displayed by **68** and **70** could be attributed to the substitution of $–CH_3$ at C-24 position with $-CH_2OH$ and –CHO, respectively. The orientation of the hydroxyl group at C-3 seems to play an important role in the activity as its replacement with *β*-$OSO_3$ (**69**) decreased the activity. Further investigations are required to establish the SAR studies.

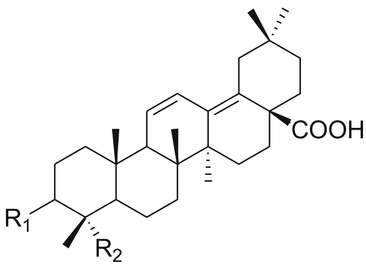


| | $R_1$ | $R_2$ |
|---|---|---|
| 68 | $\alpha$-OH | $CH_2OH$ |
| 69 | $\beta$-$OSO_3H$ | $CH_3$ |
| 70 | $\alpha$-OH | CHO |
| 75 | $\alpha$-OH | $CH_3$ |

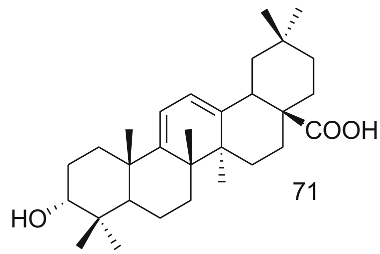


71

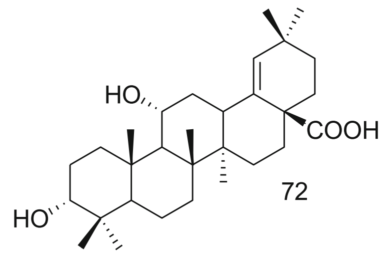


72

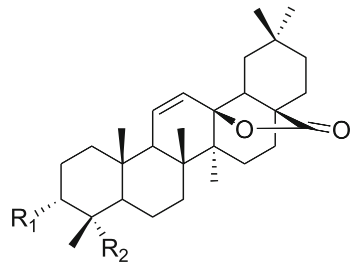


| | $R_1$ | $R_2$ |
|---|---|---|
| 74 | OH | $CH_2OH$ |
| 76 | OH | $CH_3$ |

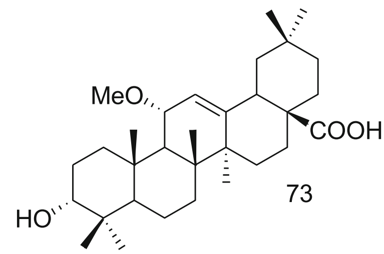


73

*Nor-terpenes*

The phytochemical investigation on the aerial parts of *Schisandra propinqua* var. *propinqua* by Lei and co-workers resulted in the isolation of propindilactones P-S (**77–80**), wuweizidilactones B and H (**81** and **82**); the 18-*nor*-schiartane framework (C28) bearing triterpenoids (Lei et al. 2010). The report further highlights that among the compounds evaluated (**78**, **79**, **81**, and **82**) against HBV activity in Hep G 2.2.15 cell line using lamivudine as a positive control, only **81** was reported to possess high cytotoxicity and low activity against both antigens (HBsAg and HBeAg) with an SI value $< 1.0$ while other compounds were inactive (Lei et al. 2010). Careful examination of structural features with reported activities suggests that **81** containing a five-membered F ring is more active compared to those bearing a six-membered F ring. This indicates that compound **77** may also exhibit the activity with due consideration of substitution at the C-7 position, however, due to the small quantity it was not tested (Lei et al. 2010).

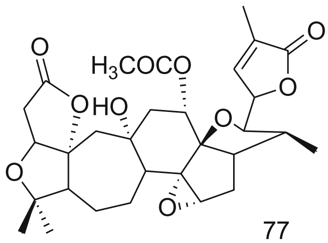


77

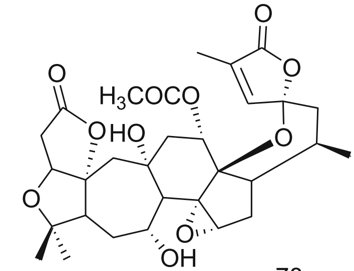


78

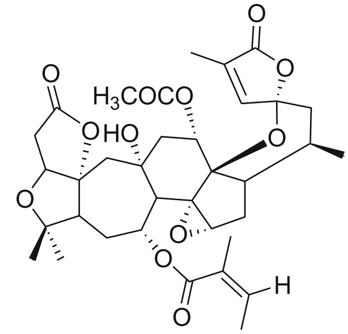


79

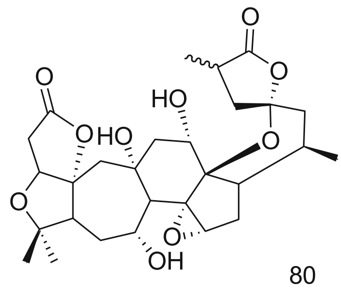


80

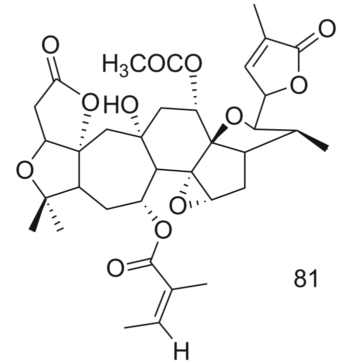


81

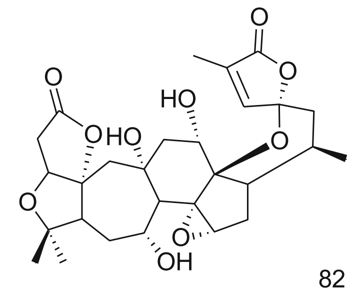


82

*Shionone triterpenes*

Shionane class of triterpenoids isolated from the roots and rhizomes of *Aster tataricus* in three independent studies were evaluated against HBV. The first study published in 2010 reported the isolation of three shionane-type triterpenes, shion-22-methoxy-20(21)-en-3-one (**83**), shion-22(30)-en-3,21-dione (**84**), shion-22-methoxy-20(21)-en-3$\beta$-ol (**85**). Among these, the tested compounds **83** and **84** showed inhibitory activities on HBsAg with $IC_{50}$ values of 0.89 and 4.49 µg/mL, respectively. Additionally, **83** showed inhibitory activity on HBeAg with an $IC_{50}$ value of 0.83 µg/mL (Table 1) (Zhou et al. 2010).

In the second study shionane triterpenes astataricusones A-D, astataricusol A, epishionol (**86–91**) were evaluated for HBV antigen and DNA replication in the HepG 2.2.15 cell line. Herein **87** displayed inhibitory activities on HBsAg secretion ($IC_{50}$ 23.5 µM), while **87** and **91** exhibited inhibitory potential on HBeAg secretion ($IC_{50}$ 18.6 and 40.5 µM), and cytotoxicity on HepG 2.2.15 cells ($CC_{50}$ 172.4 and 137.7 µM), respectively (Table 1). Compounds **87** and **91** also displayed inhibitory actions on HBV (hepatitis B virus) DNA replication with $IC_{50}$ values of 2.7 and 30.7 µM, respectively (Table 1). Lamivudine (3TC) was used as a positive control (Zhou et al. 2013).

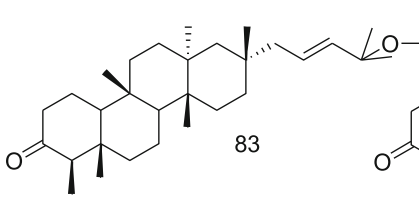
83

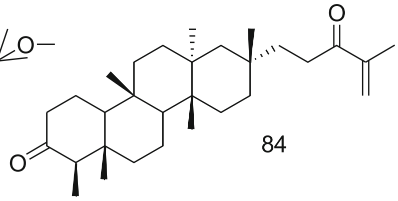
84

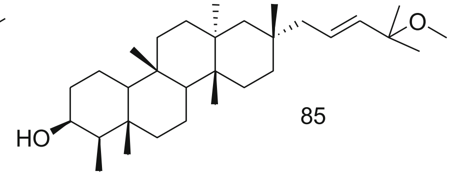
85

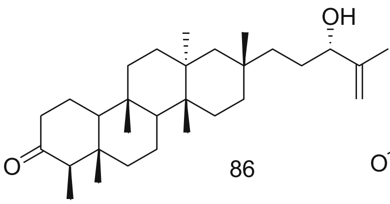
86

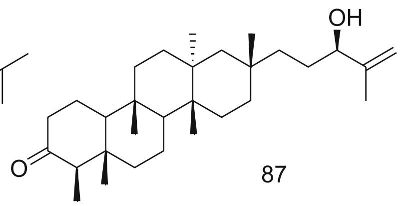
87

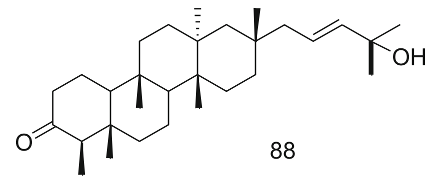
88

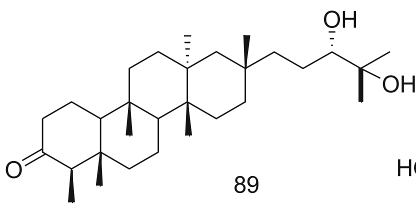
89

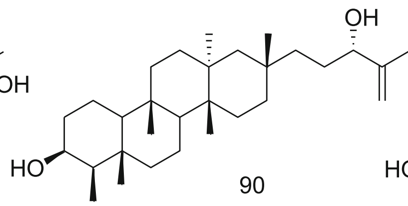
90

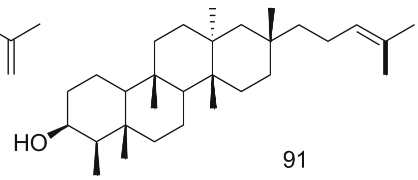
91

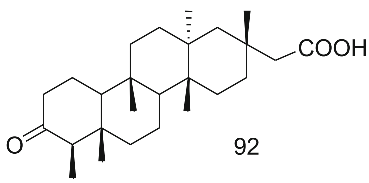
92

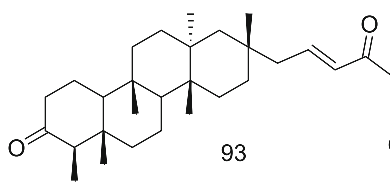
93

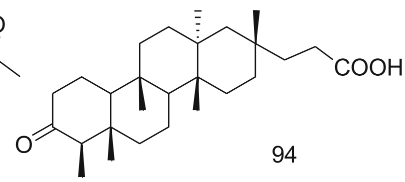
94

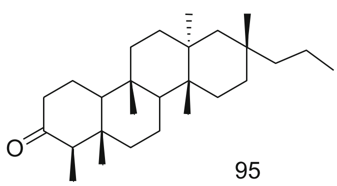
95

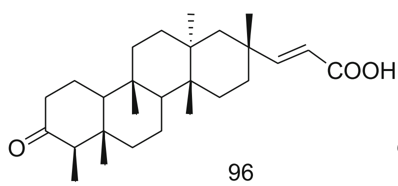
96

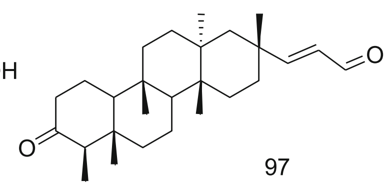
97

The third study in this series resulted in the identification of astershionones A-F (**92–97**), where **94** displayed inhibitory potential against HBsAg and HBeAg secretion ($IC_{50}$ 23.0 and 23.1 µM), and cytotoxicity against HepG 2.2.15 cells ($CC_{50}$ 170.5 µM). It also demonstrated inhibitory properties against HBV DNA replication with an $IC_{50}$ value of 22.4 µM. HepG 2.2.15 cells (Table 1) (Zhou et al. 2014).

A comparison of these studies suggests that shionone side chain might be playing an important role in displaying anti-HBsAg activity since the tested compounds **83**, **84**, **87**, and **94** have similar A-D ring orientations. Further, the presence of the $-C(CH_3)_2-OCH_3$ group in the side chain might improve the potency. Similarly, **83** also displayed potent anti-HBsAg activity whereas compounds with modified side chains lead to a decrease in the activity. It is also evident from these studies that the length of the side chain may also have a significant role as 2–3 carbon-bearing side chains containing compounds (**92**, **94**, **95–97**) were inactive.

*Ursane triterpenes*

An investigation on the aerial parts of *Elsholtzia bodinieri* resulted in the isolation of ursane saponin bodiniosides O (**98**) and P (**99**), which displayed potent anti-HCV activities with $IC_{50}$/SI of 0.41 nM/30.63 and 1.58 nM/9.08, respectively (Table 1) (Xiang et al. 2019). Another study on the same plant yielded ursane-type saponins namely bodiniosides M (**100**) and N (**101**), oblonganoside I (**102**), and bodinioside A (**103**). Of these **100** ($EC_{50}$ 11.50 nM, SI 6.53) and **103** ($EC_{50}$ 32.86 nM, SI 4.41) were reported to possess potent activity against HCV, while the other two compounds **101** ($EC_{50}$ 13.25 nM) and **102** ($EC_{50}$ 160.36 nM) displayed SI 1.0 and 0.078 respectively in the Huh7.5.1 cells infected with HCV J6/JHH-1 viral particles (Table 1). Ribavirin was used as a reference standard ($EC_{50}$ 9.57 and SI 10.03) (Zhong et al. 2016).

Collectively these studies suggest that the ursane skeleton favors the activity with **98** being most potent, having SI as high as 30.63, featuring –$CH_2$–O–CO–$CH_3$ group at C-23 position along with glycosylation at C-3 and C-28 positions. The substitutions at C-23 and C-28 position and ring modifications influence the activity, thus signifying the role of A and E rings for the activity.

Herpes virus (HSV)

Herpes simplex viruses (HSV) are enveloped, double-stranded DNA virus that contains 74 genes in their genome. They are a member of Alphaherpesvirinae, a sub family of Herpesviridae. The worldwide prevalence rate of infection is estimated to be about 65–90%. It has two sub-types HSV-1 and HSV-2, of these HSV-1 mainly cause herpes labialize, herpetic stomatitis, and keratitis and is considered to be a pervasive and extremely contagious human pathogen that has a high capability in disrupting host cell functions. The HSV-2 virus is responsible for the transmission of genital herpes (James et al. 2020; Madavaraju et al. 2021; Kumar et al. 2016).

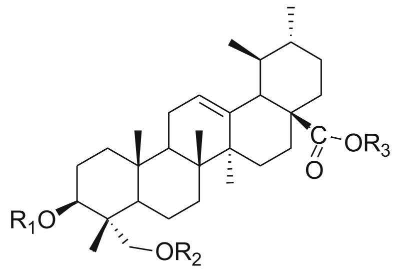


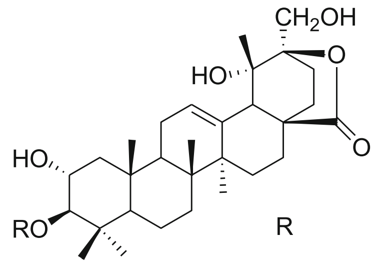


R

101 β-D-Glc

| | R1 | R2 | R3 |
|---|---|---|---|
| 98 | β-D-Xyl | -CO-$CH_3$ | β-D-Xyl-(1→6)-[β-D-Glc-(1→4)-α-L-Rhm-(1→2)]-β-D-Glc |
| 99 | β–D-Xyl | H | α-L-Rhm-(1→2)-β-D-Glc |

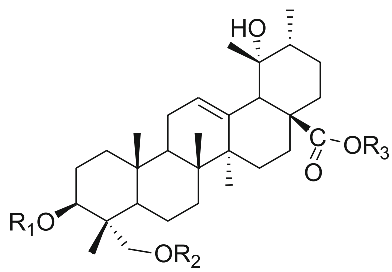


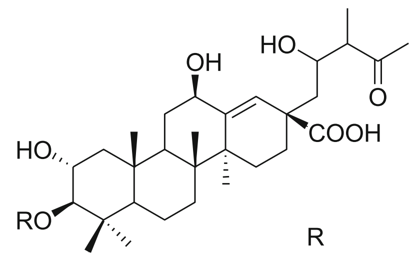


R

103 β-D-Glc

| | R1 | R2 | R3 |
|---|---|---|---|
| 100 | β-D-Xyl | -CO-$CH_3$ | α-L-Rhm-(1→2)-β-D-Glc |
| 102 | β-D-Xyl | OH | β-D-Glc |

The pathogenesis of HSV starts with its binding to the cells of the skin and mucous membrane; releases Vhs and degrades mRNA of the host cell to establish primary infection and latency. The latent virus is activated by factors such as sun exposure, psychological stress, physical trauma, etc., thus establishing the recurrent infection (Kimberlin et al. 2011). Its treatment includes general anti-viral agents such as aciclovir and valaciclovir to interfere with the virus replication, decrease the severity of lesions outbreak, and lower the risk of transmission. The ubiquitous use of anti-HSV drugs resulted in drug resistance, thus, new effective drugs are needed. In January 2020, a comprehensive review article highlighted the promising anti-HSV natural products (Treml et al. 2020).

All together 96 anti-HSV triterpenoids of 7 different classes are documented here, among these, cycloartane and *seco*-cycloartane skeleton bearing triterpenoids appear to exert better activity. However, non-identical test conditions and the absence of target-specific evaluation emphasize further extensive preclinical evaluation for the development of clinically relevant drug candidates.

*Cycloartane triterpenes*

A series of cycloartane triterpenoids, pseudolarnoids (**104–113**), isolated from the seeds of *Pseudolarix amabilis* (J. Nelson) Rehder were evaluated for their anti-viral effect against HSV-1 *in-vitro* via the cytopathic effect (CPE) assay. Among these, pseudolarnoid F (**107**), pseudolarolide C (**108**), and pseudolarolide C acid (**109**) demonstrated potent anti-viral effects on HSV-1 with $IC_{50}$ 15.3 ± 1.9, 1.1 ± 0.2, and 4.3 ± 0.4 μM and TI of 2.4 ± 0.3, 6.8 ± 0.9, and 7.8 ± 0.7, respectively (Table 1) against acyclovir as a positive control ($IC_{50}$11.9-± 1.4, TI > 50), while others were inactive (Zhao et al. 2020). The report further emphasized that among the compounds bearing the 3,4-*seco*-cycloartane with a spiro lactone moiety (**104**, **106**, **108**, and **109**), only **108** could demonstrate a potent anti-HSV effect owing to the presence of C-3 -OMe and a saturated *γ*-lactone (ring F) with a C-25 *β*-Me. Further, among the cycloartanes possessing side chains at C-17 (**107** and **110**), the unsaturation has diminishing effect (Zhao et al. 2020).

Another investigation, reported that among the cycloartanes (**10–23**) of *Lyonia ovalifolia*, **10**, **11** and **13** displayed potent inhibition with $IC_{50}$ values of 11.1 ± 2.31, 3.7 ± 1.35, and 11.1 ± 1.65 μM (Table 1) while 3α-[(6-*O*-acetyl-*β*-D-glucopyranosyl)-oxy]-24S-[(α-L-arabinopyranosyl)-oxy]-25-hydroxy-9,10-*seco*-cycloartan-1(10)-en-30-oic acid (lyonifoloside H; **20**) displayed moderate activity ($IC_{50}$ 19.3 ± 3.31 μM). They displayed SI of 2.1, 4.3, 5.2, and > 5.2 respectively (Lv et al. 2016). Aglycone devoid of C-3 glycosidic linkage demonstrated greater activity this suggests the possible involvement of the C-3 –OH group. Further, the side chain bearing different substitutions was also important for the activity.

An investigation, by Shamsabadipour and co-workers, on the aerial parts of an Iranian plant, *Euphorbia denticulate,* afforded 24-methylene-cycloart-3-ol, cycloart-23*Z*-ene-3*β*,25-diol and cycloart-23*E*-ene-3*β*,25-diol (**114**); wherein **114** showed anti-viral effect with an $EC_{50}$ value of 86.63 ± 0.03 μg/mL, and SI of 12.57 (Table 1) (Shamsabadipour et al. 2013).

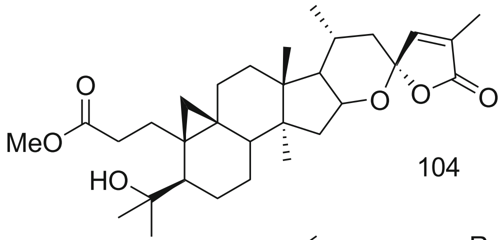

104

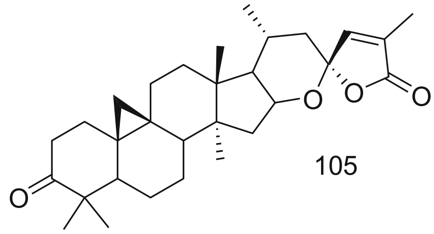

105

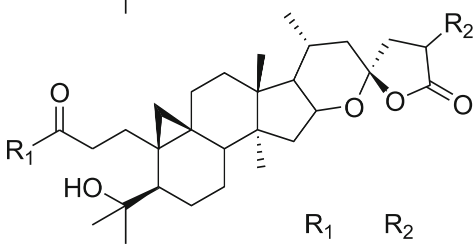

| | $R_1$ | $R_2$ |
|---|---|---|
| 106 | OMe | α-Me |
| 108 | OMe | β-Me |
| 109 | OH | β-Me |

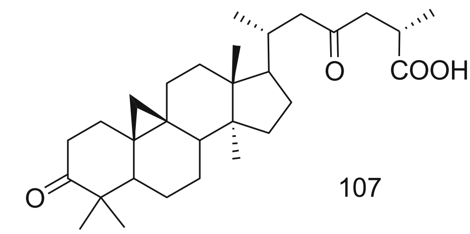

107

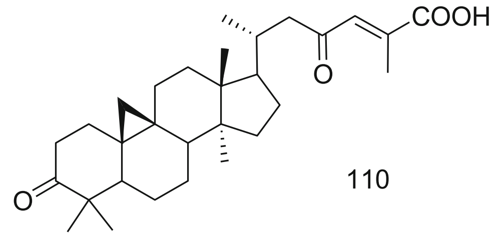

110

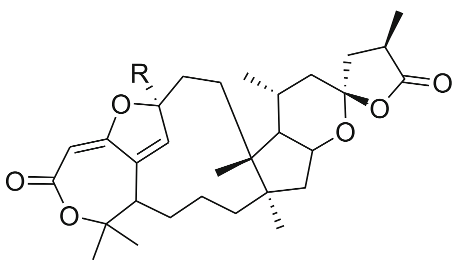

| | R |
|---|---|
| 111 | OH |
| 112 | H |

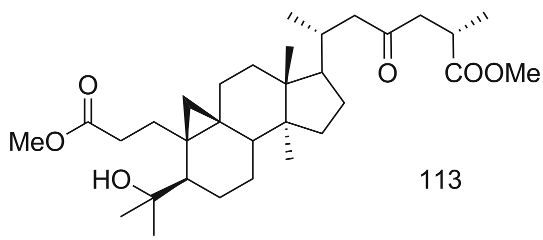

113

*Dammarane triterpenes*

An investigation on the fruits and leaves of *Aglaia erythrosperma*, reported the isolation of dammarane triterpenoids, among which cabraleahydroxylactone (**115**) showed anti-viral activity against herpes simplex virus type-1 ($IC_{50}$ 3.20 mg/mL) (Table 1), in comparison with the acyclovir ($IC_{50}$1.90 mg/mL) as a positive control. Whereas, aglinin A (**116**) was reported as a moderate inhibitor of HSV-1 (Phongmaykin et al. 2011). The greater activity demonstrated by **115** could be attributed to the basic dammarane skeleton whereas the A-ring opening (**116**) decreased the activity.

*Lanostane triterpenes*

The 24-methyl-lanostane triterpenoids, fomitopsins D-F (**117–119**), **120**, and other compounds were reported from fruiting bodies of the basidiomycete *Fomitopsis feei*. Fomitopsin D (**117**) showed activity against HSV-1 with an $IC_{50}$ value of 17 μg/mL while other compounds displayed $IC_{50}$ value > 50 μg/mL (Table 1) (Isaka et al. 2017). It is observed that the C-12 –OH bearing **117** has displayed better activity than **119** which is devoid of the –OH group. At the same time cyclization of the side-chain decreased the activity.

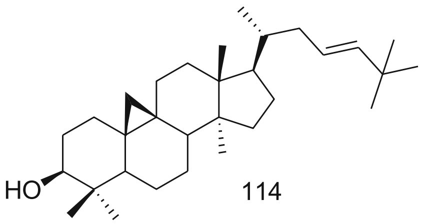

114

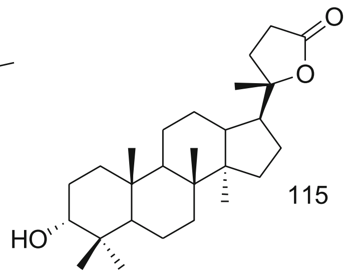

115

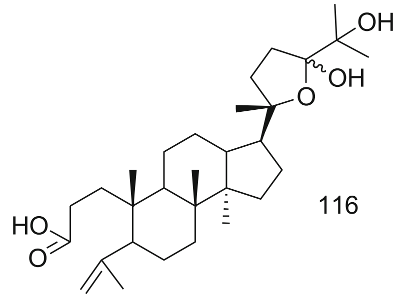

116

Among the lanostane triterpenes (**28–35**) reported by Lv et al. 2016 from leaves and twigs of *Lyonia ovalifolia* the aglycone, lyonifolic acid C (**29**), lyonifoloside M (**30**), 24(S)-[(*β*-D-glucopyranosyl)-oxy]-3α,25- dihydroxylanost-8-en-30-oic acid (lyonifoloside M; **31**) and 3α-[(6-*O*-acetyl-*β*-D-glucopyranosyl)-oxy]-24(S)-[(α-L-arabinopyranosyl)-oxy]-25-hydroxylanost-8-en- 30-oic acid (lyonifoloside P; **33**) has displayed potent activity against HSV-1 with $IC_{50}$ values of 2.1 ± 1.13, 6.4 ± 3.32, 23.1 ± 7.23, 14.3 ± 2.10 μM/L and $TC_{50}$ of 16.0 ± 2.30, 19.3 ± 0.86, 57.7 ± 6.46 and > 100 μM/L, respectively (Table 1). The better activity reported for **29** could be attributed to the absence of glycosylations; suggesting the inverse role of the bulky group against viral inhibition. This in turn signifies the role of hydroxyl groups at C-3 and the side chain. Further, acetylated-*β*-D-Glc at the C-3 position (**30**) has displayed better activity in comparison with non-acetylated-*β*-D-Glc.

*Lupane triterpenes*

Lupane skeleton bearing pentacyclic triterpenes, **121–123**, reported from *Bursera simaruba* were recorded to possess anti-HSV-1 activity with $EC_{50}$ of 26.0 ± 10.2, 17.7 ± 1.5, and 75.3 ± 6.1 μg/mL, in CPE assay, and 11.9 ± 7.0, 13.7 ± 0.3, and 88.5 ± 9.3 μg/mL, in plaque assay, respectively (Table 1). The $EC_{50}$ recorded against HSV-2 were 14.9 ± 1.4, 9.6 ± 3.6, and 110.6 ± 5.9 μg/mL, in CPE assay, and 12.4 ± 1.5, 11.8 ± 0.4, and 90.8 ± 16.3 μg/ml, in plaque assay, respectively for **121–123** (Table 1) (Álvarez et al. 2015). Among these **122** containing an additional olefinic bond exerted better activity against both HSV-1 and HSV-2 in CPE assay, however, differing results were observed in the plaque assay. Nevertheless, the lupane skeleton devoid of the –OH group at C-28 has better inhibitory potential. Similarly, betulin (**123**) from *Euphorbia denticulate* was reported for anti-HSV-1 activity ($EC_{50}$ 84.37 ± 0.02 μg/mL; Vero cells $CC_{50}$ 660.718 ± 0.072 μg/mL) and SI of 7.83 (Shamsabadipour et al. 2013).

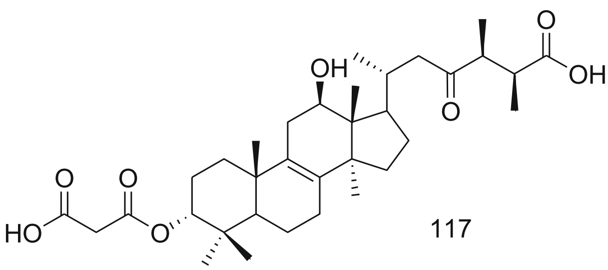

117

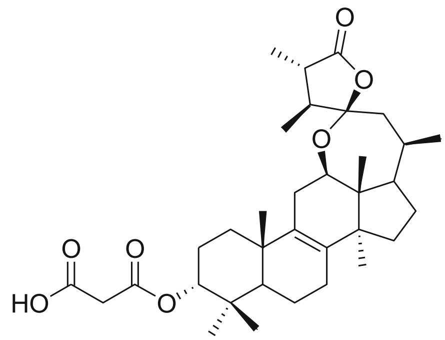

119

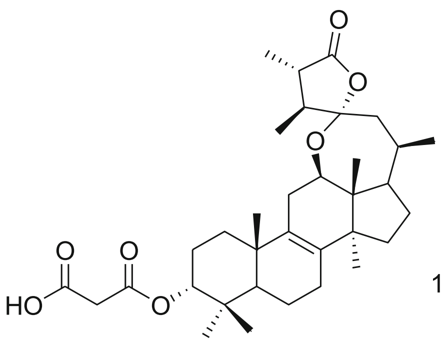

118

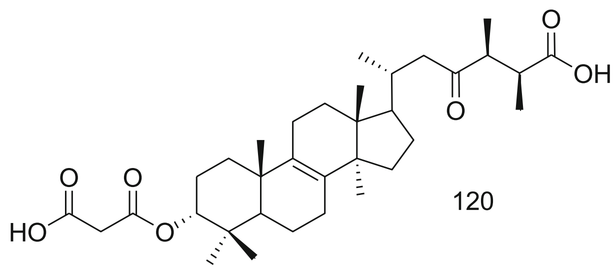

120

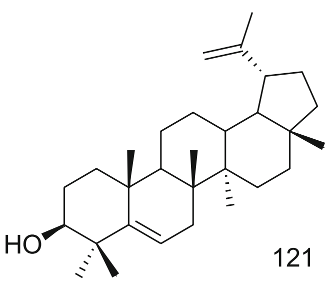

121

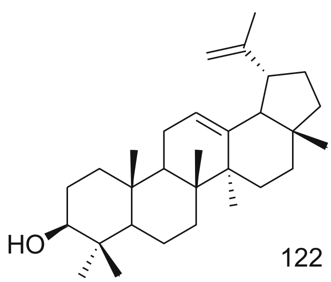

122

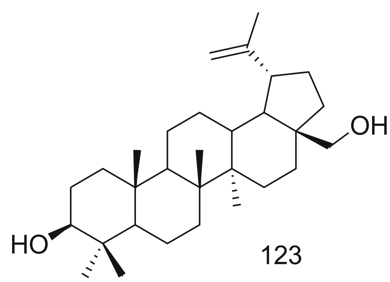

123

In another extensive phytochemical investigation on the *Rhododendron latoucheae* resulted in the isolation of 36 triterpenoids belonging to lupane, **124–132**, and ursane class. Among the lupanes, **132** and **130** displayed potent activity against HSV-1 with $IC_{50}$ of 0.71 $\pm$ 0.06 and 3.70 $\pm$ 0.2 μM, while **124** and **125** demonstrate moderate activities (Table 1). Other compounds were reported to possess $IC_{50}$ greater than 33.3 μM (Liu et al. 2019). This suggests a possible involvement of trans-feruloyl substitution at the C-3 position for enhancement of the activity. However, cis-feruloyl substitution led to a decrease in potency. Furthermore, 3,20-dioxo-30 nor-lupane skeleton (**124**, **125**) displayed moderate activity, confirming the importance of the C-3 position.

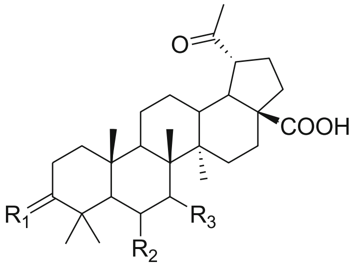

| | R1 | R2 | R3 |
|---|---|---|---|
| 124 | =O | H | $\beta$–OH |
| 125 | =O | $\alpha$–OH | H |
| 126 | $\beta$–OH | *H* | H |

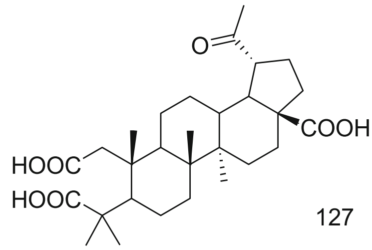

127

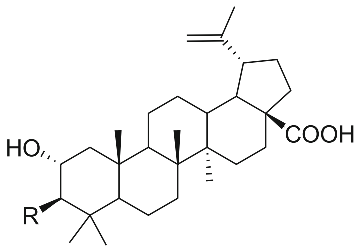

| | R |
|---|---|
| 128 | OH |

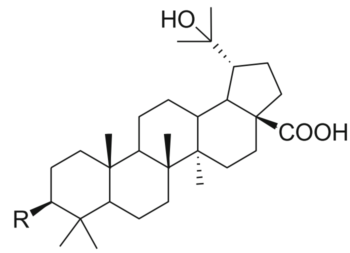

| | R |
|---|---|
| 131 | OH |

132

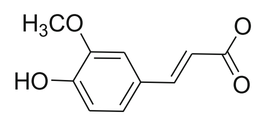

129

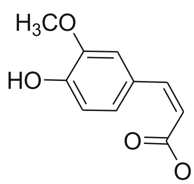

130

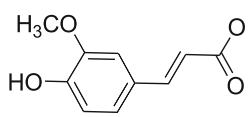

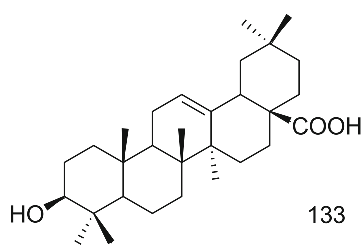

133

*Oleanane triterpenes*

Oleanolic acid (**133**) from the roots of *Achyranthes aspera* is reported by Mukherjee and co-workers to possess anti-HSV-1 and 2 potentials with $EC_{50}$ 6.8 and 7.8 µg/mL (Table 1), respectively. It is reported a maximum activity at 2–6 h post-infection and exerted its action by inhibiting early-stage multiplication with an SI value of 12 (Mukherjee et al. 2013).

GA (**36**) well known to appear from the *Glycyrrhiza glabra* demonstrated strong anti-HSV-1 activity in HeLa cells on simultaneous addition with the viruses, whereas rapamycin had no activity. An improved antiviral effect was reported on the addition of **36** to the cells 24 h before the viruses due to the production of a higher amount of autophagy activator Beclin 1 by establishing resistance to the HSV-1 replication. Under these settings, rapamycin was reported to display a significant anti-HSV-1 activity (Laconi et al. 2014).

In another investigation, acylated oleanane triterpenes, **134–138**, were isolated from the hydrolysis product of the extract obtained from the flower buds of *Camellia sinensis*. These compounds demonstrated anti-HSV-1 effects at 10 µM in Vero cells; wherein **138** displayed 20.5% inhibition at 2.5 µM, an equivalent inhibitory effect as oleanolic acid [inhibition (%): 13.1 ± 1.8 at 2.5 µM] (Table 1) (Yoneda et al. 2018). This suggests that the modifications are favorable for the activity in comparison with oleanolic acid (**133**), however, these may be considered as moderate inhibitors.

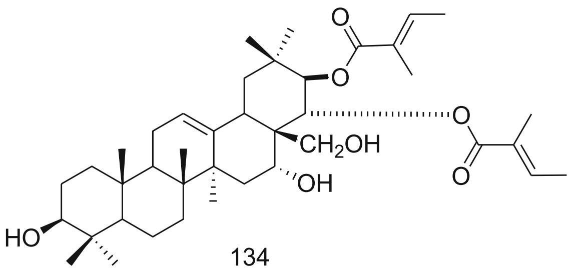

134

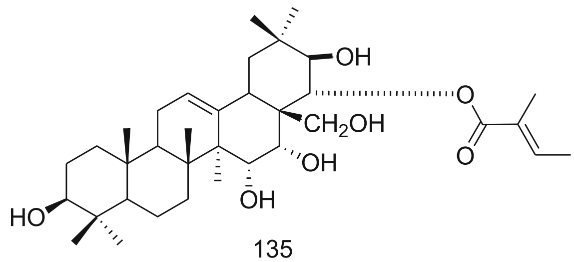

135

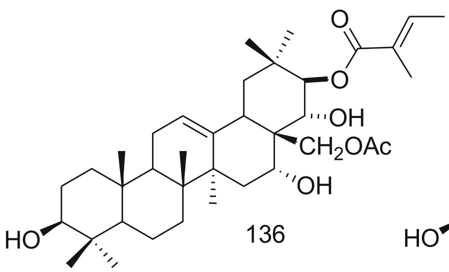

136

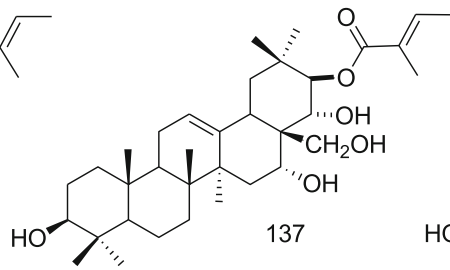

137

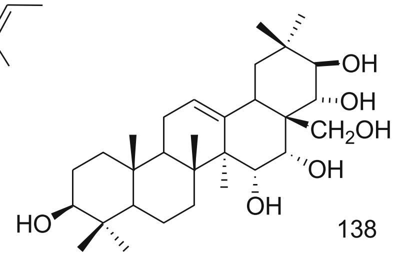

138

The oleanane triterpenoids of *Rhododendron latoucheae*, **139–145**, were evaluated against HSV-1 wherein **139**, **140**, and **143** displayed potent inhibition of the virus with $IC_{50}$ of 3.70 ± 0.3, 8.62 ± 0.5, and 3.70 ± 0.3 μM respectively against HSV-1 F strain VR 733 in the Vero cells (Table 1) (Liu et al. 2019). Among these, the quinonoid triterpenoids **139** and **140** displayed greater inhibition suggesting the possible involvement of A-ring in the potentiation of the activity. It is pertinent to mention that the substitution pattern on the A ring is crucial for the activity as the methylation at the C-4 position resulted in an almost three-fold decrease in the activity. Another compound, **143**, bearing a trans-feruloyl substitution at the C-3 position also exerted comparable activity with that of **139**. Other oleanane derivatives displayed $IC_{50}$ > 33.3 μM suggests that cis-feruloyl substitution at C-3 position is unfavorable for the activity along with 11–12 epoxidation (**145**) and poly hydroxylation at A ring (**144**) (Liu et al. 2019).

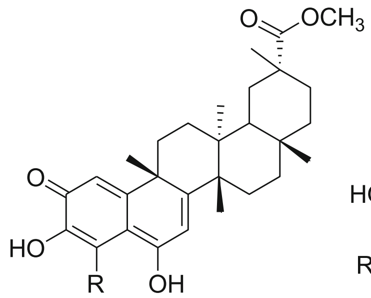


| | R |
|---|---|
| 139 | H |
| 140 | $CH_3$ |

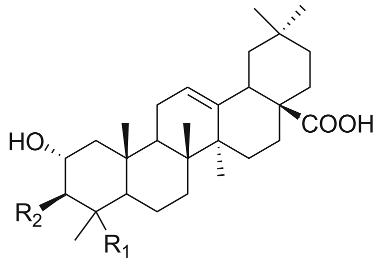


| | R1 | R2 |
|---|---|---|
| 141 | $CH_3$ | OH |
| 142 | $CH_3$ | 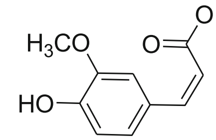 |
| 143 | $CH_2OH$ | 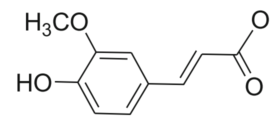 |

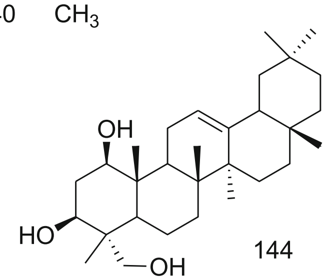


144

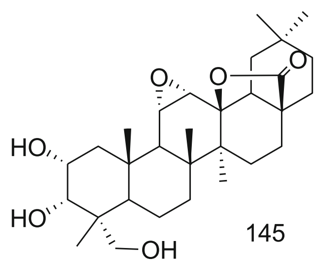


145

*Ursane triterpenes*

Among the rhodoterpenoids A (**146**), B (**147**), C, and D (**148**), isolated from *Rhododendron latoucheae* by Liu and co-worker, **146** and **148** were reported as excellent anti-HSV-1 triterpenes with $IC_{50}$ values of 8.62 and 6.87 μM (Table 1) and SI of 2.2 and 7.0, respectively in comparison with the acyclovir ($IC_{50}$ 0.41 μM; SI > 100) (Liu et al. 2017). The **146** and **147** were reported to possess an unprecedented 5/7/6/6/6-fused pentacyclic ring system. It was further detailed by the authors that the methylene at C-16 in **146** is extremely essential for the anti-HSV-1 activity. Its replacement with the keto group resulted in the loss of activity (**147**) (Liu et al. 2017).

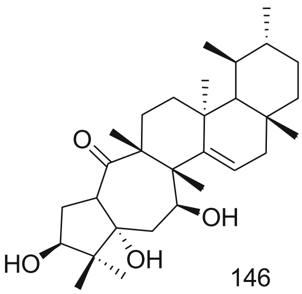

146

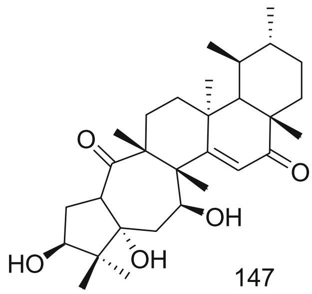

147

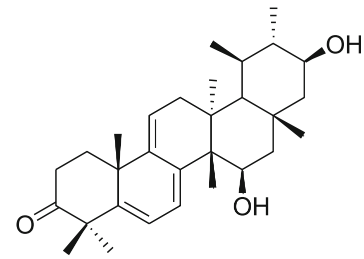

148

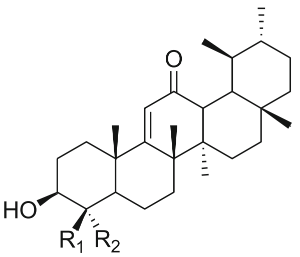

| | $R_1$ | $R_2$ |
|---|---|---|
| 149 | $CH_3$ | $CH_2OH$ |
| 150 | $CH_2OH$ | $CH_3$ |
| 151 | COOH | $CH_3$ |

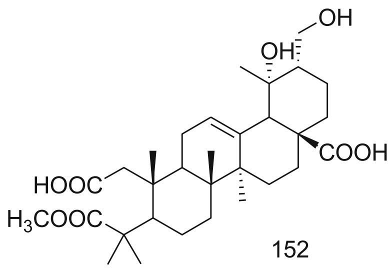

152

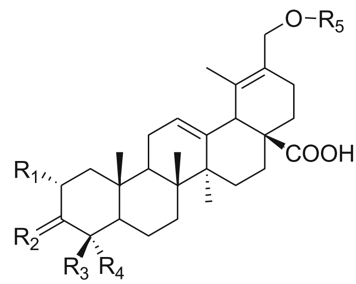

| | $R_1$ | $R_2$ | $R_3$ | $R_4$ | $R_5$ |
|---|---|---|---|---|---|
| 153 | OH | α-OH | $CH_3$ | $CH_2OH$ | $CH_2CH_3$ |
| 154 | H | α-OH | $CH_2OH$ | $CH_3$ | $CH_2CH_3$ |
| 155 | H | =O | $CH_2OH$ | $CH_3$ | H |

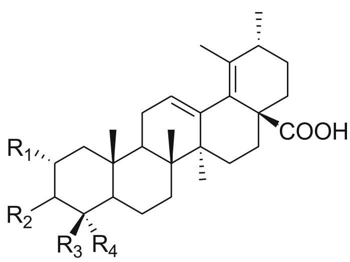

| | $R_1$ | $R_2$ | $R_3$ | $R_4$ |
|---|---|---|---|---|
| 156 | OH | α-OH | $CH_2OH$ | $CH_3$ |
| 157 | OH | α-OH | $CH_3$ | $CH_2OH$ |

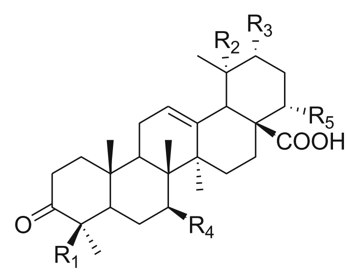

| | $R_1$ | $R_2$ | $R_3$ | $R_4$ | $R_5$ |
|---|---|---|---|---|---|
| 158 | $CH_2OH$ | OH | $CH_3$ | H | OH |
| 159 | $CH_3$ | H | $CH_2OH$ | OH | H |

Another investigation on *Rhododendron latoucheae* identified **149–168** displaying $IC_{50}$ in the range of 1.23 to 33.33 μM (Table 1) (Liu et al. 2019). Ursane triterpenes bearing trans-feruloyl substitution at the C-3 position (**166**, **167**) displayed potent activity, while cis-feruloyl led **168** to lose the activity. A-ring opened **152** also displayed significant activity, thus signifying the potential role of the A-ring pattern and substitution towards the potency. Further modification and substitutions at different positions decreased the potency.

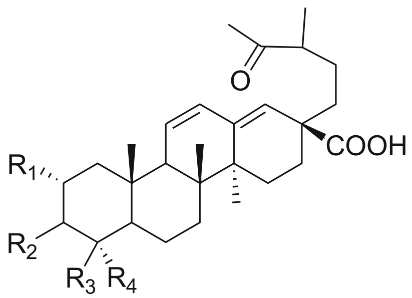

| | $R_1$ | $R_2$ | $R_3$ | $R_4$ |
|---|---|---|---|---|
| 160 | H | β-OH | $CH_2OH$ | $CH_3$ |
| 161 | OH | β-OH | $CH_3$ | $CH_3$ |

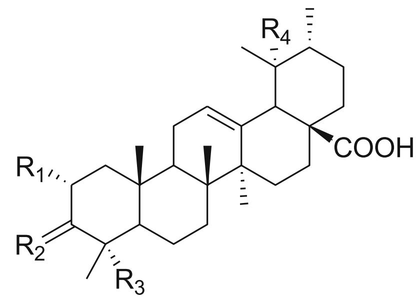

| | $R_1$ | $R_2$ | $R_3$ | $R_4$ |
|---|---|---|---|---|
| 162 | OH | β-OH | $CH_3$ | H |
| 163 | H | =O | $CH_2OH$ | OH |
| 164 | H | β-OH | $CH_3$ | OH |
| 165 | OH | α-OH | $CH_2OH$ | OH |

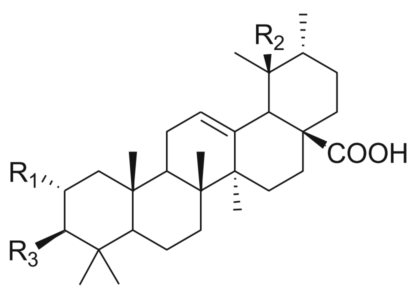

| | $R_1$ | $R_2$ | $R_3$ |
|---|---|---|---|
| 166 | H | OH | 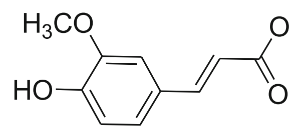 |
| 167 | OH | H | 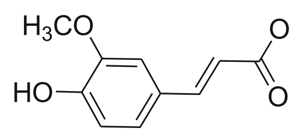 |
| 168 | H | OH | 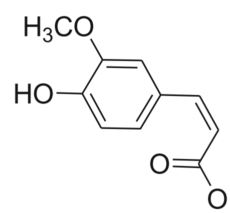 |

In another investigation, two interesting sulfur-containing triterpenoid saponins, asprellanoside A (**169**) and oblonganoside H (**170**), were reported from the roots of *Ilex asprella*, which showed anti-HSV-1 activities with a total inhibitory concentration of 0.14 and 0.18 mM (Table 1), respectively, while their maximal noncytotoxic concentrations (MNCC) against Vero cells (African green monkey kidney cells) were higher than 1.00 mM, wherein acyclovir displayed $IC_{50}$ of 0.0043 mM (Zhou et al. 2012). These compounds may be considered as moderate inhibitors of the HSV-1; however, the role of the $SO_3H$ group should be explored further as the other saponins devoid of this group were reported inactive in this study.

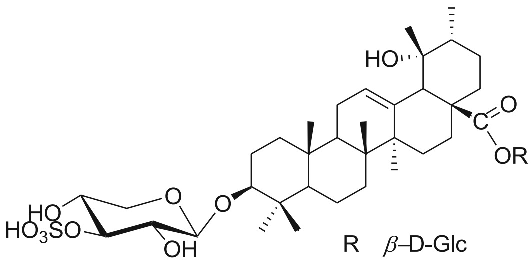


169

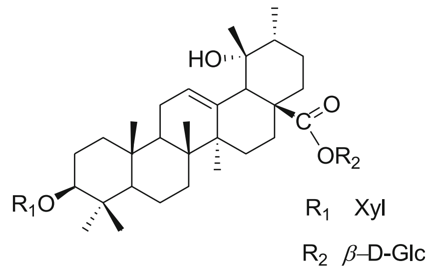


170

*Nor-terpenes*

The last investigation document here reported a bioassay-guided fractionation and purification of 14 triterpenoids namely schinchinenins A-H, schinchinenlactones A-C, and henrischinins A-C (**171–176**), from the leaves and stems of *Schisandra chinensis.* Among these **175** was found to be the most active inhibitor of HSV-2, with an excellent selectivity index of 29.95 (Song et al. 2013).

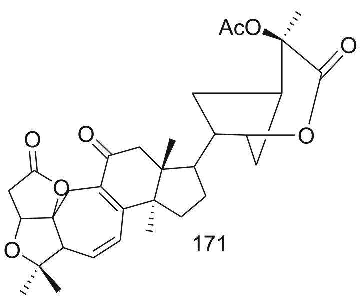

171

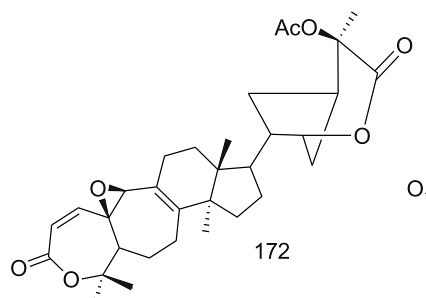

172

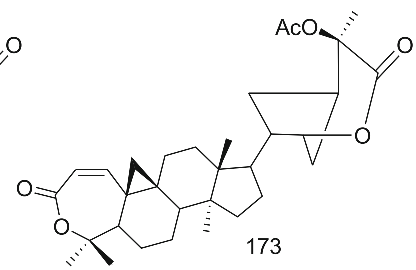

173

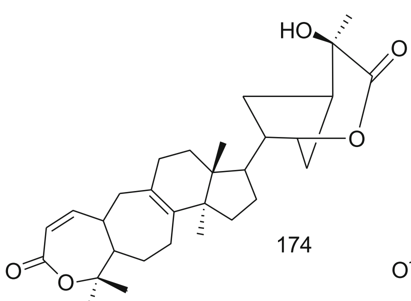

174

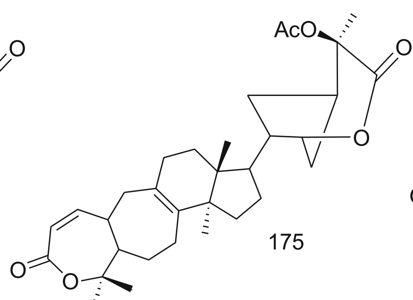

175

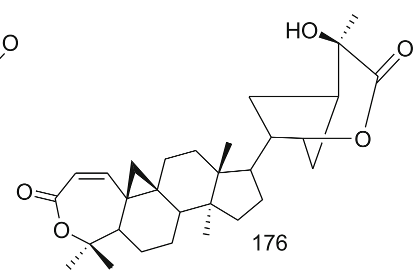

176

Broadly these triterpenes can be classified under the *seco*-cycloartanes type terpenes bearing a unique 5/5/7/6/5-fused pentacyclic ring system with a 3-one-2-oxabicyclo-[3.2.1]-octane moiety. Further, it could be noted that substitution at the C-25 position with acetyl/hydroxyl groups is essential for the activity (Song et al. 2013; Xia et al. 2015).

Human Immunodeficiency Virus (HIV)

HIV (human immunodeficiency virus) is a single-stranded RNA retrovirus that belongs to the genus *Lentivirus.* The viral RNA is converted to double-stranded DNA using reverse transcriptase (RT) enzyme which is an RNA-dependent DNA polymerase enzyme. HIV primarily shakes the human immune system by attacking $CD4^+$ T cells and macrophages. The destruction of CD4 cells reduces cell-mediated immunity among infected patients thus increasing the risk for the development of opportunistic infections like pneumonia, tuberculosis, other common bacterial and viral infections. When $CD4^+$ T-lymphocyte count drops due to gradual destruction by HIV, this stage is referred to as Acquired Immunodeficiency Syndrome (AIDS). Patients with AIDS are particularly susceptible to lymphomas and Kaposi's sarcoma (Barré-Sinoussi et al. 2013; Deeks et al. 2021; Vijayan et al. 2017).

The development of anti-retroviral therapy (ART) has resulted in the slow progression of the disease and lower viral loads among HIV patients enabling them to live a healthy and productive life. ART also reduces the risk of transmission of HIV during pregnancy and breastfeeding (Simon et al. 2006; Bell and Noursadeghi 2018). Despite this only 67% of people out of 38 million cases globally have access to anti-retroviral drugs and around 7.1 million cases went undiagnosed (https://www.avert.org/global-hiv-and-aids-statistics). Being a virus of severe health concern, several studies have chalked out the role of triterpenoids against HIV as summarized below.

All together 66 triterpenoids belonging to five classes were retrieved from the literature during the study period and they displayed activity in the μM or μg level, however, non-uniform experimental conditions across the studies make it strenuous to draw a determinative conclusion. Nevertheless, 6/6/6/6/5 and 6/6/6/5 skeleton bearing triterpenes i.e. lupane and dammarane have displayed potent activities. The anti-HIV triterpenes also displayed a higher number of structural modifications through side-chain cyclization, ring-opening, and ring expansions. Thus these molecules could offer better selectivity towards other viruses as well and need experimental validation for their clinical development.

*Cycloartane triterpenes*

An investigation by Wu et al. 2019 on the roots of *Souliea vaginata* resulted in the isolation of cycloartane triterpenoids (**177–188**). They feature unique structural modifications on the side chain resulting in additional rings. Among these, beesioside I (**177**), a tetracyclic cycloartane bearing pendant tetrahydrofuran at C-17, exhibited the highest potency against HIV-1NL 4–3 in MT-4 cells with an $EC_{50}$ value of 2.32 ± 0.46 μM ($CC_{50}$ > 40 mM) (Table 1) using azidothymidine (AZT) as a standard drug. It was further reported that the presence of oxygen bridge between C-18/C-24 and substituent present on side-chain might also influence the anti-HIV activity; as **178**, **180**, and **186** displayed significant loss in the activity, while **179**, **181**, and **185** were inactive. Further, acetylation of hydroxyl groups at C-15 and C-16 on the D-ring favored the activity (Wu et al. 2019). Several semi-synthetic derivatives were also prepared wherein small modification on aglycone moiety of the **177** could remarkably enhance the antiviral activity. Mainly, the introduction of an acyl group at the C-3 position led to significant enhancement in both anti-HIV potency and selectivity index (Wu et al. 2019)

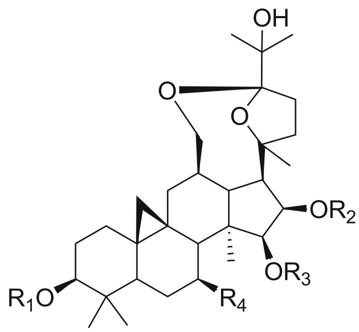

| | $R_1$ | $R_2$ | $R_3$ | $R_4$ |
|---|---|---|---|---|
| 177 | β-D-Xyl | Ac | Ac | H |
| 178 | β-D-Xyl | Ac | H | H |
| 179 | β-D-Xyl | Ac | H | OH |

Ac = $-COCH_3$

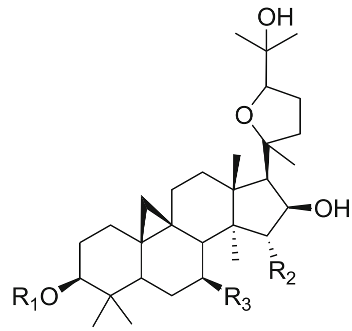

| | $R_1$ | $R_2$ | $R_3$ |
|---|---|---|---|
| 180 | β-D-Xyl | OAc | H |
| 181 | β-D-Xyl | OH | OH |
| 182 | α-L-Rha(1→2)-β-D-Xyl | H | OH |
| 183 | β-D-Glc(1→3)-α-L-Rha(1→2)-β-D-Xyl | H | H |

.

On the same line triterpenoids, **189–196**, isolated from *Kadsura heteroclite* were tested for their potential to inhibit HIV-1 protease and reverse transcriptase (RT) (Xu et al. 2010). Among these **194** and **195** showed strong and **196** showed moderate inhibition of HIV-1 PR, while others were weakly active (Table 1). The greater activity displayed by **194** and **195** could be attributed to the groups generated due to A-ring opening i.e. 3,4-*seco*-cycloartane skeleton. Further cyclization of the side-chain led to a decrease in the activity (Xu et al. 2010).

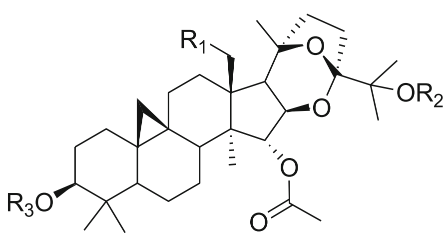

| | $R_1$ | $R_2$ | $R_3$ |
|---|---|---|---|
| 184 | H | H | β-D-Xyl |
| 185 | OH | H | β-D-Xyl |
| 186 | H | β-D-Glc | β-D-Xyl |

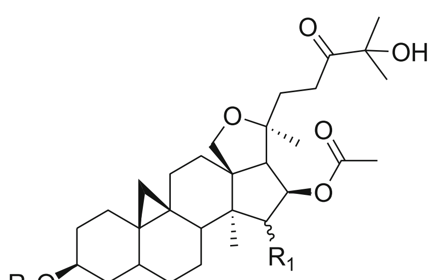

| | $R_1$ | $R_2$ |
|---|---|---|
| 187 | α-OH | β-D-Xyl |
| 188 | β-OAc | β-D-Xyl |

Another study reported the isolation of cycloartane nigranoic acid (**195**), lancifoic acid A (**197**), schisphendilactone A and B (**198–199**), and lanostane triterpenes from the stems of *Schisandra sphenanthera*. Among these **197**, possessing a 2,3-*seco*-cycloartane skeleton bearing –COOH and –OH groups, showed promising anti-HIV-1 activity ($EC_{50}$ 0.52 μg/mL) with a TI of 117.12 (Liang et al. 2014). The absence of the –OH group, as in **195**, resulted in a multifold loss of activity (TI 2.03) (Table 1) (Liang et al. 2014).

*Dammarane triterpene*

A 3,4-*seco*-dammarane triterpenoid, dammarenolic acid (**200**), was identified from the bark of *Aglaia ignea* to inhibit HIV-1 (NL4-3) ($IC_{50}$ 0.48 μg/mL; Table 1) (Esimone et al. 2010). It also displayed cytotoxicity and inhibited cell proliferation at a relatively higher concentration of 10.69 μg/mL. The methyl ester analog, methyldammarenolate, was found to be inactive against HIV-1; thus signifies the role of the acid group for the activity (Esimone et al. 2010).

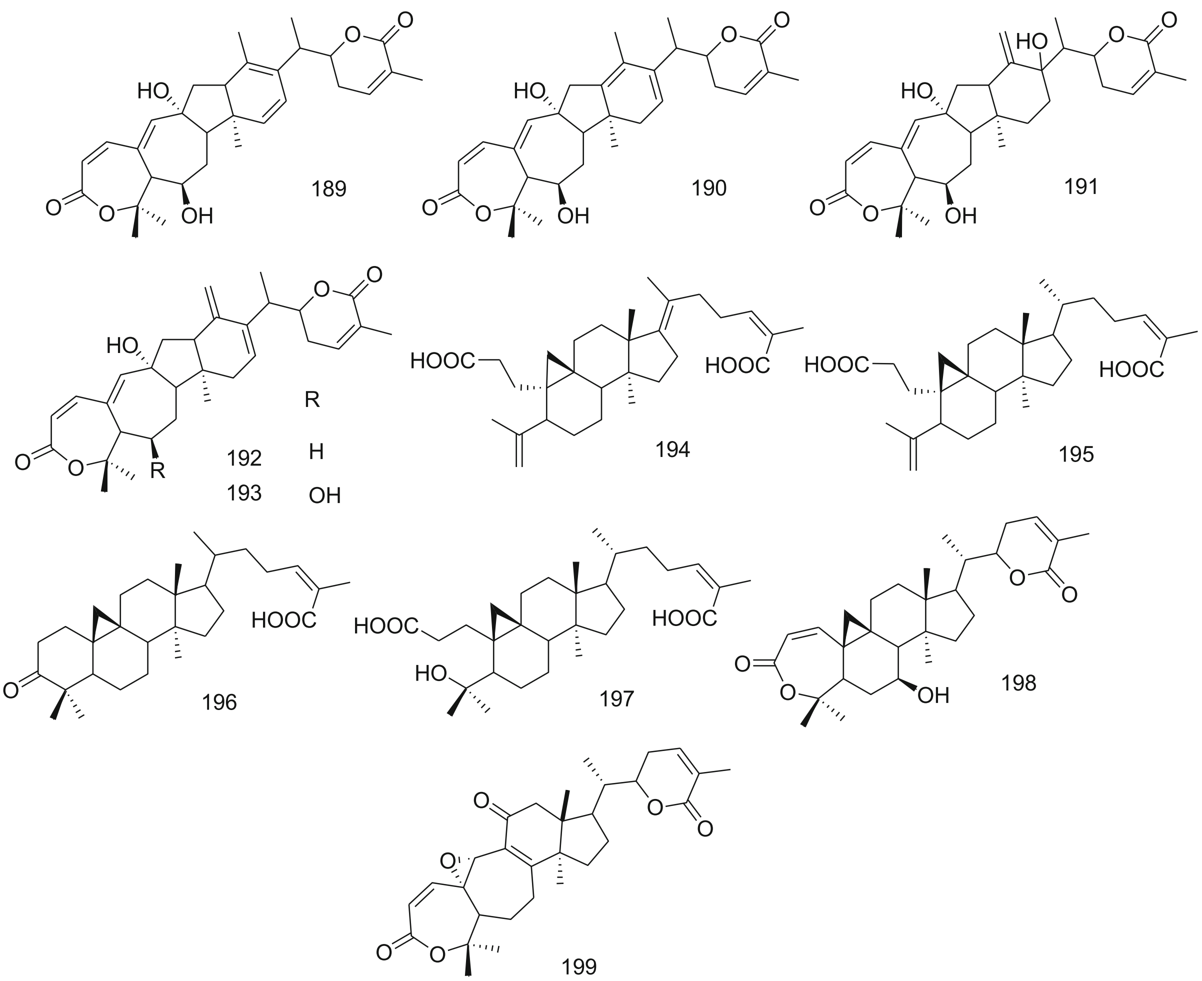

*Lanostane triterpenes*

Among the lanostanes, kadcotriones A – C (**201–203**), and 12-$\beta$-hydroxycoccinic acid (**204**) isolated from stems of *Kadsura coccinea*, **201** and **204** were reported to exert anti-HIV-1 activities ($EC_{50}$ 30.29 and 54.81 µM) and considered weak inhibitor in comparison with AZT ($EC_{50}$ 0.02 µM) (Table 1). Compound **201** featured a 12,14-$\beta$-dimethyl 6/6/6-fused tricyclic skeleton, while **202** and **203** were possessing a 6/6/5-ring system (Liang et al. 2013). As mentioned in the cycloartane section, the lanostanes, kadsuric acid (**205**)**,** of *Schisandra sphenanthera* also displayed considerable activity ($EC_{50}$ 8.23 µg/mL; TI 5.98) (Table 1) (Liang et al. 2014).

*Lupane triterpenes*

An investigation on the stem of *Cassine xylocarpa* and root bark of *Maytenus cuzcoina* resulted in the identification lupane type triterpenoids (**206–231**) possessing an inhibitory effect on HIV replication in type 1 X4 tropic recombinant virus (NL4.3-Ren) infected in a lymphoblastoid cell line (MT-2) (Callies et al. 2015). The triterpenoids **206–208**, **212**, **215–217**, **220**, **222**, **227**, **228**, and **230** had displayed more than 50% inhibition at 10 µM, among which 3-oxolup-20(29)-en-30-al (**212**) exhibited the most potent activity with $IC_{50}$ of 1.4 ± 0.2 µM (Table 1).

Contrastingly, **217** and **215** displayed selectivity index (SI: ratio $CC_{50}/IC_{50}$) as high as 24.5 and 14.3 suggesting that these triterpenes could be further developed as potential leads (Callies et al. 2015). Further, the investigator detailed that oxygenation led to an increase in the activity as compound bearing two oxygen groups displayed better activity (**222**, **227**, **123**, and **229** in comparison with **221**; **220** with **219** and **206** with **213**) (Table 1) (Callies et al. 2015).

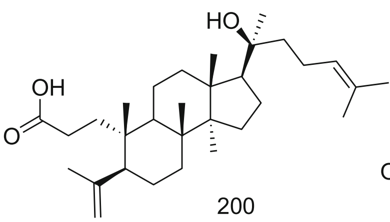

200

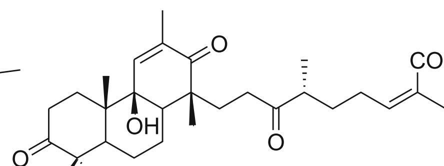

201

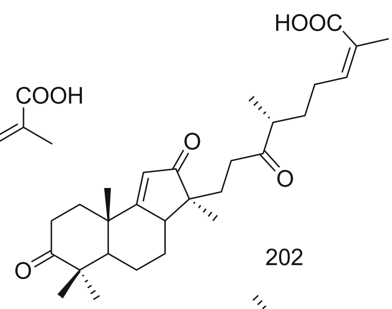

202

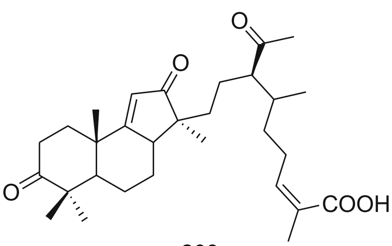

203

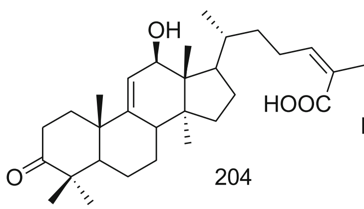

204

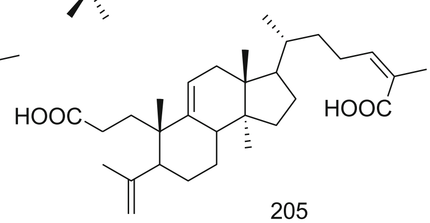

205

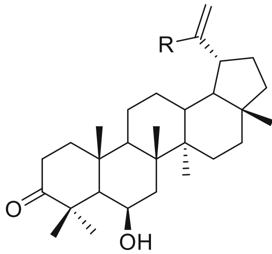

| | R |
|---|---|
| 206 | $CH_2OH$ |
| 207 | CHO |

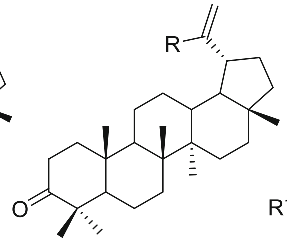

| | R |
|---|---|
| 208 | COOH |
| 212 | CHO |
| 213 | $CH_2OH$ |
| 214 | H |

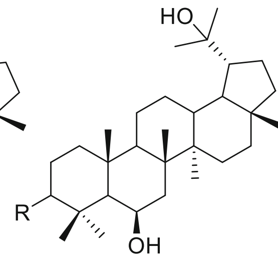

| | R |
|---|---|
| 209 | OH |
| 215 | =O |

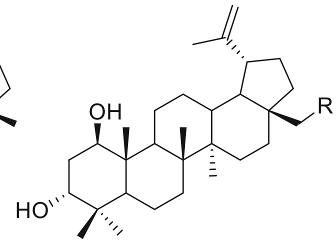

| | R |
|---|---|
| 210 | OH |
| 216 | H |

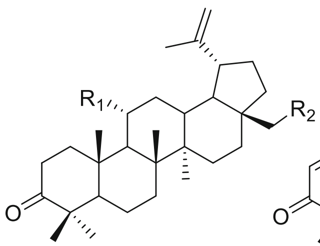

| | $R_1$ | $R_2$ |
|---|---|---|
| 211 | OH | OH |
| 217 | H | OH |
| 218 | OH | H |

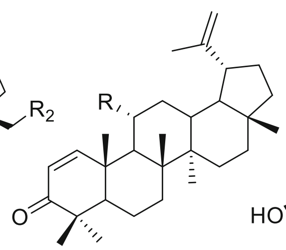

| | R |
|---|---|
| 219 | H |
| 220 | OH |

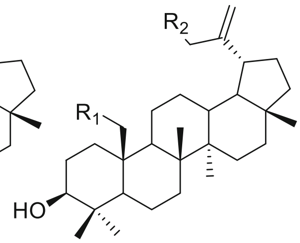

| | $R_1$ | $R_2$ |
|---|---|---|
| 221 | H | H |
| 222 | OH | H |
| 223 | H | OH |

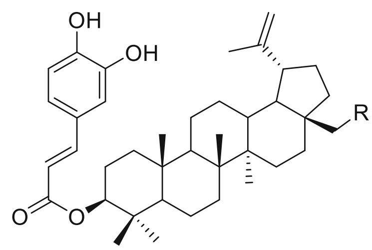

| | R |
|---|---|
| 224 | H |
| 225 | OH |

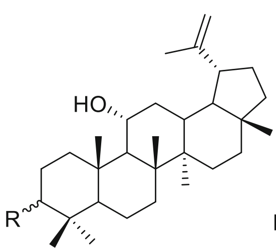

| | R |
|---|---|
| 226 | $\alpha$-OH |
| 227 | $\beta$-OH |

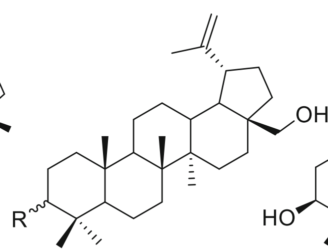

| | R |
|---|---|
| 228 | $\alpha$-OH |

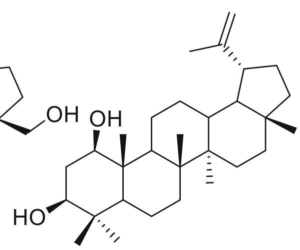

229

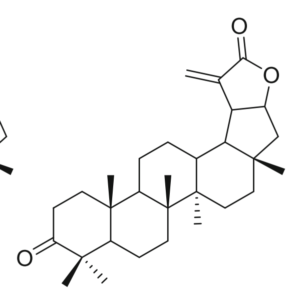

230

*Oleanane triterpenes*

An extensive investigation on *Glycyrrhiza uralensis* by Song et al. 2014c reported licorice saponin E2 (**231**), licorice saponin B2 (**232**), araboglycyrrhizin (**233**), 22$\beta$-acetoxyglycyrrhizin (**234**), 22$\beta$-acetoxyglycyrrhetaldehyde, and 3-*O*-$\beta$-D-glucuronopyranosylglycyrrhetinic acid (**235**) to possess anti-HIV potential

(Li-Yang et al. 2007; Kitagawa et al. 1993; Song et al. 2014c). These compounds were found to be weak inhibitors of the virus in comparison with efavirenz ($IC_{50}$ of 0.0015 μM) (Table 1). The glycyrrhetinic acid without substitution at C-3 position displayed better activity led the author to conclude that substitution with gluA is not favored for the activity (Song et al. 2014c).

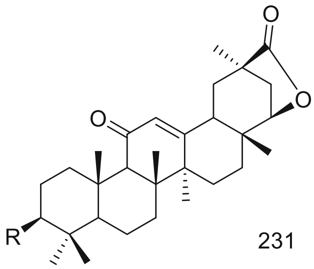


231

R

3–O–[β-D-gluA-(1→2)-β-D-gluA]

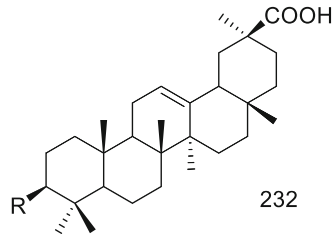


232

R

3–O–[β-D-gluA-(1→2)-β-D-gluA]

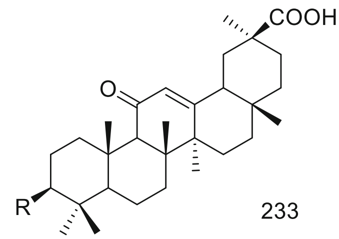


233

R

3–O–[α-L-ara-(1→2)β-D-gluA)]

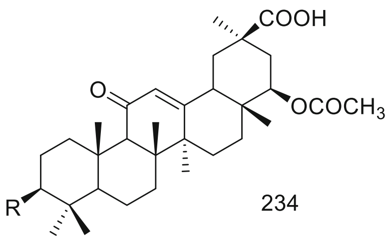


234

R

3–O–[β-D-gluA-(1→2)-β-D-gluA]

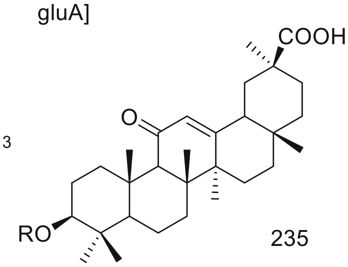


235

R

β-D-GluA

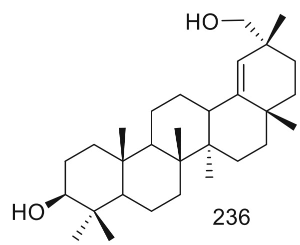


236

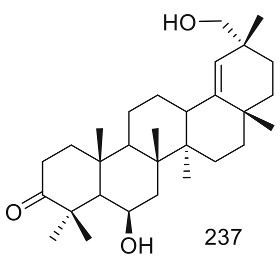


237

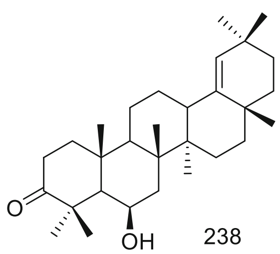


238

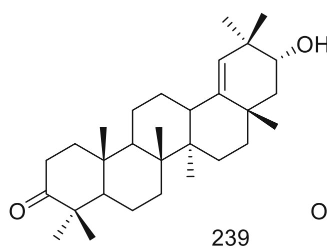


239

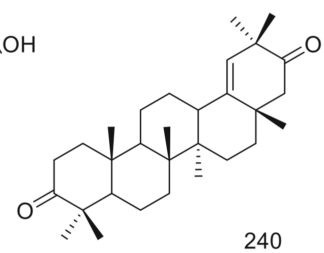


240

Another investigation reported potent anti-HIV oleanane triterpenes, **236–240**, from the stems of *Cassine xylocarpa*. All the compounds displayed varying inhibition of HIV replication in the X4 tropic HIV (NL4.3-Ren) infected MT-2 cells, out of which **236** and **240** were most potent with $IC_{50}$ values of 10.38, and 4.038 μM (Table 1), respectively (Osorio et al. 2012). It is observed that the substitution pattern on the A and E-ring is crucial for the activity.

## Influenza virus (IV)

Influenza viruses (IV), causing flu, are enveloped negative sensed RNA viruses with eight segmented genomes that are members of the Orthomyxoviridae family. Four main types of influenza virus, influenza A, B, C, and D are known, among which influenza A-C can infect human beings, whereas type D is assumed to have the potential to infect animals. A subtype of influenza A virus H1N1 is liable to cause Spanish flu pandemics in 1918 and swine flu in 2009 (Lim and Mahmood 2011; Li et al. 2019b). The surface glycoproteins such as hemagglutinin (HA or H) and neuraminidase (NA or N) are responsible for the differentiation between the subtypes of influenza A. The available therapeutic interventions include yearly vaccination as recommended by WHO and anti-viral agents like oseltamivir. However, these viruses regularly change their surface glycoprotein hemagglutinin (HA or H) leading to antigenic variations. Despite the availability of vaccines, the continuous changes in the antigenic variations and emergence of drug-resistant strains such as Tamiflu-resistant 2005 H5N1 influenza A are the major threats caused by this virus (Das 2012).

The life cycle of the influenza virus briefly includes the following steps—(i) cell surface binding via hemagglutinin (HA) and fusion (ii) release of viral ribonucleoprotein complex (vRNP) into the host cell cytoplasm mediated by M2 protein, (iii) transcription and replication (iv) viral assembly and budding (Watanabe et al. 2017). Some of these processes have been utilized for the development of potential drug targets includes M2 ion channel protein inhibitors, neuraminidase inhibitors (Das 2012), virus nucleoprotein inhibitors (Hu et al. 2017), and hemagglutinin inhibitor (Li et al. 2015), besides viral replication inhibitors and others. It is relevant to highlight that several natural products have been reported to possess anti-influenza activity and summarized earlier (Musarra-Pizzo et al. 2021).

A large number of triterpenes (117) were found in the literature to possess anti-IV potential in the eight different studies bearing four triterpenoid skeletons. Unlike other viruses discussed above all the studies against influenza virus were performed in the virus-infected MDCK cells but some studies were target specific i.e. Neuraminidase (NA) inhibitors. Nevertheless, most of these compounds have displayed activities in μg or μM level with $IC_{50}$ as low as 0.05 μM displayed by an oleanane triterpene. Interestingly except for the lanostanes, most of the active compounds are decorated with bulky groups such as glycosidic linkages or feruloyl moieties, suggesting their possible role in potentiating the activity. However, further experimental validation and SAR studies are required for clinical lead development.

*Cycloartane triterpenes*

In an investigation, **10–23** were evaluated for the anti-influenza A activity (A/95 −359) by the CPE inhibition method in the MDCK cells and the $IC_{50}$ values are displayed in Table 1. Aglycones (**11**, **13**) obtained by hydrolysis were reported to be the most potent compounds; suggesting that C-3 –OH is essential for the activity; whereas oxidation of hydroxyl to ketone at C-24 significantly improved the potency (Lv et al. 2016).

*Lanostane triterpenes*

Among the lanostane triterpenoids (**28–35**) reported by Lv et al. 2016, **29**, **30**, and **33** have displayed $IC_{50}$ of 3.7 ± 1.08, 11.1 ± 3.29, 33.3 ± 6.31 μM/L. Similar to the cycloartanes, C-3 –OH group and C-24 –C=O on the lanostanes were reported to be essential for the potency (Lv et al. 2016).

Neuraminidase (NA) inhibitors are the potential anti-viral agents for treating influenza. The investigation by Zhu et al. 2015 evaluated triterpenoids isolated from mushroom *Ganoderma lingzhi* against NA of several strains (H1N1, 09) NA(H1N1, N295S) NA(H3N2, E119V) NA (H5N1), and NA(H7N9). Among these triterpenoids, **241–270**, ganoderic acid T-Q (**241**), and TR (**242**) were found to be potent inhibitors of H5N1 and H1N1 NAs.

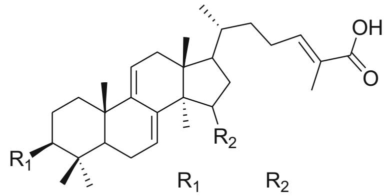

| | $R_1$ | $R_2$ |
|---|---|---|
| 241 | O | $OCOCH_3$ |
| 242 | O | OH |
| 243 | OH | $OCOCH_3$ |
| 244 | O | H |
| 245 | O | H |

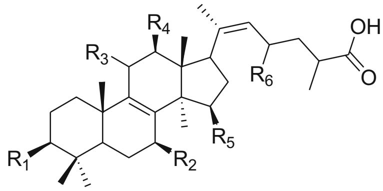

| | $R_1$ | $R_2$ | $R_3$ | $R_4$ | $R_5$ | $R_6$ |
|---|---|---|---|---|---|---|
| 247 | O | OH | O | H | OH | O |
| 251 | OH | O | O | H | O | O |
| 254 | O | O | O | H | O | O |
| 255 | OH | OH | O | H | OH | O |
| 256 | O | OH | O | H | O | H |

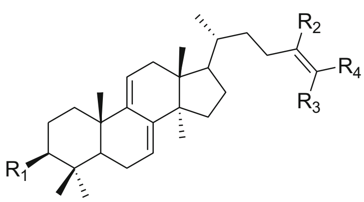

| | $R_1$ | $R_2$ | $R_3$ | $R_4$ |
|---|---|---|---|---|
| 264 | O | H | $CH_3$ | $CH_2OH$ |
| 265 | OH | H | $CH_3$ | $CH_2OH$ |
| 266 | O | H | $CH_2OH$ | $CH_2OH$ |
| 269 | OH | H | $CH_3$ | CHO |

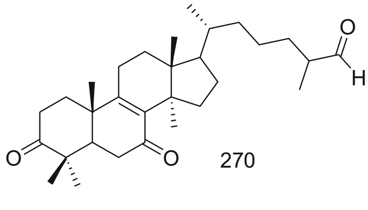

270

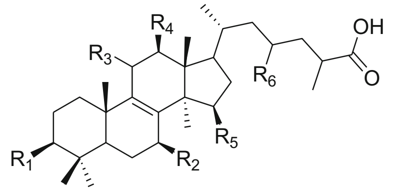

| | $R_1$ | $R_2$ | $R_3$ | $R_4$ | $R_5$ | $R_6$ |
|---|---|---|---|---|---|---|
| 246 | O | OH | O | H | OH | O |
| 248 | OH | OH | O | H | OH | O |
| 249 | OH | O | O | H | O | O |
| 250 | OH | OH | O | $OCOCH_3$ | O | O |
| 252 | OH | O | O | $OCOCH_3$ | O | O |
| 253 | OH | OH | O | H | O | O |
| 257 | OH | O | O | OH | O | O |
| 258 | O | OH | O | H | O | O |
| 260 | O | H | O | H | OH | O |
| 263 | O | O | O | $OCOCH_3$ | O | O |

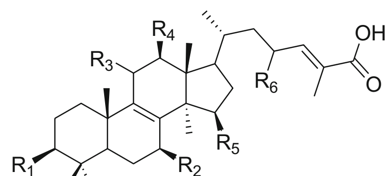

| | $R_1$ | $R_2$ | $R_3$ | $R_4$ | $R_5$ | $R_6$ |
|---|---|---|---|---|---|---|
| 259 | O | O | H | H | H | H |
| 261 | OH | O | O | H | O | OH |
| 262 | O | OH | O | H | O | OH |

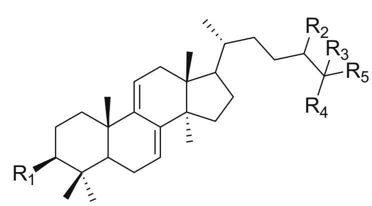

| | $R_1$ | $R_2$ | $R_3$ | $R_4$ | $R_5$ |
|---|---|---|---|---|---|
| 267 | O | OH | OH | $CH_3$ | $CH_3$ |
| 268 | O | OH | OH | $CH_3$ | $CH_2OH$ |

Among these tested triterpenoids, **241**, **242**, and **243** displayed the highest activities against the NA(H1N1,09) at 200 μM concentrations. Similarly, **241**, **242**, and **244** against NA (H1N1, N295S); **241**, **242**, and **248** against NA(H3N2, E119V); **241**, **242**, and **243** against NA (H5N1) and **251**, **254**, and **256** against NA (H7N9) displayed potent activities. However, greater inhibition was displayed by triterpenoids against H1N1, 09, and H5N1 neuraminidase with $IC_{50}$ values ranging from 1.2 ± 1.0 μM to > 200 μM. The $IC_{50}$ against H5N1 is displayed in Table 1 (Zhu et al. 2015). The in-silico studies by authors revealed that amino-acid residues Arg292 and/or Glu119 of NA were essential for the inhibition of H5N1 and H1N1. The SAR studies by the author indicated that among the three backbone skeletons, backbone A (**241–245**), unsaturation at C7/C8 and C9/C11, and carboxylic acid in the side chain were the critical determinants for the activity against N1 NA (Zhu et al. 2015). It was further detailed that $R_5$ is a critical position and acetyl or hydroxy moieties favored N1 NA inhibition (Zhu et al. 2015).

*Lupane triterpenes*

Triterpene betulinic aldehyde (**271**), isolated from the bark of *Alnus japonica* was reported to possess an anti-influenza effect against KBNP-0028 ($IC_{50}$ 12.5 μg/mL) (Table 1) compared to oseltamivir ($IC_{50}$ 0.063 μg/mL), in the egg-bit assay. Other compounds displayed $IC_{50}$ > 100 μg/mL (Tung et al. 2010).

Another study reported lupane triterpenoid saponins, **272–275**, from bark extract of *Burkea africana*. The bark extract displayed promising anti-viral effects against H3N2 influenza virus A/Hong kong/68 (HK/68) ($IC_{50}$ of 5.5 μg/mL), with no notable cytotoxicity in Madin Darby canine kidney cells. Among these saponins **272**, **274**, and **275** containing disaccharide chain, displayed weak to no anti-influenza virus activity, whereas **273** containing a branched trisaccharide moiety displayed potent inhibition with $IC_{50}$ values of 1.1 and 1.9 μM against HK/68 and Jena/8178, respectively. The $IC_{50}$ values against Jena/8178 are displayed in Table 1 (Mair et al. 2018).

The chemical investigation by Gong et al. 2017 on the aerial parts of the mangrove plant *Sonneratia paracaseolaris* resulted in the identification of compounds bearing lupane, ursane, oleanane, and cycloartane skeleton, however among these only **276** ($IC_{50}$ 28.4 μg/mL) exhibited > 50% inhibition (50 μM) against influenza A H1N1 virus (IAV) employing CPE (the cytopathic effects) assay in comparison with positive control ribavirin ($IC_{50}$ 24.6 μg/mL). The better activity of the **276** might be due to the presence of two hydroxyl moieties at C-1 and C-3, which were not seen in other isolated compounds. Other compounds (**277–281**, **221**, **123**, **128 and 38**) displayed 7–46% inhibition. This shows that the hydroxyl group substitution on A-ring might influence the activity against the H1N1 virus. Further, substitution with larger groups like *p*-coumaroyl also resulted in a significant loss in the activity (Gong et al. 2017).

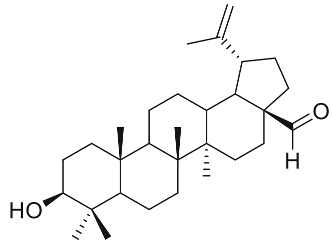

271

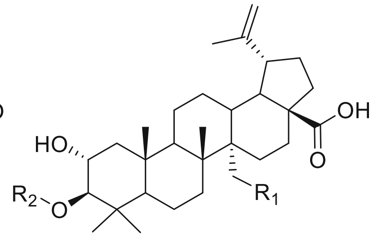

| | $R_1$ | $R_2$ |
|---|---|---|
| 272 | H | -β-Glc(2→1)-β-Xyl |
| 273 | H | -β-Glc-[(2→1)-β-Xyl]-(4→1)-α-Rha |
| 274 | OH | -β-Glc(2→1)-β-Xyl |
| 275 | OH | -β-Glc(2→1)-β-Glc |

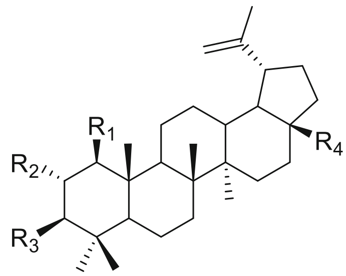

| | $R_1$ | $R_2$ | $R_3$ | $R_4$ |
|---|---|---|---|---|
| 276 | OH | H | OH | $CH_2OH$ |
| 277 | OH | H | a | $CH_2OH$ |
| 278 | OH | H | b | $CH_2OH$ |
| 279 | H | OH | a | $CH_2OH$ |
| 280 | H | OH | b | COOH |
| 281 | H | H | a | COOH |

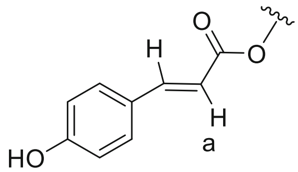

a

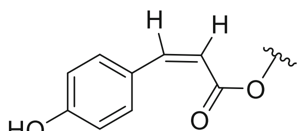

b

*Oleanane triterpenes*

In an interesting report, a total of 28 oleanane triterpenoid saponins, **36**, **231–235**, **282–303**, isolated from the roots of *Glycyrrhiza uralensis* Fisch were evaluated against influenza virus A/WSN/33 (H1N1) in MDCK cells employing Cell Titer-Glo luminescent cell viability assay (Song et al. 2014c). The oleananes were reported to have inhibitory activity against H1N1 ranging from 47.5–82.5% at 100 μM concentration; the same concentrations were significantly non-cytotoxic in the uninfected MDCK cells. Uralsaponin M (**282**), uralsaponin S (**288**), uralsaponin T (**289**), and 22β-acetoxyglycyrrhizin (**234**) exhibited good activities (Table 1) in comparison with the positive control oseltamivir phosphate ($IC_{50}$ 45.6 μM). GA (**36**), the major saponin in licorice, showed an $IC_{50}$ value of 158.0 μM (Song et al. 2014c). Saponins bearing a –$OCOCH_3$ at C-22 and –COOH at C-30 (**234**, **282**) or substitution at C-29 and C-30 (**288**, **289**) have displayed better activity than those having substitutions at other positions (**283**, **284**, **290**, **292**, **294–303**). Further studies are required to ascertain the role of the sugar chain, its length, and position.

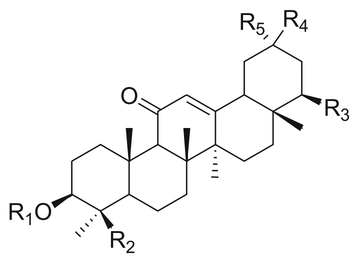

| | $R_1$ | $R_2$ | $R_3$ | $R_4$ | $R_5$ |
|---|---|---|---|---|---|
| 282 | S2 | $CH_3$ | $OCOCH_3$ | COOH | $CH_3$ |
| 283 | S2 | $CH_2OH$ | H | COOH | $CH_3$ |
| 290 | S1 | $CH_2OH$ | H | $CH_3$ | COOH |
| 292 | S1 | $CH_3$ | H | COH | $CH_3$ |
| 293 | S7 | $CH_3$ | $OCOCH_3$ | COOH | $CH_3$ |

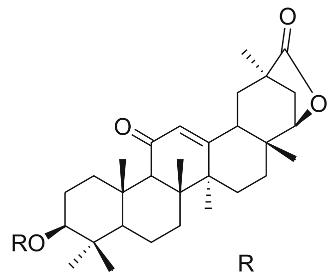

| | R |
|---|---|
| 284 | S2 |
| 294 | S7 |

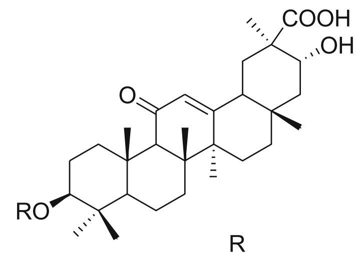

| | R |
|---|---|
| 285 | S3 |
| 286 | S4 |
| 287 | S5 |
| 288 | S6 |

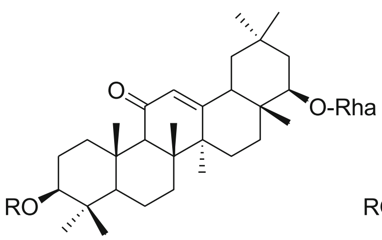

| | R |
|---|---|
| 289 | S1 |

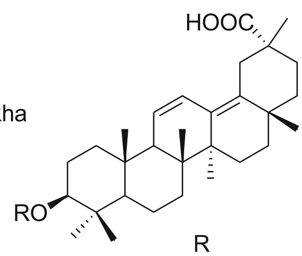

| | R |
|---|---|
| 291 | S1 |

| | |
|---|---|
| S1 | β-D-GluA(2→1)-β-D-GluA |
| S2 | β-D-GluA(2→1)-β-D-GalA |
| S3 | β-D-GluA(2→1)-β-D-Gal |
| S4 | β-D-GluA(2→1)-β-D-Xyl-(2→1)-α-L-Rha |
| S5 | β-D-GalA(2→1)-β-D-Glu-(2→1)-α-L-Rha |
| S6 | β-D-GluA(2→1)-β-D-Glu-(2→1)-α-L-Rha |
| S7 | β-D-GluA(2→1)-β-D-GluA-(2→1)-α-L-Rha |

Mair and co-workers reported the promising antiviral effects of **304–309** (*Burkea africana*) against H3N2 influenza virus A/Hong kong/68 (HK/68). The saponins **304–307** and their aglycones **308–309** displayed $IC_{50}$ in the range of 0.05 to 11.3 μM against HK/68 while **305–309** displayed $IC_{50}$ of 1.8 ± 0.03, 0.27 ± 0.13, 0.16 ± 0.07, 6.9 ± 2.97, and 6.8 ± 4.12 μM, respectively, against Jena/8178. The results revealed that branched or linear trisaccharide and tetrasaccharide exerted greater activity compared to that of disaccharides and their respective aglycones (Mair et al. 2018).

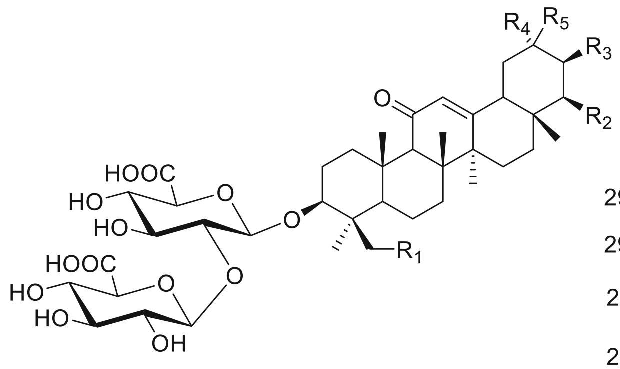

S1

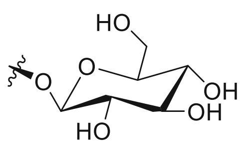

| | $R_1$ | $R_2$ | $R_3$ | $R_4$ | $R_5$ |
|---|---|---|---|---|---|
| 295 | H | OH | H | $CH_3$ | $CH_2OH$ |
| 296 | OH | $OCOCH_3$ | H | $CH_3$ | COOH |
| 297 | H | H | H | $CH_3$ | CO-$S_1$ |
| 298 | OH | H | H | $CH_3$ | COOH |
| 299 | H | H | H | COOH | $CH_3$ |
| 302 | H | $OCOCH_3$ | H | $CH_3$ | CHO |

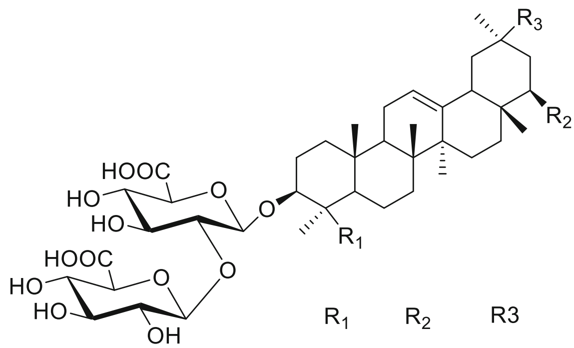

| | $R_1$ | $R_2$ | R3 |
|---|---|---|---|
| 300 | H | H | COOH |
| 301 | OH | H | COOH |

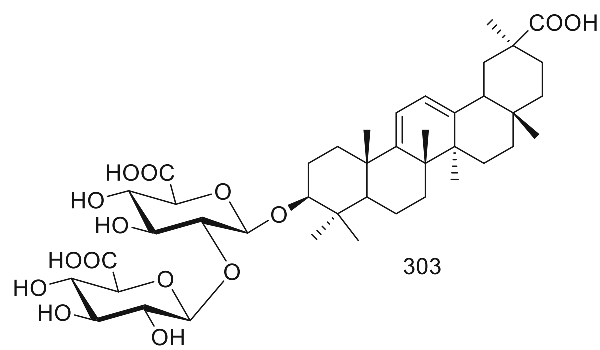

303

A saikosaponins, **310–323**, of *Bupleurum marginatum* var. *stenophyllum* were reported to possess inhibitory potential against influenza A virus A/WSN/33 (H1N1) in 293 T-Gluc cells using ribavirin ($EC_{50}$ 17.95 μM, SI > 11.42) as a positive control (Fang et al. 2017). The study further detailed that **315** displayed the most potent inhibition with $IC_{50}$ of 2.14 ± 0.72 μM but a poor SI (1.33) possibly due to the presence of 13,28-epoxy group which enhances the anti-viral potency as well as cytotoxicity; so is the case for **311**, **317**. The best SI (> 26.08) was displayed by **323** with an $IC_{50}$ of 7.67 ± 2.48 μM. It was also observed by the authors that the sugar chain (**318**, **319**, **323**), type of olefinic bond (**314**, **319**, **322**, **323**) and substitutions at C-11 and C-16 positions (**313**, **319**, **320**, **321**) may have an impact on the activity and SI (Fang et al. 2017).

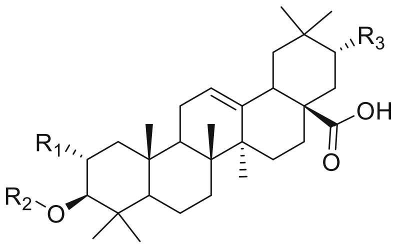


S = 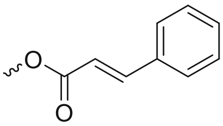


| | $R_1$ | $R_2$ | $R_3$ |
|---|---|---|---|
| 304 | OH | -β-Glc-[(2→1)-β-Xyl]-(4→1)-α-Rha | H |
| 305 | OH | -β-Glc-[(2→1)-β-Xyl]-(4→1)-α-Rha | S |
| 306 | H | -β-Xyl(2→1)-β-Xyl(2→1)-α-Rha | S |
| 307 | H | -β-Xyl-[(2→1)-β-Xyl(2→1)-α-Rha]-(4→1)-α-Rha | S |
| 308 | OH | H | S |
| 309 | H | H | S |

Porcine epidemic diarrhea virus (PEDV)

Porcine epidemic diarrhea virus (PEDV) is an enteric coronavirus causing high morbidity and mortality in porcine herds. It belongs to subgenus of *Pedacovirus* of genus *Alphacoronavirus* and family of Coronaviridae. PEDV is a positive sensed, enveloped, single-stranded RNA having a genomic size of 28 kb (Jung and Saif 2015; Pascual-iglesias et al. 2019). It is relatively an old virus first identified in China in the year 1980 however it gained attention in the year 2010 when a large outbreak cause severe economic concerns (Wang et al. 2016) and it further marked its presence in the USA in late 2013 (Scott et al. 2016); now it is present globally.

Some of the targets against which drugs are being developed include 3CL protease, main protease, and kinase inhibitors (Wang et al. 2017, 2020; Ye et al. 2020a; Raghuvanshi and Bharate 2021). Few natural products, quercetin, and homoharringtonine (Dong et al. 2018; Li et al. 2020b), and plant extracts (Trinh et al. 2021) have also displayed potential against PEDV including one study describing the promising role of oleanane triterpenes.

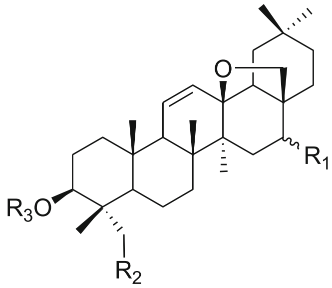


| | $R_1$ | $R_2$ | $R_3$ |
|---|---|---|---|
| 310 | β-OH | OH | 3-O-[6''-O-crotonyl]-β-D-Glc-(1→3)-β-D-Fuc |
| 315 | β-OH | H | 3-O-β-D-Glc-(1→3)-β-D-Fuc |
| 316 | =O | OH | 3-O-β-D-Glc-(1→3)-β-D-Fuc |

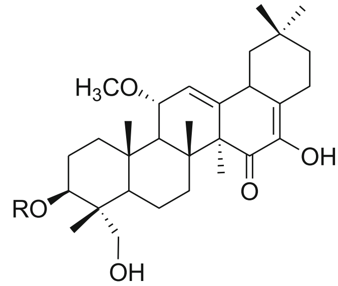


| | R |
|---|---|
| 311 | 3-O-β-D-Glc-(1→3)-β-D-Fuc |

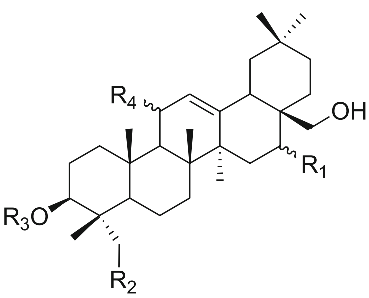


| | $R_1$ | $R_2$ | $R_3$ |
|---|---|---|---|
| 313 | α-OH | OH | 3-O-β-D-Glc-(1→3)-β-D-Fuc |
| 319 | β-OH | OH | 3-O-β-D-Glc-(1→3)-β-D-Fuc |

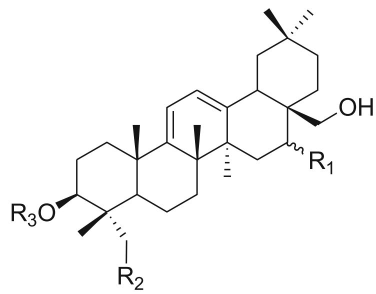


| | $R_1$ | $R_2$ | $R_3$ | $R_4$ |
|---|---|---|---|---|
| 320 | β-OH | H | 3-O-β-Glc-(1→6)-[-α-L-Rha(1→4)]-β-D-Glc | α–$OCH_3$ |
| 321 | β-OH | OH | 3-O-β-Glc-(1→6)-[-α-L-Rha(1→4)]-β-D-Glc | H |

*Oleanane triterpenes*

In an investigation, fifteen oleanane triterpenes (**324–338**), isolated from the flowers of *Camellia japonica*, were evaluated for their anti-viral activity against PEDV replication, wherein potent inhibitors (Table 1) displayed their effects on PEDV replication by inhibiting genes encoding GP6 nucleocapsid, GP2 spike, and GP5 membrane protein synthesis. Further studies by Yang and co-workers confirmed inhibition of PEDV GP6 nucleocapsid and GP2 spike protein synthesis during viral replication. Thus these compounds could serve as a templet for further lead optimization (Yang et al. 2015). The SAR detailed by the authors suggests that substitution pattern at C-16 and C-17 positions, type of sugar attachments, presence of additional double bond at C-17/C-18 have influential effects on the SI, potency, and cytotoxicities (Yang et al. 2015).

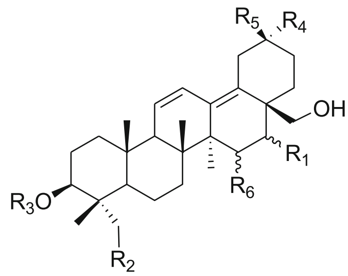


| | $R_1$ | $R_2$ | $R_3$ | $R_4$ | $R_5$ | $R_6$ |
|---|---|---|---|---|---|---|
| 312 | =O | OH | 3-*O*-*β*-D-Glc-(1→3)-*β*-D-Fuc | $CH_3$ | $CH_3$ | *α*–OH |
| 314 | *β*-OH | OH | 3-*O*-*β*-D-Glc-(1→3)-b-D-Fuc | $CH_3$ | $CH_2OH$ | H |
| 317 | *β*-OH | OH | 3-*O*-*β*-D-Fuc | $CH_3$ | $CH_3$ | H |
| 318 | =O | OH | 3-*O*-*β*-D-Glc-(1→3)-*β*-D-Fuc | $CH_3$ | $CH_3$ | H |
| 322 | *β*-OH | OH | 3-*O*-*β*-Glc-(1→6)-[-*α*-L-Rha(1→4)]-*β*-D-Glc | $CH_3$ | $CH_3$ | H |
| 323 | *β*-OH | H | 3-*O*-*β*-Glc-(1→6)-[-*α*-L-Rha(1→4)]-*β*-D-Glc | $CH_3$ | $CH_3$ | H |

Respiratory syncytial virus (RSV)

Respiratory syncytial virus (RSV) is a negative sensed, single-stranded RNA virus of genus *Orthopneumovirus* and family Pneumoviridae. It is a major contagious and common pathogen of the lower respiratory tract of infants and in elderly adults. RSV was isolated in 1956 from chimpanzees having a common cold-like illness and subsequently from young children having a pulmonary disease (Nam and Ison 2019). Aerosolized ribavirin is a licensed drug for the patient with the highest risk of RSV while palivizumab and motavizumab are the FDA-approved monoclonal antibody for RSV prophylaxis in immature infants born with the cardiopulmonary disorder. Several biological and pharmacological approaches are being tested for the safe and effective vaccine and drug development against RSV infection (Griffiths et al. 2017). No wonder traditional medicines and natural products have also been explored against RSV and summarized earlier (Lin et al. 2016; Hu et al. 2021); surprisingly only one study could be traced comprising triterpenes as anti-RSV agents.

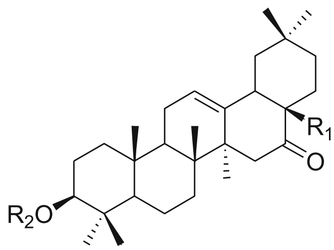

| | $R_1$ | $R_2$ |
|---|---|---|
| 324 | OH | β-D-GluA |
| 325 | OH | 6′-methoxy–β-D-GluA |
| 326 | OH | 6′-ethoxy-β-D-GluA |
| 327 | OH | β-D-Glu(1→2)-β-D-Gal(1→3)-β-D-GluA |
| 328 | OH | [β-D-Gal(1→2)]-β-D-Glc(1→2)-β-D-Gal(1→3)]-β-D-GlcA |
| 329 | $CH_2OH$ | H |

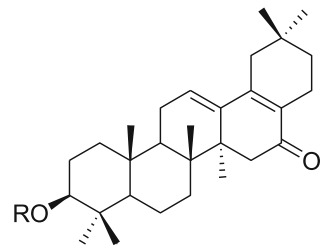

| | R |
|---|---|
| 335 | H |
| 336 | 6′-methoxy-β-D-GluA |
| 337 | 6′-methoxy-α-D-GluA |

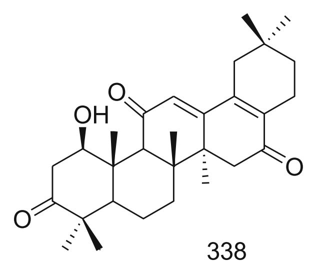

338

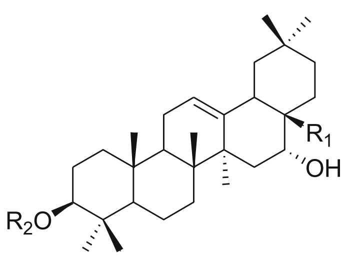

| | $R_1$ | $R_2$ |
|---|---|---|
| 330 | $CH_2OH$ | β-D-GluA |
| 331 | $CH_2OH$ | H |
| 332 | CHO | β-D-GluA |
| 333 | COOH | [β-D-Gal(1→2)]-β-D-Glc(1→2)-β-D-Gal(1→3)]-β-D-GlcA |
| 334 | COOH | β-D-GluA |

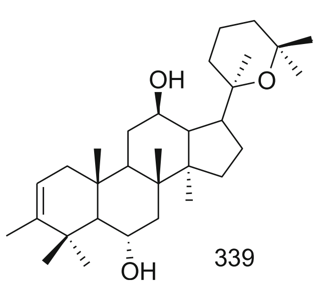

339

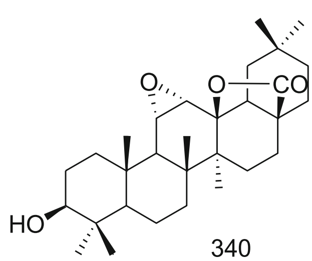

340

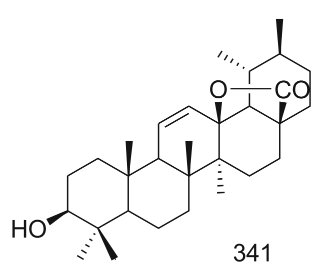

341

*Dammarane triterpenes*

(20R)-20,25-epoxy-3-methyldammaran-2-en-6α,12β-diol,(20R)-20,25-epoxydammaran-2-en-6α, 12β-diol (**339**), isolated from the flowers of *Lilium speciosum* var. *gloriosoides* Baker displayed potent activity against the respiratory syncytial virus (RSV) ($IC_{50}$ 2.9 µg/mL; SI 11.3) compared to ribavirin while other were moderate to weak inhibitor (Chen et al. 2019b).

Semliki Forest Virus (SFV)

The Semliki Forest virus (SFV), the positive-stranded RNA virus, contains approximately 13,000 base pair genomes which encode nine proteins. Uganda Virus Research Institute first identified SFV from mosquitoes of the Semliki Forest in 1942 and it spreads by mosquito bites (Atkins et al. 1999; Contu et al. 2021; Fazakerley 2002).

No specific anti-viral drugs are available and treatment lies around supportive care (Ekstroöm et al. 2006). Very few studies concerning natural products having inhibitory potential against SFV are reported. However, one study investigated in-silico exploration of a handful of natural products including triterpenes acteol which selectively interacted with SINV protease (Byler et al. 2016).

*Oleanane and ursane triterpenes*

Among the four triterpenoids, **133, 340–341** and **37** isolated from the leaves of *Fadogia tetraquetra* var. *tetraquetra*, showed strong activity against the SFV ($IC_{50}$ 14.7 μM) but also reported to possess significant cytotoxicity (68% reduction in cell viability after 24 h exposure at 50 μM) towards baby hamster kidney (BHK21) host cells (Mulholland et al. 2011). The activity result suggests that the basic skeleton (**37**) favored the activity.

Zika virus (ZIKV)

Zika virus (ZIKV; genus *Flavivirus*, family Flaviviridae) is an arthropod-borne viral disease first isolated from a non-human primate rhesus monkey in 1947, from mosquito species in 1948, and humans in 1952 (MacNamara 1954; Newman et al. 2017). The clinical presentation of the Zika virus is similar to dengue and chikungunya and can be transmitted by several mosquito species. The first ZIKV outbreak occurred in 2007 in the western pacific island of Yap and was followed by the larger epidemic in 2013–2014 in the south Pacific where infection-associated neurological complications were reported for the first time (Duffy et al. 2009; Musso and Gubler 2016). ZIKV circulated silently for decades in the human population in sporadic form, and sudden outbreaks were believed to be due to environmental factors and changes in genetics and virulence (Strottmann et al. 2019). The viral entry into humans occurs mostly by mosquito bite wherein skin cells such as epidermal keratinocytes, dermal fibroblast, and dendritic cells and adhesion factors SIGN, AXL, Tyro, and TIM-1 play an important role (Hamel et al. 2015). Currently, no vaccine is available and according to the CDC guideline best way to protect one from the ZIKA virus is to avoid *Aedes* mosquito bites (https://www.cdc.gov/zika/prevention/index.html).

Although the ZIKV is known for many years, recent outbreaks promoted the research towards drug development, and many synthetic compounds are being developed as anti-ZIKV agents; recently Bernatchez and group have summarized the possible drug targets and therapeutic interventions including the natural products and their derivatives as anti-ZIKV agents (Bernatchez et al. 2019). The only traceable study on the triterpenes as anti-ZIKV agents highlights the potential role of taraxeranes.

*Taraxerane triterpenes*

From the root bark of *Stillingia loranthacea* four 28-*nor*-taraxarenes derivatives, loranthones A-D along with diterpenoids were isolated by Abreu and coworkers. Compound loranthones B (**342**) exhibited significant anti-viral activity with 1.7 log10 $TCID_{50}$/mL reduction in ZIKV replication against an epidemic Zika virus (ZIKV) strain circulating in Brazil (ZIKV/H. sapiens/Brazil/PE243/2015) (Abreu et al. 2019).

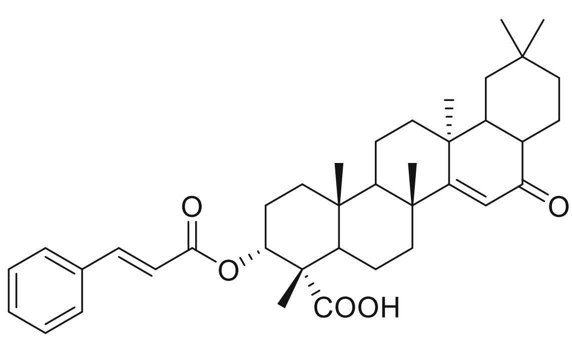


342

## Summary

Isoprene polymers, particularly triterpenes, are an important group for biologically active natural compounds with numerous new derivatives being reported every year. Only a small portion of these studies explored them for anti-viral properties. All together 342 triterpenoids representing 10 sub-classes have been covered in this review (2010–2020) displaying varying anti-viral potential against 14 different viruses (Fig. 12). Of those so explored, have shown potent to mild/weak activity in preliminary screening. Most of these studies are indicative, lacking a systematic exploration of their anti-viral properties in *in-vitro* and *in-vivo* models; except the studies concerning 20(S)-protopanaxtriol (**24**), oleanolic acid (**133**), and GA (**36**). This indicates that in-depth exploration was carried out for the compounds available in large quantities while the studies on the structure elucidation of new triterpenes were restricted to the initial anti-viral activity only. This could be attributed to the dubiety of getting the new to nature triterpenes in the quantity sufficient for the detailed *in-vitro* and *in-vivo* exploration.

On the same line, the most abundant triterpenes such as GA (**36**), ursolic acid (**37**), betulinic acid (**38**), ginsenosides (**24–27**) and betulin (**123**) were studied against more than one virus; which signify their

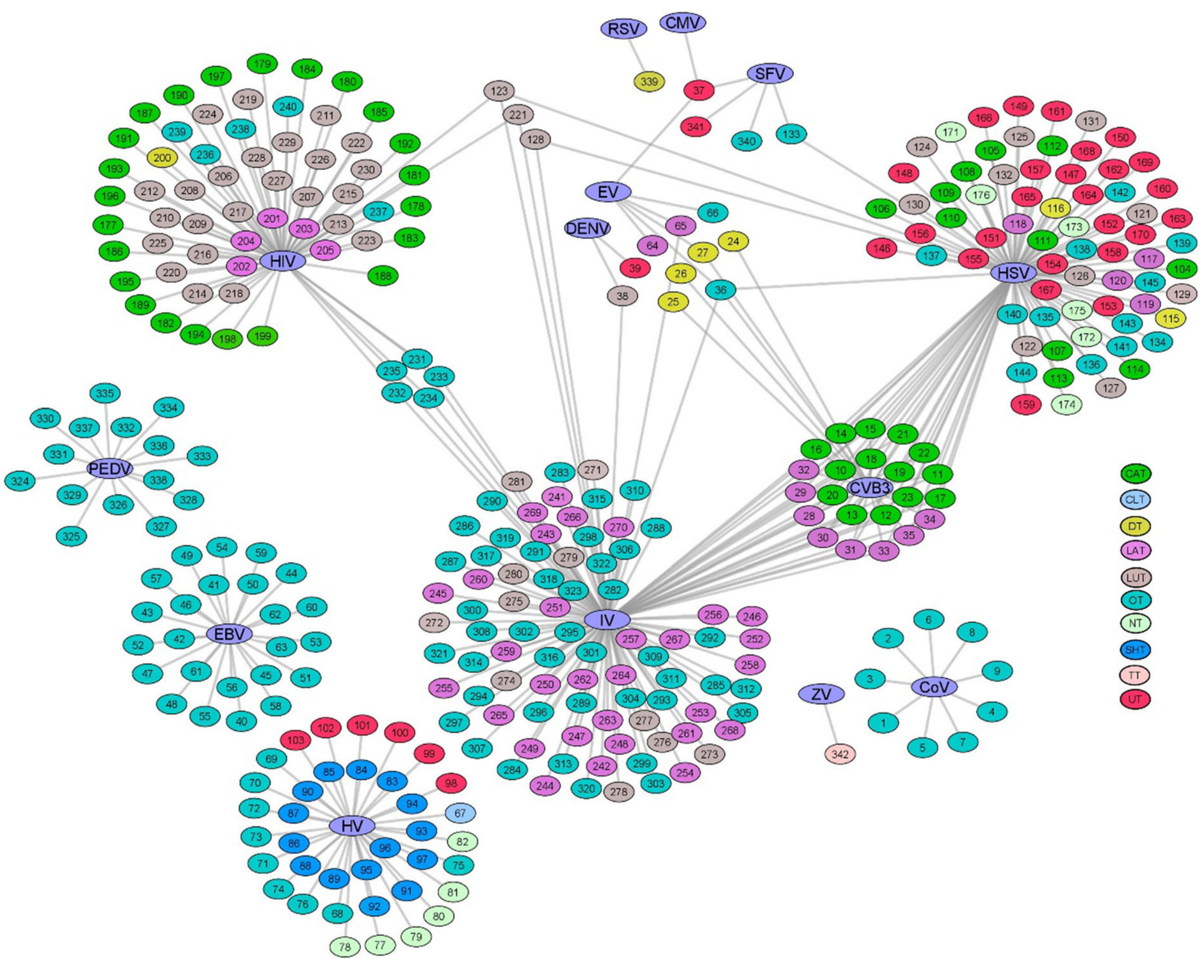


**Fig. 12** Cytoscape network depicting the correlation between 14 viruses (purple nodes) and 342 triterpenes. Interaction of viruses and triterpenes is indicated by grey edges. The most abundant oleanane terpenes are active against most of the viruses, followed by lanostane, ursane, lupane, and cycloartane. Triterpenes like cyclolanostane, dammarane, nor-terpenoids, taraxerane, and shionone displayed inhibitory effect on limited number of viruses. Each color indicates a different class of triterpenoid. Triterpene **36**, **37**, and **123** are the most interacting triterpenes

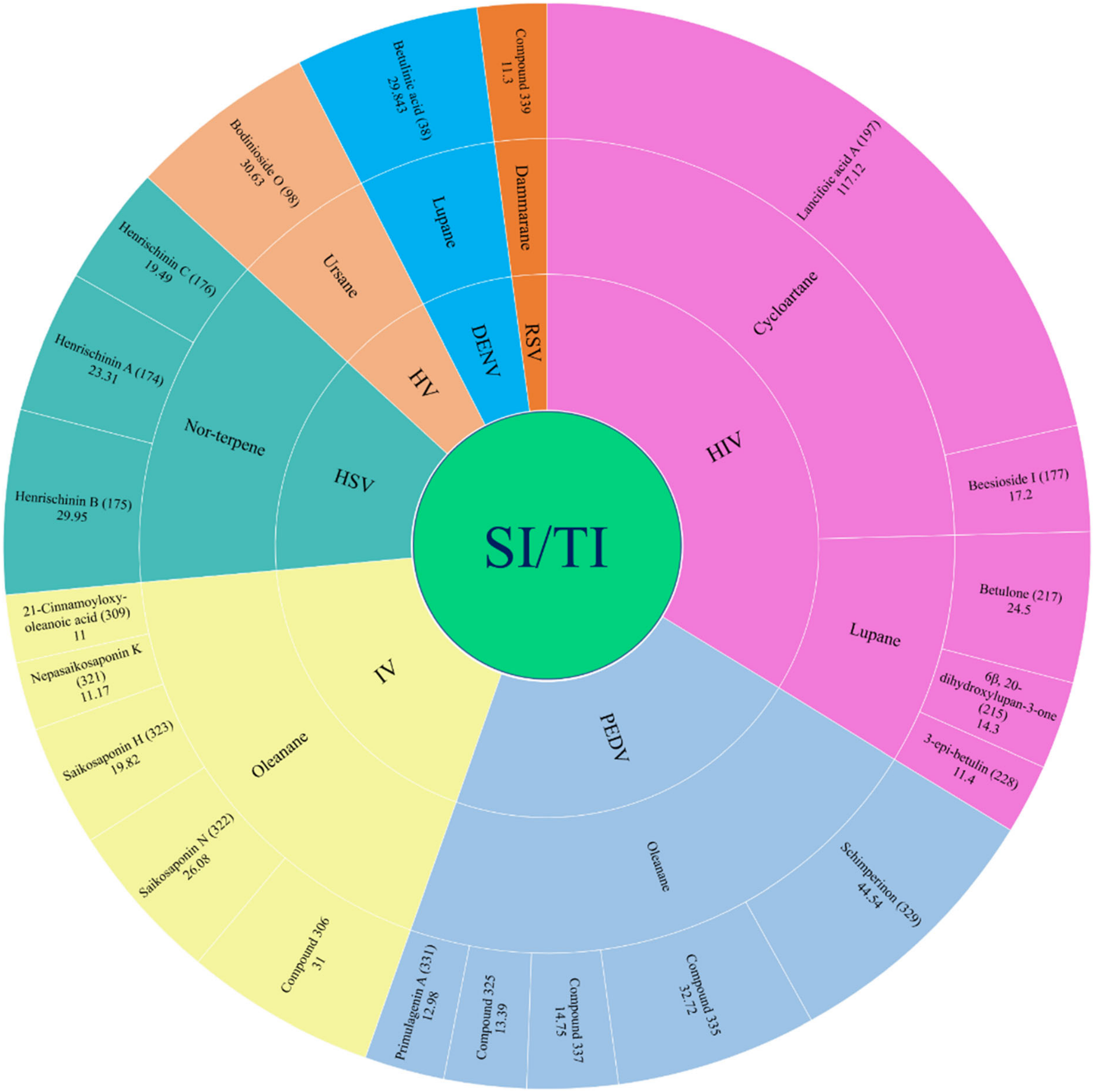


**Fig. 13** Sunburst chart representing the selective/therapeutic index of triterpenoids, against different viruses. The chart depicts the three groups, in which the first group represents the virus, the second represents the class of triterpenoid and the third group shows the triperpenes having SI/TI > 10

affinity towards different targets of viral lifecycles. On the other hand, the mode of action of unfamiliar triterpenoids against the specific virus is still unmapped. Further to depict the correlation between the triterpenes evaluated against different viruses a network is constructed (Fig. 12); wherein among the most abundant triterpenes the GA (**36**) is showing antiviral properties against the most number of viruses namely CVB3, EV, IV, and HSV distinctly; followed by **37** and **123** having activity against CMV/EV/SFV and HIV/HSV/IV, respectively. Interestingly, CVB3 and EV belong to the same virus family yet, the interaction of **36** occurs at different stages of replication. Among the 22 compounds isolated from *Lyonia ovalifolia,* (**10–23**, **28–35**), **11** and **13** have shown viral inhibition against all three tested viruses i.e. CVB3, HSV, and IV. This suggests that cycloartane triterpenes bearing 6/7/6/5 ring possessing carboxylic group at C-14, and hydroxyl or ketone group at C-21, without any glycosylation, may act on similar target or life stage of different viruses. Moreover, a little variation in structure may alter its activity against same or different viruses as observed for the **29, 30, 31** and **33** against CVB3, HSV and IV. It also suggest the influence of glycosylation at the C-3 position against these viruses (Lv et al. 2016). Therefore, triterpenes having activity against more than one virus can be studied for their mechanism of action to understand their complex relationship with different viruses for the development of potential drug candidates.

On the biosynthetic front mevalonic acid or non-mevalonate pathway generates 30 carbon-bearing 2,3-oxidosqualene, the divergent point for the biosynthesis of different skeletons catalyzed by relevant OSCs. Further, similar modifications observed on the basic skeletons such as cyclization of the side chain, ring-opening cascades, glycosylations, feruloylation, hydroxylations, or acetylations signifies their chemotaxonomic relevance within the family they belong to. For example, triterpenes, **115–116** and **200** reported from the plant of Meliaceae family belong to dammarane class, and across these species, **116** and **200** displayed 3,4-*seco* derivatization possibly due to the presence of similar catalytic enzymes. Similarly, five species belonging to the Schisandraceae have generated triterpenes **77–82** (nor-terpene), **171–176** (nor-terpene), **189–197** (cycloartane), and **201–205** (lanostane) of diverse chemical structures. Cycloartane and lanostane follow a similar biosynthetic route while the discussed nor-terpenoids are generated from the cycloartane, suggesting the presence of relevant OSCs owing to the genetic similarities. A careful examination suggests that these triterpenes represent structural uniqueness such as A or D ring-opening, A and B ring expansion, side-chain cyclization, or combinations of ring-opening, expansion, and cyclizations possible due to the presence of similar catalytic system among the plants of Schisandraceae family. At the same time, different classes of triterpenoids i.e. cycloartane (**10–23**), lanostane (**28–35**), lupane (**124–132**), oleanane (**139–145**), and ursane (**149–168**) are also reported from the species belonging to the same family i.e. Ericaceae.

Besides the OSCs, the role of heme-containing cytochrome P450 mono-oxygenase enzymes is indispensable for catalyzing different reactions such as C–C and C-O bond coupling, rearrangements, cyclization, hydroxylations, and reductions, etc. The specific role of the cytochrome P450 enzyme-catalyzed reactions is described in the reviews published earlier (Banerjee and Hamberger, 2017; Guengerich and Munro, 2013; Kumari et al. 2013) and these multi-step reactions including rearrangements are complex processes for which a lot more is yet to be unveiled.

In the present review, the most complex and structurally unique nor-triterpenes **77** and **171** displayed an inimitable skeleton bearing 7 ring system. It is evident that the nor-terpenes are generated from cycloartanes and the plausible biosynthesis of **77** and **171** may start with the genesis of 9,10-*seco* cycloartane (**F11a**) from the 3-oxo-cycloartenoids (**F11**) followed by ring opening of the 3-oxo bearing A-ring giving rise to a 3,4-*seco*/9,10-*seco* derivative (**F11b**). The relevant enzymes may catalyze the formation of lactone (**F11c**) and hydro furan ring (**F11e**). Genesis of **F11c** may also follow the 3,4-*seco* derivatization followed by 9,10-*seco* modifications (F11-F11d-F11c or F11-F11d-F11b-F11c). The next step involves rearrangements at the side chain leading to the genesis of complex bicyclic systems of **77** and **171** (Fig. 11). These complex steps must have been catalyzed by the relevant cytochrome P450 enzymes present in the Schisandraceae family.

In general, triterpenoids derivatives with glycosidic linkages were relatively less active, whereas substitution such as acetylation or oxidation led to an increase in the potency. This indicates that the increase in the hydrophilicity imparted by bulky sugar groups is unfavorable for the activity while the introduction of small and/or lipophilic groups improved the potency. Also, the possible involvement of the point of attachments needs in-depth analysis. Therefore, the futuristic medicinal chemistry approach considering SAR studies should be undertaken for further leads optimization. For this purpose, the triterpenes displaying better SI/TI could be considered for drug development against respective viruses. Muller and co-workers have critically discussed different aspects of TI (Muller and Milton, 2012); by and large, the higher the selectivity index or therapeutic index, the drug is likely to be safe and effective in *in-vivo* conditions during any viral infection; as the SI/TI is a measure of the ratio of cytotoxicity and anti-viral efficacy (Muller and Milton, 2012). A higher SI/TI is obtained when a drug is toxic at a higher concentration while displaying its anti-viral activity at a fairly low concentration.

As displayed in Fig. 13 20 triterpenes with SI/TI greater than 10 were traced belonging to cycloartane, dammarane, lupane, nor-terpene, ursane, and oleanane classes against seven different viruses (DENV, HV, HSV, HIV, IV, PEDV, and RSV). Among these oleanane (**306**, **309**, **321–323**) appears to be the therapeutically better triterpenes against IV and most of them featured glycosidic linkages at the C-3 position. As discussed, in most of the cases the C-3 position of triterpenes is important for the anti-viral activity; however, at the same time, C-3 functionalities might have improved the cytotoxicities and thus lowered their SI/TI. Therefore, C-3 glycosides have displayed better SI/TI and must be developed further with suitable substitutions at C-3 positions to improve the SI/TI. In this context, nor-terpenes (**174–176**) of Schisandraceae family also displayed satisfactory SI against the HSV virus.

Lancifoic acid A (**197**), the *seco*-cycloarate triterpene, of *Schisandra sphenanthera* (Schisandraceae) displayed the most promising TI of 117.12 against HIV in comparison with AZT (TI 234,520.60) (Liang et al. 2014). Since the cycloartane and cycloartane derivatives (nor-terpenes) have displayed better therapeutic indexes, these triterpenes should be taken up and preferred over triterpene glycosides as a template for further lead optimization and drug discovery. Also, cycloartanes, especially the *seco*-derivatives, may be explored against other viruses as well.

The last couple of centuries have introduced several new viruses to the human race crossing species barrier and many of them have been proven fatal counting millions of lives. In the present review, we could trace the triterpenoids having efficacy against 14 different viruses during the study period of 2010–2020, among which SARS-CoV-2 is of major health concern now. This pandemic emphasized the role of traditional medicines in absence of any proven drug with challenges of new drug discovery taking a long time. In this context, large-scale exploration of the triterpenes against different strains of SARS-Cov-2 is of great importance wherein the friedelan skeleton-bearing compounds and quinone-methides could play a major role. Moreover, the possible role of shionones as anti-covid agents cannot be ruled out as they bear a similar skeleton on the A/B/C rings.

## Conclusion and future direction

Triterpenes are therapeutically important natural products of which only a few were explored systematically for their anti-viral properties. In general, the natural products obtained employing a bio-assay guided approach provide an important template for the medicinal chemistry-based lead optimization and activity-guided rational drug design. In the present review, most of the studies had focused on the structural characterization of unreported triterpenes; nevertheless, few reports also adopted the futuristic approach of target-specific SAR-guided lead optimization. At the same time, many studies have not documented the TI or SI of the identified triterpenes which makes it arduous to conclude. In near future, the triterpenes displaying better SI or TI may serve as the potential leads for drug development with due consideration of their multi-target potential.

At the same time multi-directional efforts – (i) application of synthetic biology for the large scale production, (ii) development of sustainable cultivation, conservation, and extraction technologies, (iii) utilization of synthetic chemistry for the total synthesis of the potential leads, (iv) medicinal chemistry-based lead optimization, and (v) pre-clinical validation and clinical studies, are required for the development of triterpenoidal drug candidates. Moreover, with the emergence of potential markets for botanical drugs and nutraceutical products, future research may also focus on the development of these plant-based drugs with an amalgamation of ethnopharmacology and traditional knowledge with the modern scientific interventions such as the network pharmacology approach with quality marker analysis for standardization. Parallel investigations for the identification of new to nature triterpenes should be promoted employing bio-assay-guided approach to generate a pool of triterpenes for further development. This may be facilitated with the emergence of newer hyphenated instrument based de-replication and quality marker strategies.

It is evident that the major complications and fatalities arising from viral infections are due to the overexpression of pro-inflammatory cytokines, this event is known as 'cytokine storm'. Therefore, for viral infections, including SARS-CoV-2, anti-inflammatory, and immunomodulatory therapy may improve the outcome (Fajgenbaum and June 2020; Ye et al.

2020b). When all is said and done, the anti-inflammatory potential of the triterpenes should be leveraged in concurrence with their anti-viral properties.

**Acknowledgements** The authors are thankful to Director, CSIR-IICB Kolkata for providing the necessary facilities. We also wish to thank the anonymous reviewers for their fruitful comments. PD and SSS acknowledge the fellowship from NIPER-K and NBA respectively.

**Author contribution** PD and SSS: Drafting, network analysis; AKS and RB: Valuable suggestions; DK: Conceptualization, literature collection, drafting, correction, revision, and overall supervision.

**Declarations**

**Conflict of interest** No conflict of interest.

## References

Abreu LS, Nascimento YMD, Costa RDS et al (2019) Tri- and diterpenoids from *Stillingia loranthacea* as inhibitors of zika virus replication. J Nat Prod 82:2721–2730. https://doi.org/10.1021/acs.jnatprod.9b00251

Almeida A, Dong L, Appendino G, Bak S (2020) Plant triterpenoids with bond-missing skeletons: biogenesis, distribution and bioactivity. Nat Prod Rep 37:1207–1228. https://doi.org/10.1039/c9np00030e

Álvarez ÁL, Habtemariam S, Parra F (2015) Inhibitory effects of lupene-derived pentacyclic triterpenoids from *Bursera simaruba* on HSV-1 and HSV-2 in vitro replication. Nat Prod Res 29:2322–2327. https://doi.org/10.1080/14786419.2015.1007456

Andrei G, Trompet E, Snoeck R (2019) Novel therapeutics for epstein–barr virus. Molecules 24:1–20. https://doi.org/10.3390/molecules24050997

Arai A (2021) Chronic active epstein-barr virus infection: the elucidation of the pathophysiology and the development of therapeutic methods. Microorganisms 9:1–11. https://doi.org/10.3390/microorganisms9010180

Atkins GJ, Sheahan BJ, Liljeström P (1999) The molecular pathogenesis of semliki forest virus: a model virus made useful? J Gen Virol 80:2287–2297. https://doi.org/10.1099/0022-1317-80-9-2287

Banerjee A, Hamberger B (2017) P450s controlling metabolic bifurcations in plant terpene specialized metabolism. Phytochem Rev 17:81–111. https://doi.org/10.1007/S11101-017-9530-4

Bar-On YM, Flamholz A, Phillips R, Milo R (2020) Sars-cov-2 (Covid-19) by the numbers. Elife 9:1–15. https://doi.org/10.7554/elife.57309

Barré-Sinoussi F, Ross AL, Delfraissy JF (2013) Past, present and future: 30 years of HIV research. Nat Rev Microbiol 11:877–883. https://doi.org/10.1038/nrmicro3132

Behnam MAM, Nitsche C, Boldescu V, Klein CD (2016) The medicinal chemistry of dengue virus. J Med Chem 59:5622–5649. https://doi.org/10.1021/acs.jmedchem.5b01653

Bell LCK, Noursadeghi M (2018) Pathogenesis of HIV-1 and *Mycobacterium tuberculosis* co-infection. Nat Rev Microbiol 16:80–90. https://doi.org/10.1038/nrmicro.2017.128

Bernatchez JA, Tran LT, Li J et al (2019) Drugs for the treatment of zika virus infection. J Med Chem 63:470–489. https://doi.org/10.1021/acs.jmedchem.9b00775

Bourjot M, Leyssen P, Eydoux C et al (2012) Flacourtosides A-F, phenolic glycosides isolated from *Flacourtia ramontchi*. J Nat Prod 75:752–758. https://doi.org/10.1021/np300059n

Byler KG, Collins JT, Ogungbe IV, Setzer WN (2016) Alphavirus protease inhibitors from natural sources: a homology modeling and molecular docking investigation. Comput Biol Chem 64:163–184. https://doi.org/10.1016/j.compbiolchem.2016.06.005

Callies O, Bedoya LM, Beltrán M et al (2015) Isolation, structural modification, and HIV inhibition of pentacyclic lupane-type triterpenoids from *Cassine xylocarpa* and *Maytenus cuzcoina*. J Nat Prod 78:1045–1055. https://doi.org/10.1021/np501025r

Chang FR, Yen CT, Ei-Shazly M et al (2012) Anti-human coronavirus (anti-HCoV) triterpenoids from the leaves of *Euphorbia neriifolia*. Nat Prod Commun 7:1415–1417. https://doi.org/10.1177/1934578x1200701103

Chen JJ, Wu RF, Hsiao JW et al (2019a) A new triterpenoid and bioactive constituents of *Eriobotrya deflexa f. buisanensis*. Chem Nat Compd 55:74–78. https://doi.org/10.1007/s10600-019-02616-8

Chen W, Zhang H, Wang J, Hu X (2019b) A new triterpenoid from the bulbs of *Lilium speciosum var. gloriosoides*. Chem Nat Compd 55:289–291. https://doi.org/10.1007/s10600-019-02669-9

Cheng SY, Wang CM, Hsu YM et al (2011) Oleanane-type triterpenoids from the leaves and twigs of *Fatsia polycarpa*. J Nat Prod 74:1744–1750. https://doi.org/10.1021/np2002435

Chu LL, Montecillo JAV, Bae H (2020) Recent advances in the metabolic engineering of yeasts for ginsenoside biosynthesis. Front Bioeng Biotechnol 8:139. https://doi.org/10.3389/fbioe.2020.00139

Colpitts CC, Verrier ER, Baumert TF (2016) Targeting viral entry for treatment of hepatitis B and C virus infections. ACS Infect Dis 1:420–427. https://doi.org/10.1021/acsinfecdis.5b00039

Contu L, Balistreri G, Domanski M et al (2021) Characterisation of the Semliki Forest Virus-host cell interactome reveals the viral capsid protein as an inhibitor of nonsense-mediated mRNA decay. PLOS Pathog 17:e1009603. https://doi.org/10.1371/journal.ppat.1009603

Corsino J, De Carvalho PRF, Kato MJ et al (2000) Biosynthesis of friedelane and quinonemethide triterpenoids is compartmentalized in *Maytenus aquifolium* and *Salacia campestris*. Phytochemistry 55:741–748. https://doi.org/10.1016/S0031-9422(00)00285-5

Cui H, Xu B, Wu T et al (2014) Potential antiviral lignans from the roots of *Saururus chinensis* with activity against epstein-barr virus lytic replication. J Nat Prod 77:100–110. https://doi.org/10.1021/np400757k

Das K (2012) Antivirals targeting influenza A virus. J Med Chem 55:6263–6277. https://doi.org/10.1021/JM300455C
Deeks SG, Archin N, Cannon P et al (2021) Research priorities for an HIV cure: International AIDS Society Global Scientific Strategy 2021. Nat Med 27:2085–2098. https://doi.org/10.1038/s41591-021-01590-5
Dong H-J, Wang Z-H, Meng W et al (2018) The natural compound homoharringtonine presents broad antiviral activity in vitro and in vivo. Viruses 10:601. https://doi.org/10.3390/V10110601
Duffy MR, Chen T-H, Hancock WT et al (2009) Zika virus outbreak on Yap island, federated states of Micronesia. N Engl Med 360:2536–2543. https://doi.org/10.1056/NEJMoa0805715
Ekstroöm M, Garoff H, Andersson H (2006) Semliki forest virus expression system. Cell Biol 4:63–67. https://doi.org/10.1016/B978-012164730-8/50194-5
El-Tantawy WH, Temraz A (2020) Natural products for the management of the hepatitis C virus: a biochemical review. Arch Physiol Biochem 126:116–128. https://doi.org/10.1080/13813455.2018.1498902
Ernberg I, Andersson J (1986) Acyclovir efficiently inhibits oropharyngeal excretion of epstein-barr virus in patients with acute infectious mononucleosis. J Gen Virol 67:2267–2272. https://doi.org/10.1099/0022-1317-67-10-2267
Eschenmoser A, Ruzicka L, Jeger O, Arigoni D (1955) Zur kenntnis der triterpene. 190. mitteilung. eine stereochemische interpretation der biogenetischen isoprenregel bei den triterpenen. Helv Chim Acta 38:1890–1904. https://doi.org/10.1002/hlca.19550380728
Esimone CO, Eck G, Nworu CS et al (2010) Dammarenolic acid, a secodammarane triterpenoid from *Aglaia* sp. shows potent anti-retroviral activity in vitro. Phytomedicine 17:540–547. https://doi.org/10.1016/j.phymed.2009.10.015
Fajgenbaum DC, June CH (2020) Cytokine Storm. N Engl J Med 383:2255–2273. https://doi.org/10.1056/nejmra2026131/suppl_file/nejmra2026131_disclosures.pdf
Fang W, Yang YJ, Guo BL, Cen S (2017) Anti-influenza triterpenoid saponins (saikosaponins) from the roots of *Bupleurum marginatum* var. *stenophyllum*. Bioorganic Med Chem Lett 27:1654–1659. https://doi.org/10.1016/j.bmcl.2017.03.015
Fang Z, Zhang T, Chen S et al (2019) Cycloartane triterpenoids from *Actaea vaginata* with anti-inflammatory effects in LPS-stimulated RAW264.7 macrophages. Phytochemistry 160:1–10. https://doi.org/10.1016/j.phytochem.2019.01.003
Fazakerley JK (2002) Pathogenesis of semliki forest virus encephalitis. J Neurovirol 8:66–74. https://doi.org/10.1080/135502802901068000
Feuer R, Mena I, Pagarigan R et al (2002) Cell cycle status affects coxsackievirus replication, persistence, and reactivation in vitro. J Virol 76:4430–4440. https://doi.org/10.1128/jvi.76.9.4430-4440.2002
Fukushima EO, Seki H, Ohyama K et al (2011) CYP716A subfamily members are multifunctional oxidases in triterpenoid biosynthesis. Plant Cell Physiol 52:2050–2061. https://doi.org/10.1093/pcp/pcr146
Gershburg E, Pagano JS (2005) Epstein-barr virus infections: prospects for treatment. J Antimicrob Chemother 56:277–281. https://doi.org/10.1093/jac/dki240
Glover BJ (2011) Pollinator attraction: the importance of looking good and smelling nice. Curr Biol 21:R307–R309. https://doi.org/10.1016/j.cub.2011.03.061
Gong KK, Li PL, Qiao D et al (2017) Cytotoxic and antiviral triterpenoids from the mangrove plant *Sonneratia paracaseolaris*. Molecules 22:1–11. https://doi.org/10.3390/molecules22081319
Griffiths C, Drews SJ, Marchant DJ (2017) Respiratory syncytial virus: Infection, detection, and new options for prevention and treatment. Clin Microbiol Rev 30:277–319. https://doi.org/10.1128/CMR.00010-16
Griffiths PD, Whitley RJ (2002) In: Boucher CAB, Galasso GA, Katzenstein DA, Cooper DA (eds) Practical guidelines in antiviral therapy. Elsevier Inc. https://doi.org/10.1016/B978-044450884-3/50007-6
Guengerich FP, Munro AW (2013) Unusual Cytochrome P450 enzymes and reactions. J Biol Chem 288:17065–17073. https://doi.org/10.1074/JBC.R113.462275
Gunatilaka AAL (1996) In: Herz W, Kirby GW, Moore RE, Steglich W, Tamm C (eds) Fortschritte der chemie organischer naturstoffe/progress in the chemistry of organic natural products. Springer, Vienna . https://doi.org/10.1007/978-3-7091-9406-5_1
Guzman MG, Halstead SB, Artsob H et al (2010) Dengue: a continuing global threat. Nat Rev Microbiol 8:S7–S16. https://doi.org/10.1038/nrmicro2460
Halstead SB (2015) Pathogenesis of dengue: Dawn of a new era. F1000Research 4:1–8. https://doi.org/10.12688/f1000research.7024.1
Hamel R, Dejarnac O, Wichit S et al (2015) Biology of zika virus infection in human skin cells. J Virol 89:8880–8896. https://doi.org/10.1128/JVI.00354-15
Haralampidis K, Trojanowska M, Osbourn AE (2002) Biosynthesis of triterpenoid saponins in plants. Adv Biochem Eng Biotechnol 75:31–49. https://doi.org/10.1007/3-540-44604-4_2
Harrison SC (2008) Viral membrane fusion. Nat Struct Mol Biol 15:690–698. https://doi.org/10.1038/nsmb.1456
Haudecoeur R, Ahmed-Belkacem A, Yi W et al (2011) Discovery of naturally occurring aurones that are potent allosteric inhibitors of hepatitis C virus RNA-dependent RNA polymerase. J Med Chem 54:5395–5402. https://doi.org/10.1021/jm200242p
Hou M, Wang R, Zhao S, Wang Z (2021) Ginsenosides in *Panax* genus and their biosynthesis. Acta Pharm Sin B 11:1813–1834. https://doi.org/10.1016/j.apsb.2020.12.017
Hu Y, Sneyd H, Dekant R, Wang J (2017) Influenza A virus nucleoprotein: a highly conserved multi-functional viral protein as a hot antiviral drug target. Curr Top Med Chem

17:2271–2285. https://doi.org/10.2174/1568026617666170224122508
Hu D, Gao H, Yao X (2020a) Biosynthesis of triterpenoid natural products. Compr Nat Prod 3:577–612. https://doi.org/10.1016/B978-0-12-409547-2.14678-5
Hu Z, Lin J, Chen J et al (2021) Overview of viral pneumonia associated with influenza virus, respiratory syncytial virus, and coronavirus, and therapeutics based on natural products of medicinal plants. Front Pharmacol 12:1–21. https://doi.org/10.3389/fphar.2021.630834
Hu D, Gao H, Yao X et al (2020b) In: Liu HWB, Begley TP (eds) Comprehensive Natural Products III, 3rd edn. Elsevier Inc. https://doi.org/10.1016/B978-0-12-409547-2.14678-5
Hunter WN (2007) The non-mevalonate pathway of isoprenoid precursor biosynthesis. J Biol Chem 282:21573–21577. https://doi.org/10.1074/jbc.R700005200
Isah T (2019) Stress and defense responses in plant secondary metabolites production. Biol Res 52:1–25. https://doi.org/10.1186/S40659-019-0246-3
Isaka M, Chinthanom P, Srichomthong K, Thummarukcharoen T (2017) Lanostane triterpenoids from fruiting bodies of the bracket fungus *Fomitopsis feei*. Tetrahedron Lett 58:1758–1761. https://doi.org/10.1016/j.tetlet.2017.03.066
James C, Harfouche M, Welton NJ et al (2020) Herpes simplex virus: global infection prevalence and incidence estimates. Bull World Health Organ 98:315–329. https://doi.org/10.2471/BLT.19.237149
Jenson HB (2011) Epstein-Barr virus. Pediatr Rev 32:375–384. https://doi.org/10.1542/pir.32-9-375
Jung K, Saif LJ (2015) Porcine epidemic diarrhea virus infection: etiology, epidemiology, pathogenesis and immunoprophylaxis. Vet J 204:134–143. https://doi.org/10.1016/j.tvjl.2015.02.017
Kapadia GJ, Azuine MA, Tokuda H et al (2002) Inhibitory effect of herbal remedies on 12-o-tetradecanoylphorbol-13-acetate-promoted Epstein-Barr virus early antigen activation. Pharmacol Res 45:213–220. https://doi.org/10.1006/phrs.2001.0936
Keith KA, Hartline CB, Bowlin TL, Prichard MN (2018) A standardized approach to the evaluation of antivirals against DNA viruses: Polyomaviruses and lymphotropic herpesviruses. Antiviral Res 159:122–129. https://doi.org/10.1016/j.antiviral.2018.09.016
Kimberlin DW, Whitley RJ, Wan W et al (2011) Oral acyclovir suppression and neurodevelopment after neonatal herpes. N Engl J Med 365:1284–1292. https://doi.org/10.1056/nejmoa1003509
Kitagawa I, Hori K, Taniyama T et al (1993) Saponin and sapogenol. XLVII. On the constituents of the roots of *Glycyrrhiza uralensis* fischer from northeastern China. (1). Licorice-Saponins A3, B2, and C2. Chem Pharm Bull 41:43–49. https://doi.org/10.1248/cpb.41.43
Kralj A, Nguyen MT, Tschammer N et al (2013) Development of flavonoid-based inverse agonists of the key signaling receptor US28 of human cytomegalovirus. J Med Chem 56:5019–5032. https://doi.org/10.1021/jm4003457
Krishna BA, Wills MR, Sinclair JH (2019) Advances in the treatment of cytomegalovirus. Br Med Bull 131:5–17. https://doi.org/10.1093/bmb/ldz031
Kumar SP, Chandy ML, Shanavas M et al (2016) Pathogenesis and life cycle of *Herpes simplex* virus infection-stages of primary, latency and recurrence. J Oral Maxillofac Surg Med Pathol 28:350–353. https://doi.org/10.1016/j.ajoms.2016.01.006
Kumari S, Priya P, Misra G, Yadav G (2013) Structural and biochemical perspectives in plant isoprenoid biosynthesis. Phytochem Rev 122(12):255–291. https://doi.org/10.1007/S11101-013-9284-6
Laconi S, Madeddu MA, Pompei R (2014) Autophagy activation and antiviral activity by a licorice triterpene. Phyther Res 28:1890–1892. https://doi.org/10.1002/ptr.5189
Lasrado N, Gangaplara A, Massilamany C et al (2021) Attenuated strain of CVB3 with a mutation in the CAR-interacting region protects against both myocarditis and pancreatitis. Sci Rep 11:1–20. https://doi.org/10.1038/s41598-021-90434-w
Lee S, Chung YH, Lee C (2017) US28, a virally-encoded GPCR as an antiviral target for human cytomegalovirus infection. Biomol Ther 25:69–79. https://doi.org/10.4062/biomolther.2016.208
Lei C, Huang SX, Xiao WL et al (2010) Bisnortriterpenoids possessing an 18-nor-schiartane skeleton from *schisandra propinqu*a var. *propinqua*. Planta Med 76:1611–1615. https://doi.org/10.1055/s-0029-1241018
Li F (2016) Structure, function, and evolution of coronavirus spike proteins. Annu Rev Virol 3:237–261. https://doi.org/10.1146/annurev-virology-110615-042301
Li F, Ma C, Wang J (2015) Inhibitors targeting the influenza virus hemagglutinin. Curr Med Chem 22:1361–1382. https://doi.org/10.2174/0929867322666150227153919
Li YL, Xue LJ, Li J et al (2019a) Abinukitrine A, a unique 17,18-cyclolanostane triterpenoid from *Abies nukiangensis*. Org Biomol Chem 17:2107–2109. https://doi.org/10.1039/C8OB03117G
Li YT, Linster M, Mendenhall IH et al (2019b) Avian influenza viruses in humans: lessons from past outbreaks. Br Med Bull 132:81–95. https://doi.org/10.1093/bmb/ldz036
Li H, Sun J, Xiao S et al (2020a) Triterpenoid-mediated inhibition of virus-host interaction: is now the time for discovering viral entry/release inhibitors from nature? J Med Chem 63:15371–15388. https://doi.org/10.1021/acs.jmedchem.0c01348
Li Z, Cao H, Cheng Y et al (2020b) Inhibition of porcine epidemic diarrhea virus replication and viral 3C-like protease by quercetin. Int J Mol Sci 21:1–13. https://doi.org/10.3390/IJMS21218095
Liang CQ, Shi YM, Li XY et al (2013) Kadcotriones A-C: Tricyclic triterpenoids from *Kadsura coccinea*. J Nat Prod 76:2350–2354. https://doi.org/10.1021/np400546z
Liang CQ, Luo RH, Yan JM et al (2014) Structure and bioactivity of triterpenoids from the stems of *Schisandra sphenanthera*. Arch Pharm Res 37:168–174. https://doi.org/10.1007/s12272-013-0133-3
Lim BH, Mahmood TA (2011) Influenza A H1N1 2009 (swine flu) and pregnancy. J Obstet Gynecol India 61:386–393. https://doi.org/10.1007/s13224-011-0055-2
Lin YJ, Lai CC, Lai CH et al (2013) Inhibition of enterovirus 71 infections and viral IRES activity by *Fructus gardeniae* and geniposide. Eur J Med Chem 62:206–213. https://doi.org/10.1016/j.ejmech.2012.12.038

Lin LL, Shan JJ, Xie T et al (2016) Application of traditional chinese medical herbs in prevention and treatment of respiratory syncytial virus. Evidence-Based Complement Altern Med 2016:1–13. https://doi.org/10.1155/2016/6082729

Liu F, Wang YN, Li Y et al (2017) Rhodoterpenoids A-C, three new rearranged triterpenoids from *Rhododendron latoucheae* by HPLC-MS-SPE-NMR. Sci Rep 7:1–10. https://doi.org/10.1038/s41598-017-06320-x

Liu F, Wang YN, Li Y et al (2019) Triterpenoids from the twigs and leaves of *Rhododendron latoucheae* by HPLC-MS-SPE-NMR. Tetrahedron 75:296–307. https://doi.org/10.1016/j.tet.2018.11.059

Liu DX, Liang JQ, Fung TS (2021) In: Bamford DH, Zuckerman M (eds) Encyclopedia of virology, 4th edn. Elsevier Inc. 10.1016/B978–0–12–809633–8.21501-X

Li-Yang J, Nakajima JI, Kimura N et al (2007) Oleanane-type triterpene glycosides from *Glycyrrhiza uralensis*. Nat Prod Commun 2:243–248. https://doi.org/10.1177/1934578X0700200304

Loe MWC, Hao E, Chen M, et al (2020) Betulinic acid exhibits antiviral effects against dengue virus infection. Antiviral Res 184:in press. https://doi.org/10.1016/j.antiviral.2020.104954

Lu Y, Zhou J, Hu T et al (2018) A Multifunctional Oxidosqualene Cyclase from *Tripterygium Regelii* that produces both α- and *β*-Amyrin. RSC Adv 8:23516–23521. https://doi.org/10.1039/c8ra03468k

Lurain NS, Chou S (2010) Antiviral drug resistance of human cytomegalovirus. Clin Microbiol Rev 23:689–712. https://doi.org/10.1128/CMR.00009-10

Lv XJ, Li Y, Ma SG et al (2016) Antiviral triterpenes from the twigs and leaves of *Lyonia ovalifolia*. J Nat Prod 79:2824–2837. https://doi.org/10.1021/acs.jnatprod.6b00585

Lyu H, Chen J, Li W-L (2016) Natural triterpenoids for the treatment of diabetes mellitus: a review. Nat Prod Commun 11:1579–1586. https://doi.org/10.1177/1934578X1601101037

Ma Y, Shang C, Yang P et al (2018) 4-Iminooxazolidin-2-one as a bioisostere of the cyanohydrin moiety: inhibitors of enterovirus 71 3C protease. J Med Chem 61:10333–10339. https://doi.org/10.1021/acs.jmedchem.8b01335

MacNamara F (1954) Zika virus: a report on three cases of human infection during an epidemic of jaundice in Nigeria. Trans R Soc Trop Med Hyg 48:139–145. https://doi.org/10.1016/0035-9203(54)90006-1

Madavaraju K, Koganti R, Volety I et al (2021) Herpes Simplex Virus cell entry mechanisms: an update. Front Cell Infect Microbiol 10:852. https://doi.org/10.3389/fcimb.2020.617578

Mair CE, Grienke U, Wilhelm A et al (2018) Anti-influenza triterpene saponins from the bark of *Burkea africana*. J Nat Prod 81:515–523. https://doi.org/10.1021/acs.jnatprod.7b00774

Manosroi A, Jantrawut P, Ogihara E et al (2013) Biological activities of phenolic compounds and triterpenoids from the Galls of *Terminalia chebula*. Chem Biodivers 10:1448–1463. https://doi.org/10.1002/cbdv.201300149

Martín R, Cordova C, San Román JA et al (2014) Oleanolic acid modulates the immune-inflammatory response in mice with experimental autoimmune myocarditis and protects from cardiac injury. Therapeutic implications for the human disease. J Mol Cell Cardiol 72:250–262. https://doi.org/10.1016/j.yjmcc.2014.04.002

Milstone AM, Petrella J, Sanchez MD et al (2005) Interaction with coxsackievirus and adenovirus receptor, but not with decay-accelerating factor (DAF), induces a-particle formation in a DAF-binding coxsackievirus B3 isolate. J Virol 79:655–660. https://doi.org/10.1128/jvi.79.1.655-660.2005

Morita M, Shibuya M, Kushiro T et al (2000) Molecular cloning and functional expression of triterpene synthases from pea (*Pisum sativum*): New α-amyrin-producing enzyme is a multifunctional triterpene synthase. Eur J Biochem 267:3453–3460. https://doi.org/10.1046/j.1432-1327.2000.01357.x

Mukherjee H, Ojha D, Bag P et al (2013) Anti-herpes virus activities of *Achyranthes aspera:* An indian ethnomedicine, and its triterpene acid. Microbiol Res 168:238–244. https://doi.org/10.1016/j.micres.2012.11.002

Mulholland DA, Mohammed AMA, Coombes PH et al (2011) Triterpenoid acids and lactones from the leaves of *Fadogia tetraquetra* var. *tetraquetra* (Rubiaceae). Nat Prod Commun 6:1573–1576. https://doi.org/10.1177/1934578x1100601103

Muller PY, Milton MN (2012) The determination and interpretation of the therapeutic index in drug development. Nat Rev Drug Discov 11:751–761. https://doi.org/10.1038/nrd3801

Murugesan A, Manoharan M (2019) In: Ennaji MM (ed) Emerging and reemerging viral pathogens. Elsevier Inc, Amsterdam. https://doi.org/10.1016/B978-0-12-819400-3.00016-8

Musarra-Pizzo M, Pennisi R, Ben-Amor I et al (2021) Antiviral activity exerted by natural products against human viruses. Viruses 13:1–30. https://doi.org/10.3390/V13050828

Musso D, Gubler DJ (2016) Zika virus. Clin Microbiol Rev 29:487–524. https://doi.org/10.1128/cmr.00072-15

Naggie S, Lok AS (2021) New Therapeutics for Hepatitis B: The Road to Cure. Annu Rev Med 72:93–105. https://doi.org/10.1146/annurev-med-080119-103356

Nam HH, Ison MG (2019) Respiratory syncytial virus infection in adults. BMJ 366:371–384. https://doi.org/10.1136/bmj.l5021

Newman C, Friedrich TC, O'Connor DH (2017) Macaque monkeys in zika virus research: 1947–present. Curr Opin Virol 25:34–40. https://doi.org/10.1016/j.coviro.2017.06.011

O'leary JG, Davis GL (2010) Hepatitis C virus replication and potential targets for direct-acting agents. Therap Adv Gastroenterol 3:43–53. https://doi.org/10.1177/1756283x09353353

Oberste MS, Maher K, Kilpatrick DR, Pallansch MA (1999) Molecular evolution of the human enteroviruses: correlation of serotype with VP1 sequence and application to picornavirus classification. J Virol 73:1941–1948. https://doi.org/10.1128/jvi.73.3.1941-1948.1999

Ohyama K, Suzuki M, Kikuchi J et al (2009) Dual biosynthetic pathways to phytosterol via cycloartenol and lanosterol in

*Arabidopsis*. Proc Natl Acad Sci 106:725–730. https://doi.org/10.1073/pnas.0807675106

Osorio AA, Muñóz A, Torres-Romero D et al (2012) Olean-18-ene triterpenoids from Celastraceae species inhibit HIV replication targeting NF-kB and Sp1 dependent transcription. Eur J Med Chem 52:295–303. https://doi.org/10.1016/j.ejmech.2012.03.035

Pal M, Berhanu G, Desalegn C, Kandi V (2020) Severe acute respiratory syndrome coronavirus-2 (SARS-CoV-2): an update. Cureus 12:1–13. https://doi.org/10.7759/cureus.7423

Parvez MK, Arbab AD, Al-Dosari MS, Al-Rehaily AJ (2016) Antiviral natural products against chronic hepatitis B: recent developments. Curr Pharm Des 22:286–293. https://doi.org/10.2174/1381612822666151112152733

Pascual-iglesias A, Sanchez CM, Penzes Z et al (2019) Recombinant chimeric transmissible gastroenteritis virus (TGEV)—porcine epidemic diarrhea virus (PEDV) virus provides protection against virulent PEDV. Viruses 11:1–18. https://doi.org/10.3390/v11080682

Payne S (2017) In Payne S (ed), Viruses. Academic press, New York. https://doi.org/10.1016/B978-0-12-803109-4.00017-9

Pei Y, Wang C, Yan SF, Liu G (2017) Past, current, and future developments of therapeutic agents for treatment of chronic hepatitis B virus infection. J Med Chem 60:6461–6479. https://doi.org/10.1021/acs.jmedchem.6b01442

Peyrat LA, Eparvier V, Eydoux C et al (2017) Betulinic acid, the first lupane-type triterpenoid isolated from both a *Phomopsis* sp. and its host plant *Diospyros carbonaria* Benoist. Chem Biodivers 14:1–8. https://doi.org/10.1002/cbdv.201600171

Phongmaykin J, Kumamoto T, Ishikawa T et al (2011) Biologically active constituents of *Aglaia erythrosperma*. Nat Prod Res 25:1621–1628. https://doi.org/10.1080/14786419.2010.508038

Pollack A, Kontorovich AR, Fuster V, Dec GW (2015) Viral myocarditis-diagnosis, treatment options, and current controversies. Nat Rev Cardiol 12:670–680. https://doi.org/10.1038/nrcardio.2015.108

Poole CL, James SH (2018) Antiviral therapies for herpesviruses: current agents and new directions. Clin Ther 40:1282–1298. https://doi.org/10.1016/j.clinthera.2018.07.006

Raghuvanshi R, Bharate SB (2021) Recent developments in the use of kinase inhibitors for management of viral infections. J Med Chem in Press. https://doi.org/10.1021/acs.jmedchem.0c01467 (n press)

Rivest S, Forrest JRK (2020) Defence compounds in pollen: why do they occur and how do they affect the ecology and evolution of bees? New Phytol 225:1053–1064. https://doi.org/10.1111/nph.16230

Rokita SE (2009) In Rokita SE (ed) Quinone methides. Wiley, New York. https://doi.org/10.1002/9780470452882

Ruzicka L (1953) The isoprene rule and the biogenesis of terpenic compounds. Experientia 9:357–367. https://doi.org/10.1007/BF02167631

Ryu YB, Park SJ, Kim YM et al (2010) SARS-CoV 3CLpro inhibitory effects of quinone-methide triterpenes from *Tripterygium regelii*. Bioorganic Med Chem Lett 20:1873–1876. https://doi.org/10.1016/j.bmcl.2010.01.152

Sandjo LP, Kuete V (2013) In: Kuete C (ed) Medicinal plants research in Africa, pharmacology and chemistry. Elsevier Inc. https://doi.org/10.1016/B978-0-12-405927-6.00004-7

Sausen DG, Bhutta MS, Gallo ES et al (2021) Stress-Induced Epstein-Barr Virus Reactivation Biomolecules 11:1380. https://doi.org/10.3390/biom11091380

Sawai S, Saito K (2011) Triterpenoid biosynthesis and engineering in plants. Front Plant Sci 2:1–8. https://doi.org/10.3389/fpls.2011.00025

Sawai S, Uchiyama H, Mizuno S et al (2011) Molecular characterization of an oxidosqualene cyclase that yields shionone, a unique tetracyclic triterpene ketone of *Aster tataricus*. FEBS Lett 585:1031–1036. https://doi.org/10.1016/J.FEBSLET.2011.02.037

Schulz U, Solidoro P, Müller V et al (2016) CMV immunoglobulins for the treatment of CMV infections in thoracic transplant recipients. Transplantation 100:S5–S10. https://doi.org/10.1097/TP.0000000000001097

Schwartz DA, Graham AL (2020) Potential maternal and infant outcomes from coronavirus 2019-NCOV (SARS-CoV-2) infecting pregnant women: Lessons from SARS, MERS, and other human coronavirus infections. Viruses 12:1–16. https://doi.org/10.3390/v12020194

Scott A, McCluskey B, Brown-Reid M et al (2016) Porcine epidemic diarrhea virus introduction into the United States: Root cause investigation. Prev Vet Med 123:192–201. https://doi.org/10.1016/j.prevetmed.2015.11.013

Seema JSK (2005) Molecular mechanism of pathogenesis of dengue virus: Entry and fusion with target cell. Indian J Clin Biochem 20:92–103. https://doi.org/10.1007/bf02867407

Shamsabadipour S, Ghanadian M, Saeedi H, et al (2013) Triterpenes and steroids from *Euphorbia denticulata* lam. with anti-herpes symplex virus activity. Iran J Pharm Res 12:759–767. https://doi.org/10.22037/ijpr.2013.1400

Shehla N, Li B, Cao L et al (2020) Xuetonglactones A-F: Highly oxidized lanostane and cycloartane triterpenoids from *Kadsura heteroclita* Roxb. Craib Front Chem 7:1–13. https://doi.org/10.3389/fchem.2019.00935

Shenvi RA, Guerrero CA, Shi J et al (2008) Synthesis of (+)-cortistatin A. J Am Chem Soc 130:7241–7243. https://doi.org/10.1021/JA8023466

Shi Q, Lu S, Li D et al (2020) Cycloartane triterpene glycosides from rhizomes of *Cimicifuga foetida* L. with lipid-lowering activity on 3T3-L1 adipocytes. Fitoterapia 145:1–8. https://doi.org/10.1016/j.fitote.2020.104635

Shia KS, Li WT, Chang CM et al (2002) Design, synthesis, and structure-activity relationship of pyridyl imidazolidinones: A novel class of potent and selective human enterovirus 71 inhibitors. J Med Chem 45:1644–1655. https://doi.org/10.1021/jm010536a

Shieh JTC, Bergelson JM (2002) Interaction with decay-accelerating factor facilitates coxsackievirus B infection of polarized epithelial cells. J Virol 76:9474–9480. https://doi.org/10.1128/jvi.76.18.9474-9480.2002

Si L, Meng K, Tian Z et al (2018) Triterpenoids manipulate a broad range of virus-host fusion via wrapping the HR2 domain prevalent in viral envelopes. Sci Adv 4:1–14. https://doi.org/10.1126/sciadv.aau8408

Simon V, Ho DD, Karim QA (2006) Seminar HIV/AIDS epidemiology, pathogenesis, prevention, and treatment. Lancet 368:489–504. org/https://doi.org/10.1016/S0140-6736(06)69157-5

Sinclair J, Sissons P (2006) Latency and reactivation of human cytomegalovirus. J Gen Virol 87:1763–1779. https://doi.org/10.1099/vir.0.81891-0

Song QY, Jiang K, Zhao QQ et al (2013) Eleven new highly oxygenated triterpenoids from the leaves and stems of *Schisandra chinensis*. Org Biomol Chem 11:1251–1258. https://doi.org/10.1039/c2ob27115j

Song JH, Choi HJ, Song HH et al (2014a) Antiviral activity of ginsenosides against coxsackievirus B3, enterovirus 71, and human rhinovirus 3. J Ginseng Res 38:173–179. https://doi.org/10.1016/j.jgr.2014.04.003

Song JH, Yeo SG, Hong EH et al (2014b) Antiviral activity of hederasaponin B from *Hedera helix* against enterovirus 71 subgenotypes C3 and C4a. Biomol Ther 22:41–46. https://doi.org/10.4062/biomolther.2013.108

Song W, Si L, Ji S et al (2014c) Uralsaponins M-Y, antiviral triterpenoid saponins from the roots of *Glycyrrhiza uralensis*. J Nat Prod 77:1632–1643. https://doi.org/10.1021/np500253m

Stephenson MJ, Field RA, Osbourn A (2019) The protosteryl and dammarenyl cation dichotomy in polycyclic triterpene biosynthesis revisited: Has this "rule" finally been broken? Nat Prod Rep 36:1044–1052. https://doi.org/10.1039/c8np00096d

Strottmann DM, Zanluca C, Mosimann ALP et al (2019) Genetic and biological characterisation of Zika virus isolates from different Brazilian regions. Mem Inst Oswaldo Cruz 114:1–11. https://doi.org/10.1590/0074-02760190150

Su HG, Peng XR, Shi QQ et al (2020) Lanostane triterpenoids with anti-inflammatory activities from *Ganoderma lucidum*. Phytochemistry 173:1–7. https://doi.org/10.1016/j.phytochem.2019.112256

Suzuki M, Muranaka T (2007) Molecular genetics of plant sterol backbone synthesis. Lipids 42:47–54. https://doi.org/10.1007/s11745-006-1000-5

Suzuki M, Xiang T, Ohyama K et al (2006) Lanosterol synthase in dicotyledonous plants. Plant Cell Physiol 47:565–571. https://doi.org/10.1093/pcp/pcj031

Taddeo V, Castillo U, Martínez M et al (2019) Development and validation of an HPLC-PDA method for biologically active quinonemethide triterpenoids isolated from *Maytenus chiapensis*. Medicines 6:1–8. https://doi.org/10.3390/medicines6010036

Tang Q, Xu Z, Jin M et al (2020) Identification of dibucaine derivatives as novel potent enterovirus 2C helicase inhibitors: In vitro, in vivo, and combination therapy study. Eur J Med Chem 202:1–12. https://doi.org/10.1016/j.ejmech.2020.112310

Tansakul P, Shibuya M, Kushiro T, Ebizuka Y (2006) Dammarenediol-II synthase, the first dedicated enzyme for ginsenoside biosynthesis, in *Panax ginseng*. FEBS Lett 580:5143–5149. https://doi.org/10.1016/j.febslet.2006.08.044

Thimmappa R, Geisler K, Louveau T et al (2014) Triterpene biosynthesis in plants. Annu Rev Plant Biol 65:225–257. https://doi.org/10.1146/annurev-arplant-050312-120229

Treml J, Gazdová M, Šmejkal K et al (2020) Natural products-derived chemicals: breaking barriers to novel anti-HSV drug development. Viruses 12:1–43. https://doi.org/10.3390/v12020154

Trinh TBN, Le DH, Nguyen TTK et al (2021) In vitro antiviral activities of ethanol and aqueous extracts of Vietnamese traditional medicinal plants against porcine epidemic diarrhea virus: a coronavirus family member. Virus Dis, pp 1–7. https://doi.org/10.1007/S13337-021-00709-Z

Tuiskunen BA, Lundkvist Å (2013) Dengue viruses—an overview. Infect Ecol Epidemiol 3:1–21. https://doi.org/10.3402/iee.v3i0.19839

Tung NH, Kwon HJ, Kim JH et al (2010) An anti-influenza component of the bark of *Alnus japonica*. Arch Pharm Res 33:363–367. https://doi.org/10.1007/s12272-010-0303-5

Vijayan KKV, Karthigeyan KP, Tripathi SP, Hanna LE (2017) Pathophysiology of CD4+ T-cell depletion in HIV-1 and HIV-2 infections. Front Immunol 8:1–8. https://doi.org/10.3389/fimmu.2017.00580

Vranová E, Coman D, Gruissem W (2013) Network analysis of the MVA and MEP pathways for isoprenoid synthesis. Annu Rev Plant Biol 64:665–700. https://doi.org/10.1146/annurev-arplant-050312-120116

Wang X, Wang Y, Ren Z et al (2012) Protective effects of 20(S)-protopanaxtriol on viral myocarditis infected by coxsackievirus B3. Pathobiology 79:285–289. https://doi.org/10.1159/000331229

Wang J, Chen X, Wang W et al (2013) Glycyrrhizic acid as the antiviral component of *Glycyrrhiza uralensis* Fisch. against coxsackievirus A16 and enterovirus 71 of hand foot and mouth disease. J Ethnopharmacol 147:114–121. https://doi.org/10.1016/j.jep.2013.02.017

Wang L, Wang J, Wang L et al (2015) Anti-enterovirus 71 agents of natural products. Molecules 20:16320–16333

Wang D, Fang L, Xiao S (2016) Porcine epidemic diarrhea in China. Virus Res 226:7–13. https://doi.org/10.1016/j.virusres.2016.05.026

Wang F, Chen C, Yang K et al (2017) Michael acceptor-based peptidomimetic inhibitor of main protease from porcine epidemic diarrhea virus. J Med Chem 60:3212–3216. https://doi.org/10.1021/acs.jmedchem.7b00103

Wang P, Bai J, Liu X et al (2020) Tomatidine inhibits porcine epidemic diarrhea virus replication by targeting 3CL protease. Vet Res 51:1–18. https://doi.org/10.1186/S13567-020-00865-Y

Wang J, Guo Y, Yin X et al (2021) Diverse triterpene skeletons are derived from the expansion and divergent evolution of 2,3-oxidosqualene cyclases in plants. Crit Rev Biochem Mol Biol 1–20. https://doi.org/10.1080/10409238.2021.1979458

Watanabe K, Ishikawa T, Otaki H et al (2017) Structure-based drug discovery for combating influenza virus by targeting the PA–PB1 interaction. Sci Reports 7:1–12. https://doi.org/10.1038/s41598-017-10021-w

Weiss SR, Leibowitz JL (2011) Coronavirus pathogenesis. Adv Virus Res 81:85–164. https://doi.org/10.1016/b978-0-12-385885-6.00009-2

Wink M (1988) Plant breeding: importance of plant secondary metabolites for protection against pathogens and herbivores. Theor Appl Genet 75:225–233. https://doi.org/10.1007/BF00303957

Wohlfarth C, Efferth T (2009) Natural products as promising drug candidates for the treatment of hepatitis B and C. Acta Pharmacol Sin 30:25–30. https://doi.org/10.1038/aps.2008.5

Woo PCY, Lau SKP, Lam CSF et al (2012) Discovery of seven novel mammalian and avian corona viruses in the genus *Deltacoronavirus* supports bat coronaviruses as the gene source of *Alphacoronavirus* and *Betacoronavirus* and avian coronaviruses as the gene source of *Gammacoronavirus* and *Deltacoronavirus*. J Virol 86:3995–4008. https://doi.org/10.1128/jvi.06540-11

Wu H, Ma G, Yang Q et al (2019) Discovery and synthesis of novel beesioside I derivatives with potent anti-HIV activity. Eur J Med Chem 166:159–166. https://doi.org/10.1016/j.ejmech.2019.01.020

Xia YG, Yang BY, Kuang HX (2015) Schisandraceae Triterpenoids: a Review Phytochem Rev 14:155–187. https://doi.org/10.1007/s11101-014-9343-7

Xia S, Liu M, Wang C et al (2020) Inhibition of SARS-CoV-2 (previously 2019-nCoV) infection by a highly potent pan-coronavirus fusion inhibitor targeting its spike protein that harbors a high capacity to mediate membrane fusion. Cell Res 30:343–355. https://doi.org/10.1038/s41422-020-0305-x

Xiang L, Zhang L, Chen X et al (2019) Ursane-type triterpenoid saponins from *Elsholtzia bodinieri*. Nat Prod Res 33:1349–1356. https://doi.org/10.1080/14786419.2018.1477144

Xiao WL, Li RT, Huang SX et al (2008) Triterpenoids from the schisandraceae family. Nat Prod Rep 25:871–891. https://doi.org/10.1039/b719905h

Xu R, Fazio GC, Matsuda SPT (2004) On the origins of triterpenoid skeletal diversity. Phytochemistry 65:261–291. https://doi.org/10.1016/j.phytochem.2003.11.014

Xu LJ, Peng ZG, Chen HS et al (2010) Bioactive triterpenoids from *Kadsura heteroclita*. Chem Biodivers 7:2289–2295. https://doi.org/10.1002/cbdv.200900173

Xu M, Li X, Song L et al (2020) Lupeol alleviates coxsackievirus B3-induced viral myocarditis in mice via downregulating toll-like receptor 4. J Int Med Res 48:1–11. https://doi.org/10.1177/0300060520910908

Xue Z, Duan L, Liu D et al (2012) Divergent evolution of oxidosqualene cyclases in plants. New Phytol 193:1022–1038. https://doi.org/10.1111/J.1469-8137.2011.03997.X

Yang JL, Ha TKQ, Dhodary B et al (2015) Oleanane triterpenes from the flowers of *Camellia japonica* inhibit porcine epidemic diarrhea virus (PEDV) replication. J Med Chem 58:1268–1280. https://doi.org/10.1021/jm501567f

Ye G, Wang X, Tong X et al (2020a) Structural basis for inhibiting porcine epidemic diarrhea virus replication with the 3C-Like protease inhibitor GC376. Viruses 12:1–15. https://doi.org/10.3390/V12020240

Ye Q, Wang B, Mao J (2020b) The pathogenesis and treatment of the 'Cytokine Storm' in COVID-19. J Infect 80:607–613. https://doi.org/10.1016/J.JINF.2020.03.037

Yoneda T, Nakamura S, Ogawa K et al (2018) Oleanane-type triterpenes with highly-substituted oxygen functional groups from the flower buds of *Camellia sinensis* and their inhibitory effects against no production and HSV-1. Nat Prod Commun 13:131–136. https://doi.org/10.1177/1934578x1801300206

Yuen MF, Chen DS, Dusheiko GM et al (2018) Hepatitis B virus infection. Nat Rev Dis Prim 4:1–20. https://doi.org/10.1038/nrdp.2018.35

Zhai Y, Ma Y, Ma F et al (2016) Structure–activity relationship study of peptidomimetic aldehydes as enterovirus 71 3C protease inhibitors. Eur J Med Chem 124:559–573. https://doi.org/10.1016/j.ejmech.2016.08.064

Zhang J, Kurita M, Shinozaki T et al (2014a) Triterpene glycosides and other polar constituents of shea (*Vitellaria paradoxa*) kernels and their bioactivities. Phytochemistry 108:157–170. https://doi.org/10.1016/j.phytochem.2014.09.017

Zhang W, Tao J, Yang X et al (2014b) Antiviral effects of two *Ganoderma lucidum* triterpenoids against enterovirus 71 infection. Biochem Biophys Res Commun 449:307–312. https://doi.org/10.1016/j.bbrc.2014.05.019

Zhao J, Chen J, Liu T et al (2012) Anti-viral effects of urosolic acid on guinea pig cytomegalovirus in vitro. J Huazhong Univ Sci Technolog Med Sci 32:883–887. https://doi.org/10.1007/s11596-012-1052-0

Zhao CH, Xu J, Zhang YQ et al (2014) Inhibition of human enterovirus 71 replication by pentacyclic triterpenes and their novel synthetic derivatives. Chem Pharm Bull 62:764–771. https://doi.org/10.1248/cpb.c14-00088

Zhao XT, Yu MH, Su SY et al (2020) Cycloartane triterpenoids from *Pseudolarix amabilis* and their antiviral activity. Phytochemistry 171:1–8. https://doi.org/10.1016/j.phytochem.2019.112229

Zhong JD, Zhao XW, Chen XQ et al (2016) Two new ursane-type triterpenoid saponins from *Elsholtzia bodinieri*. Arch Pharm Res 39:771–777. https://doi.org/10.1007/s12272-016-0750-8

Zhou F, Pichersky E (2020) More is better: the diversity of terpene metabolism in plants. Curr Opin Plant Biol 55:1–10. https://doi.org/10.1016/j.pbi.2020.01.005

Zhou WB, Tao JY, Xu HM et al (2010) Three new antiviral triterpenes from *Aster tataricus*. Zeitschrift Fur Naturforsch Sect B J Chem Sci 65:1393–1396. https://doi.org/10.1515/znb-2010-1116

Zhou M, Xu M, Ma XX et al (2012) Antiviral triterpenoid saponins from the roots of *Ilex asprella*. Planta Med 78:1702–1705. https://doi.org/10.1055/s-0032-1315209

Zhou WB, Zeng GZ, Xu HM et al (2013) Astataricusones A-D and astataricusol A, five new anti-HBV shionane-type triterpenes from *Aster tataricus* L. f. Molecules 18:14585–14596. https://doi.org/10.3390/molecules181214585

Zhou WB, Zeng GZ, Xu HM et al (2014) Astershionones A-F, six new anti-HBV shionane-type triterpenes from *Aster tataricus*. Fitoterapia 93:98–104. https://doi.org/10.1016/j.fitote.2013.12.021

Zhou J, Hu T, Gao L et al (2019) Friedelane-type triterpene cyclase in celastrol biosynthesis from *Tripterygium wilfordii* and its application for triterpenes biosynthesis in yeast. New Phytol 223:722–735. https://doi.org/10.1111/nph.15809

Zhou Q (2009) Natural diterpene and triterpene quinone methides: structures, synthesis, and biological potentials. In: Rokita SE (ed) Quinone Methides, vol 1. Wiley, New York, pp 269–295

Zhu Q, Bang TH, Ohnuki K et al (2015) Inhibition of neuraminidase by *Ganoderma* triterpenoids and implications for neuraminidase inhibitor design. Sci Rep 5:1–9. https://doi.org/10.1038/srep13194

Zuckerman AJ (1996) In: Baron S (ed) Medical Microbiology 4th edn. The University of Texas Medical Branch, Galveston.

**Publisher's Note** Springer Nature remains neutral with regard to jurisdictional claims in published maps and institutional affiliations.